

Ali Shee

---

# Evaluation of Copper-Based-Catalysts for Treatment of Halogenated Organic Compounds in Water

**Evaluation of Copper-Based-Catalysts for Treatment of Halogenated Organic Compounds  
in Water**

Der Fakultät für Chemie und Mineralogie  
der Universität Leipzig

DISSERTATION

zur Erlangung des akademischen Grades

doctor rerum naturalium

(Dr. rer. nat.)

vorgelegt

von M. Sc. (Chemie) Ali Shee

geboren am 23. März 1986 in Kwale, Kenia

Leipzig, den 18.05.2021

## Bibliographic Description

Ali Shee

### **Evaluation of Copper-Based-Catalysts for Treatment of Halogenated Organic Compounds in Water**

Leipzig University, Doctoral Thesis

175 Pages, 23 Figures, 9 Tables, 198 Citations

#### Abstract:

This thesis contributes to the evaluation of  $\text{Cu}^0 + \text{NaBH}_4$  as a promising system for reductive dehalogenation of halogenated organic compounds (HOCs) in water. The first part of the thesis describes an investigation of  $\text{Cu}^0 + \text{NaBH}_4$  in order to determine product selectivity patterns and reaction pathways in dehalogenation reactions of HOCs with the general formula  $\text{CCl}_3\text{-R}$ , where  $\text{R} = \text{H, F, Cl, Br, and CH}_3$ . Selectivity patterns were determined under various experimental conditions, e.g. in water matrix and with catalyst supports. When  $\text{Cu}^0 + \text{NaBH}_4$  was applied to  $\text{CCl}_3\text{-R}$  compounds, the formation of slowly degrading intermediates such as  $\text{CH}_2\text{Cl}_2$  from  $\text{CHCl}_3$  was inevitable. Hence, optimization of  $\text{Cu}^0 + \text{NaBH}_4$  in order to ensure minimization or elimination of these intermediates is discussed. The second part of the thesis explores the reactivity of  $\text{Cu}^0 + \text{NaBH}_4$  with various HOC classes frequently encountered in water, soils, and sediments. A comparison was made between  $\text{Cu}^0 + \text{NaBH}_4$  and the common reduction systems employing nanoscale zero-valent iron (nZVI) as a reagent and Pd catalysts +  $\text{H}_2$  as the reductant for these HOC classes. Criteria for comparison were based on the HOC's reactivity presented as specific metal activities, yields, and the fate of the halogenated intermediates, metal costs, and metal stability in water. Application areas for Cu, nZVI, and Pd are discussed with regard to each

class of HOCs. Finally, water-matrix effects on the stability of Cu catalysts were investigated for reductive dehalogenation reactions.

Bibliographische Darstellung

Ali Shee

**Evaluation of Copper-Based-Catalysts for Treatment of Halogenated Organic Compounds  
in Water**

Universität Leipzig, Dissertation

175 Seiten, 23 Abbildungen, 9 Tabellen, 198 Literaturangaben

Kurzreferat:

Diese Dissertation trägt zur Untersuchung von  $\text{Cu}^0 + \text{NaBH}_4$  als einem vielversprechenden System zur reduktiven Dehalogenierung von halogenierten organischen Verbindungen (HOCs) in Wasser bei. Im ersten Teil dieser Arbeit wurde das System  $\text{Cu}^0 + \text{NaBH}_4$  untersucht, um die Produktselektivität und Reaktionswege während der reduktiven Dehalogenierung von HOCs mit der allgemeinen Formel  $\text{CCl}_3\text{-R}$  mit  $\text{R} = \text{H}, \text{F}, \text{Cl}, \text{Br}$  und  $\text{CH}_3$  zu bestimmen. Die Selektivität wurde unter verschiedenen experimentellen Bedingungen, z.B. der Zusammensetzung der Wassermatrix und Variationen des Katalysatorträgers, bestimmt. Die Bildung von halogenierten Zwischenprodukten, unter Verwendung von  $\text{Cu}^0 + \text{NaBH}_4$ , ist für diese Verbindungsklassen unvermeidlich, daher wird die Optimierung des Systems zur Minimierung oder Vermeidung der Akkumulation dieser diskutiert. Im zweiten Teil der Dissertation wurde die Reaktivität des Systems  $\text{Cu}^0 + \text{NaBH}_4$  mit verschiedenen HOC-Klassen untersucht, die häufig in Wässern, Böden und Sedimenten vorkommen. Zudem wurde ein Vergleich des  $\text{Cu}^0 + \text{NaBH}_4$  Systems mit gebräuchlicheren Reduktionsmitteln, wie nullwertigem Eisen (nZVI) und Pd-Katalysatoren +  $\text{H}_2$ , an den HOC-Klassen vorgenommen. Dabei wurden insbesondere die HOC-Reaktivität mittels der spezifischen Metall-Aktivität, die Produkt Ausbeuten, der Verbleib der halogenierten Zwischenprodukte, sowie der Katalysator- und Reduktionsmittelkosten und der Metallstabilität in

Wasser diskutiert. Des Weiteren, werden Einsatzmöglichkeiten für Cu, nZVI und Pd, im Hinblick auf die verschiedenen Klassen von HOCs, diskutiert. Abschließend wurden die Auswirkungen der Wassermatrix auf die Stabilität von Cu-Katalysatoren für die reduktive Dehalogenierung untersucht.

This thesis work was conducted in the period from October 2016 to December 2020 at the Department of Environmental Engineering, Helmholtz Centre for Environmental Research - UFZ under the supervision of Prof. Dr. Frank-Dieter Kopinke and Dr. Katrin Mackenzie. The research stay at the UFZ, Leipzig of the author was supported through a scholarship from the Germany Academic Exchange Service (DAAD).

## Table of Contents

1 Introduction.....	10
2 Theoretical Part.....	14
2.1 Reductive dehalogenation of HOCs in water.....	14
2.2 Reductive dechlorination pathways.....	15
2.2.1 Chlorinated methanes.....	15
2.2.2 Chlorinated ethanes and ethylenes.....	17
2.3 Dehalogenation of CCl <sub>3</sub> -R compounds using reagents and catalysts.....	19
2.4 Dehalogenation reactions using nZVI reagent.....	25
2.4.1 Synthesis and properties of nZVI.....	25
2.4.2 Reduction of HOCs using nZVI.....	28
2.4.3 HOC classes treatable by nZVI.....	29
2.5 Reductive dechlorination using vitamin B12.....	32
2.6 Catalytic dechlorination.....	34
2.6.1 Palladium catalysts.....	34
2.6.2 Copper catalysts.....	38
2.7 Specific activities and performance of reagents and catalysts.....	40
3 Research Methodology.....	43
3.1. Chemicals, reagents, and materials.....	43
3.1.1 Chemicals, reagents, and gases.....	43
3.1.2 Materials.....	46
3.1.3 Preparation of synthetic freshwater.....	53

3.1.4 Preparation of SRHA solution .....	54
3.2 Electrodes characterization and CF dechlorination experiments .....	54
3.2.1 Characterization of Cu and Cu/ACF electrodes by cyclic voltammetry (CV) .....	54
3.2.2 Electrochemical dechlorination of CF .....	55
3.2.3 Dehalogenation of HOCs using Cu NPs.....	56
3.2.4 Dehalogenation of HOCs using Pd NPs .....	57
3.2.5 Dehalogenation of HOCs using nZVI .....	57
3.2.6 Dechlorination of CF using Cu-modified materials .....	58
3.2.7 Evaluation of Cu stability for dechlorination of CF .....	58
3.2.8 Lifetime and regeneration of Cu-doped cation-exchange resin.....	59
3.3 Analytical techniques .....	60
3.3.1 Determination of surface area.....	60
3.3.2 Determination of Fe <sup>0</sup> content.....	60
3.3.3 Analysis of Cu <sup>2+</sup> in prepared samples .....	61
3.3.4 Measurement of HOCs and dehalogenation products .....	63
3.3.5 Analysis of halide ions by ion chromatography (IC) .....	66
4 Results and Discussion .....	68
4.1 Dehalogenation of CCl <sub>3</sub> -R compounds using the Cu <sup>0</sup> + NaBH <sub>4</sub> .....	68
4.1.1 Dechlorination of CF using Cu <sup>0</sup> + NaBH <sub>4</sub> .....	68
4.1.2 Dehalogenation of CCl <sub>4</sub> , CFCl <sub>3</sub> , CBrCl <sub>3</sub> and CCl <sub>3</sub> -CH <sub>3</sub> using Cu <sup>0</sup> + NaBH <sub>4</sub> .....	96
4.2 Application areas for Cu-, Pd- and nZVI-based systems .....	102

4.2.1 Specific metal activities for the reduction of HOCs using Cu-, Pd- and nZVI-based systems.....	103
4.2.2 Water matrix effects on the stability of Cu catalysts .....	113
4.2.3 Regeneration and lifetime of Cu-doped cation-exchange resin.....	118
4.2.4 Limitations of $\text{Cu}^0 + \text{NaBH}_4$ and the recommended application areas .....	121
5 Summary .....	123
6 Bibliography .....	136
Appendix.....	151
A1 Additional experimental details .....	151
A2 Characterization of particles and materials .....	155
A3 Additional results from the dehalogenation of $\text{CCl}_3\text{-R}$ compounds .....	156
A4 List of abbreviations.....	159
A5 List of symbols .....	164
A6 List of figures .....	167
A7 List of tables .....	170
A8 Acknowledgments .....	171
A9 Curriculum vitae.....	172

## 1 Introduction

Halogenated organic compounds (HOCs) are among the most problematic contaminants frequently encountered in surface water, groundwater, soils, and sediments. Since most HOCs are toxic and carcinogenic to humans even at very low concentrations (Huang et al., 2014), their removal from contaminated sites is important. Existing remediation techniques for HOCs are based on physical, chemical, and biological processes. Biological processes are characterized by slow reaction rates; hence most compounds persist for long times in the environment (Erable et al., 2006; Singh et al., 2009). Furthermore, microbial processes, e.g. methanogenesis may be inhibited by high concentrations of some toxic HOCs, e.g. chloroform (CF) (Bagley et al., 2000; Duhamel et al., 2002). The phase-transfer techniques for HOC removal in water, such as adsorption and air stripping, only transfer the pollutant to another compartment, where further treatment steps for the extracted HOC effluents are necessary (Li et al., 2012). Chemical remediation techniques which can achieve significant detoxification include oxidation and reduction processes.

Advanced oxidation processes (AOPs) are well-established techniques and are suitable for a wide range of contaminants. AOPs for treatment of HOCs are based on: i) Fenton-based catalysts (Teel et al., 2001), ii) photocatalysts, e.g.  $\text{TiO}_2$  (Shirayama et al., 2001; Yamazaki et al., 2001), iii) ultraviolet radiation (UV) and  $\text{O}_3$  as in UV/ $\text{O}_3$ ,  $\text{O}_3/\text{H}_2\text{O}_2$  and UV/ $\text{H}_2\text{O}_2$  (Jin et al., 2012; Wols et al., 2013), iv) electrochemical oxidation (Wang and Wang, 2008), v)  $\text{KMnO}_4$  as a reagent (Yan and Schwartz, 1999), and vi)  $\text{SO}_4^{\cdot-}$  radicals (Matzek and Carter, 2016; Oh et al., 2016). Major drawbacks of AOP technologies include low reaction selectivity, production of partially oxidized and potentially toxic byproducts (e.g. chloroacetic acids from trichloroethylene (TCE) and perchloroethylene (PCE) oxidation (Hirvonen et al., 1996)), Fe-sludge generation, and consumption of high amounts of oxidant equivalents. Reductive dehalogenation of HOCs, as an

alternative to AOPs under ambient conditions, leads to considerable detoxification of contaminated waters, although dehalogenated organic byproducts (e.g. benzene from chlorobenzenes) and sometimes byproducts with lower chlorine substitution (e.g. dichloromethane (DCM) from CF) remain. Hence, it may be necessary to couple reductive dehalogenation technologies with biological process (Dong et al., 2019; Vogel et al., 2018).

Reductive dehalogenation of HOCs using metals such as zero-valent iron (ZVI) as a reagent is widely established. ZVI is often applied *in situ* due to its environmental compatibility. Furthermore, metallic Fe is cheap and easily available. Despite these benefits, the ZVI application has some significant limitations and drawbacks. First and foremost, it shows extremely low activity towards compounds with lower chlorine substitution degrees, e.g. 1,2-dichloroethane (1,2-DCA) and DCM (Feng and Lim, 2005; Song and Carraway, 2006; Song and Carraway, 2005). ZVI also fails for cleavage of C–Cl bonds bound to aromatic structures (Balda and Kopinke, 2020; Kopinke et al., 2020). Other major drawbacks of ZVI include its rapid consumption under acidic conditions ( $\text{pH} < 7$ ) and rapid deactivation under aerobic conditions. Even in the absence of oxidants, ZVI is slowly but continuously consumed by anaerobic corrosion in water ( $\text{Fe}^0 + 2\text{H}_2\text{O} \rightarrow \text{Fe}^{2+} + \text{H}_2 + 2\text{OH}^-$ ).

Reductive dehalogenation can also employ noble metal catalysts, e.g. Rh, Pt and Pd. Among the noble metals, Pd is the most potent hydrodechlorination (HDC) metal; it is quite resistant in water against self-poisoning by hydrogen halide (HX), in particular in the presence of bases, e.g. NaOH (Benitez and Del Angel, 2000; Urbano and Marinas, 2001). The combination of Pd catalysts with a suitable hydrogen donor, e.g.  $\text{H}_2$ ,  $\text{Fe}^0$  as  $\text{H}_2$  producer,  $\text{BH}_4^-$ , formic acid or hydrazine, is essential. In this case, the reductive dehalogenation reaction occurs at the Pd surface, mediated by adsorbed surface hydrogen ( $\text{Pd-H}_{\text{ads}}$ ) (Conrad et al., 1974; Coq et al., 1986). The

benefit of Pd in comparison to ZVI is that it can be applied at a broader pH range and for a broader spectrum of HOCs. Only a few substances, such as DCM or 1,2-DCA, are rather resistant against hydrodechlorination using Pd. Pd catalysts exhibit much higher specific activities towards HOCs than ZVI (on a per-surface-area basis). They are also able to catalyze the cleavage of C–Cl bonds attached to aromatic structures. Despite these benefits, the application of Pd faces some major challenges. Pd, although required only in catalytic amounts, is more expensive than ZVI (present cost is about USD 79/g Pd) (Palladium Prices, 2021). It is also highly susceptible to deactivation by macromolecules e.g. dissolved organic matter and other catalyst poisons such as reduced sulfur species, in particular sulfide (Chaplin et al., 2012; Hildebrand et al., 2009b; Lowry and Reinhard, 2000; Navon et al., 2012). Protection of Pd against macromolecules and poisoning by reduced sulfur species is therefore very important (Comandella et al., 2016; Kopinke et al., 2010; Navon et al., 2012). Due to the severe limitations of ZVI and Pd, an alternative remediation system for the reductive dehalogenation of HOCs in water is desirable.

In this thesis, the application potential of Cu catalysts for the treatment of HOCs in water was studied more deeply in order to identify advantages and develop solutions to overcome foreseeable challenges. The study was premised on previous work that  $\text{Cu}^0 + \text{NaBH}_4$  can be used to dechlorinate 1,2-DCA and DCM (Huang et al., 2012; Huang et al., 2011). The dechlorination of compounds such as DCM and 1,2-DCA using  $\text{Cu}^0 + \text{NaBH}_4$  is known to support reaction pathways to the fully dechlorinated products such as methane ( $\text{CH}_4$ ) and ethane ( $\text{C}_2\text{H}_6$ ) as well as to the partially dechlorinated intermediates, monochloromethane (MCM), and monochloroethane (MCA) (El-Sharnouby, 2016; Huang et al., 2012). Therefore, this work studied the product yields and selectivity patterns from compounds with the general formula  $\text{CCl}_3\text{-R}$ , where  $\text{R} = \text{H}, \text{F}, \text{Cl}$ ,

Br, or CH<sub>3</sub>. The application of Cu<sup>0</sup> + NaBH<sub>4</sub> as a reductive dehalogenation system was then optimized in order to minimize the formation and accumulation of halogenated byproducts.

Since Cu<sup>0</sup> + NaBH<sub>4</sub> has until now been applied to dechlorination of 1,2-DCA (Huang et al., 2011), DCM (Huang et al., 2012), and some chlorinated aromatics (Raut et al., 2016), it was further applied in this study to other HOC classes that are commonly encountered as water contaminants. The compounds to be treated by Cu<sup>0</sup> + NaBH<sub>4</sub> were selected based upon their chemical structure, halogenation degree, alkyl chain lengths, and the functional groups adjacent to the carbon-halogen (C–X) bond to be cleaved. Based on the specific metal activities, the fate of halogenated byproducts and metal costs and stability, comparisons of the dehalogenation potentials between Cu-, Pd-, and nZVI-based systems are presented as recommendations for the most appropriate application areas of each remediation system. Finally, the influence of the water matrix on the stability of Cu catalysts was evaluated in order to determine potential catalyst promoters and deactivators. As an alternative to unmodified copper nanoparticles (Cu NPs), Cu-doped cation-exchange resins as dechlorination catalysts in the presence of NaBH<sub>4</sub> were used and evaluated in order to determine their performance, reusability and regeneration upon deactivation by sulfide/bisulfide.

## 2 Theoretical Part

### 2.1 Reductive dehalogenation of HOCs in water

Reductive dehalogenation technologies can be applied to a wide range of HOCs that are usually detected as contaminants in water, soils, and sediments (Chaplin et al., 2012; Hu et al., 2017). As shown in reaction 1, reductive dehalogenation is a process applied to R–X (representative for any HOCs) and involves the cleavage of C–X bonds and the formation of carbon-hydrogen (R–H) bonds (hydrogenolysis).



In polychlorinated compounds,  $\alpha$ - and  $\beta$ -eliminations are alternative reaction mechanisms, yielding carbene or unsaturated (olefinic or acetylenic) intermediates as shown in reactions 2 and 3, respectively.



The reducing agent can either be an electron donor or activated H-species (active H\*). A special case is the application of solvated electrons as reductants. They can be generated using alkali metals, e.g. Na in liquid NH<sub>3</sub> (Mackenzie et al., 1996; Sun et al., 2000) or the UV/I<sup>-</sup>-system in water (Iglev et al., 2005; Lehr et al., 1999). Reductive dehalogenation using metallic reagents such as ZVI as a reagent and metal catalysts, e.g. Pd are the most common and have been applied

towards treating various HOCs. The reductive dehalogenation reaction may be initiated by one of the three reaction steps, hydrogenolysis,  $\alpha$ -elimination, and  $\beta$ -elimination. One or several of these reaction steps may be involved during the dehalogenation process depending on the molecular structure of the contaminant and the substitution pattern of halogen atoms within the molecule.

## 2.2 Reductive dechlorination pathways

### 2.2.1 Chlorinated methanes

The main reaction pathways for the dechlorination of chlorinated methanes, e.g. carbon tetrachloride (CTC) are hydrogenolysis and  $\alpha$ -elimination. Electron transfer to CTC initiates the dissociation of the C–Cl bond leading to the formation of surface-bound trichloromethyl radical ( $\bullet\text{CCl}_3$ ) as shown in Figure 1 (Balko and Tratnyek, 1998; Matheson and Tratnyek, 1994; Song and Carraway, 2006).

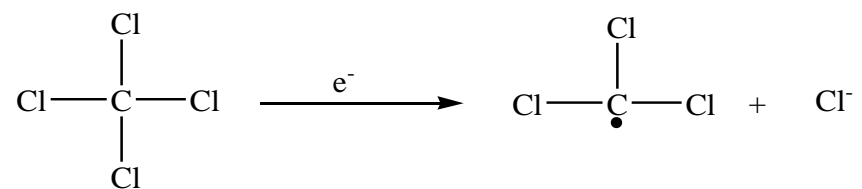


**Figure 1:** Speculated reaction step for the formation of trichloromethyl radical from carbon tetrachloride (Balko and Tratnyek, 1998; Matheson and Tratnyek, 1994; Song and Carraway, 2006).

For ZVI-driven dechlorination of CTC, the transfer of a single electron to the CTC molecule which results in cleavage of the C–Cl bond is considered rate determining. The trichloromethyl radical can undergo several reaction pathways. A second electron transfer to the trichloromethyl radical followed by protonation results in the formation of CF as shown in Figure 2.

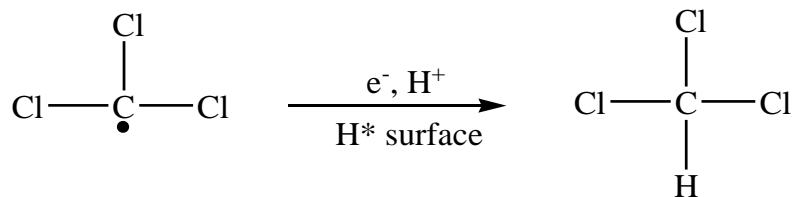


**Figure 2:** Speculated reaction step for the formation of chloroform from trichloromethyl radical (Balko and Tratnyek, 1998; Song and Carraway, 2006).

The stabilization of the surface-bound radical species can also take place by recombination with surface-bound hydrogen species ( $\text{H}^*$ ). Intermolecular reactions of trichloromethyl radicals lead to the formation of  $\geq \text{C}_2$ -chlorohydrocarbons. The detection of trace levels of ethane and ethylene in the dechlorination of CTC and CF using ZVI reagent and  $\text{Pd} + \text{H}_2$  gives evidence of radical coupling reactions (Feng and Lim, 2007; McCormick and Adriaens, 2004; Velázquez et al., 2013).

Similarly, the transfer of an electron to CF results in the formation of dichloromethyl radical ( $\bullet\text{CHCl}_2$ ) as shown in Figure 3.

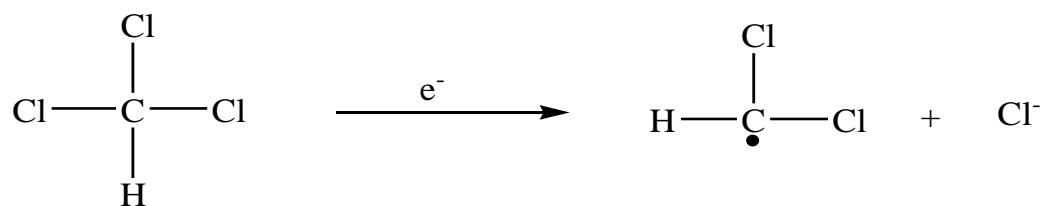


**Figure 3:** Speculated reaction step for the formation of dichloromethyl radical from chloroform (Song and Carraway, 2006).

Subsequent reactions proceed in the same way as presented above (similar process as shown in Figure 2), yielding DCM and  $\geq \text{C}_2$ -chlorohydrocarbons. Further stepwise hydrogenolysis of DCM can occur to form MCM and finally methane. For dechlorination of CTC and CF using ZVI as a reagent and  $\text{Pd} + \text{H}_2$ , DCM and MCM are highly recalcitrant intermediates.  $\text{CH}_4$  usually

appears from the onset of reaction as CTC is transformed, i.e. by a direct reaction pathway. The formation of CH<sub>4</sub> during dechlorination of CTC and CF involves concerted reductive elimination steps ( $\alpha$ -elimination) which bypasses DCM (McCormick and Adriaens, 2004; Song and Carraway, 2006). The reaction step via  $\alpha$ -elimination proceeds through the transfer of two electrons to the molecules and the elimination of two Cl-atoms bound to the same carbon. The products from the dechlorination reaction are two chloride ions and the lower-saturated aliphatic hydrocarbons.

### 2.2.2 Chlorinated ethanes and ethylenes

Dechlorination of chlorinated ethanes and ethylenes using metallic reagents and catalysts involves a combination of reactions which include hydrogenolysis,  $\alpha$ -elimination,  $\beta$ -elimination, and the hydrogenation of unsaturated bonds as shown in the reaction network in Figure 4. Reductive dechlorination via  $\alpha$ -elimination is observed for compounds with geminal halogen substituents such as in 1,1-dichloroethylene (1,1-DCE). Since MCA is rather inert using ZVI and Pd, concerted  $\alpha$ -elimination reaction steps via dichloroethyl carbene intermediates account for the formation of ethane from the dechlorination of 1,1,1-trichloroethane (1,1,1-TCA) and 1,1-dichloroethane (1,1-DCA) (Fennelly and Roberts, 1998). Reductive  $\beta$ -elimination reactions are observed for compounds containing vicinal Cl-atoms such as hexachloroethane (HCA), pentachloroethane (PCA), 1,1,1,2-tetrachloroethane (1,1,1,2-TeCA), 1,1,2,2-tetrachloroethane (1,1,2,2-TeCA), 1,1,2-trichloroethane (1,1,2-TCA), 1,2-DCA, PCE and TCE. The reductive  $\beta$ -elimination reaction involves the transfer of two electrons to the chlorinated compound and the elimination of two Cl-atoms from the molecule. For dechlorination of compounds containing vicinal Cl-atoms using ZVI,  $\beta$ -elimination is preferred over hydrogenolysis (Campbell et al., 1997; Hara et al., 2005; Roberts et al., 1996; Song and Carraway, 2005).

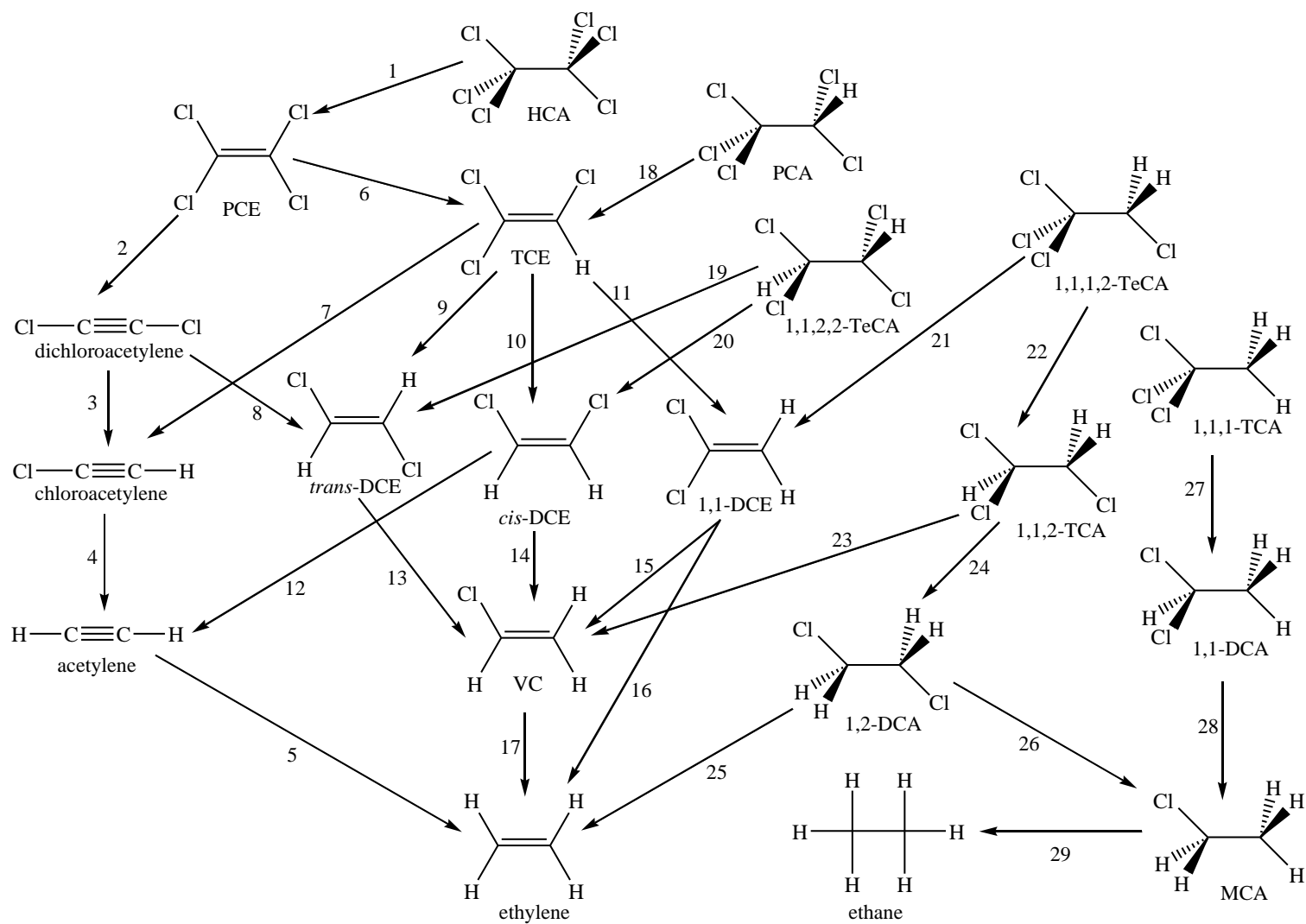


**Figure 4:** Dechlorination pathways for chlorinated ethanes and ethylenes.  $\beta$ -elimination (1, 2, 7, 12, 18, 19, 20, 21, 23, 25); hydrogenolysis (3, 4, 6, 9, 10, 11, 13, 14, 15, 17, 22, 24, 26, 27, 28, 29);  $\alpha$ -elimination (16) and hydrogenation (5, 8) (Arnold et al., 1999; Tobiszewski and Namiesnik, 2012).

In summary, the product patterns from reductive dechlorination are controlled by a complex interplay of adsorption/desorption processes with surface-mediated chemical reactions. The availability of reactive species such as electrons and hydrogen species (active  $H^*$  and  $H^+$ ) plays a key role. One could speculate that the dominance of reactive hydrogen species over electrons favors the formation of closed-shell compounds which can be released. This would result in the formation of only the partially dechlorinated byproducts.

### ***2.3 Dehalogenation of $CCl_3$ -R compounds using reagents and catalysts***

Saturated aliphatic compounds with the general structure  $CCl_3$ -R such as CF, CTC, trichlorofluoromethane ( $CFCl_3$ ), bromotrichloromethane ( $CBrCl_3$ ), and 1,1,1-TCA are among the most common water contaminants. The reduction of these compounds produces not only the total dehalogenated products e.g.  $CH_4$  and  $C_2H_6$  but also the chlorinated byproducts such as DCM and MCA. The reactivity and product patterns of  $CCl_3$ -R compounds in most cases depend on reaction pH and whether metallic reagents or catalysts are used. A comprehensive study has been done to elucidate the mechanism of the reductive dechlorination of CTC and TCE at several metal surfaces, among them bare ZVI, palladized ZVI, and nickel (Li and Farrell, 2000, 2001; Wang et al., 2004; Wang and Farrell, 2003). The reduction of  $CCl_4$  has clear parallels to that of  $CHCl_3$ , in particular the competition between stepwise and total dechlorination. Different electrochemical tools were applied to provide a deeper insight into elementary reaction steps, in particular concerning the roles of electron-transfer reactions and local concentration of active  $H^*$  (Li and Farrell, 2000, 2001; Wang et al., 2004; Wang and Farrell, 2003). We consider these studies among the most thorough studies on this topic. Therefore, the results and mechanistic conclusions are discussed in more detail.

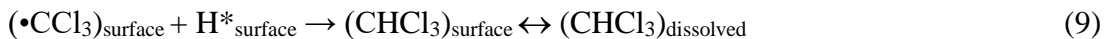
In the first study of this series, Li and Farrell described the dechlorination of CCl<sub>4</sub> in an iron-based, electrochemical flow-through reactor (Li and Farrell, 2000). At the cathodic potentials of -755 mV and -1200 mV versus standard hydrogen electrode (SHE), the primary reaction mechanism is a direct electron transfer. Methane which accounted for nearly 95 mol-% of CTC converted was by far the dominant product (only < 2 mol-% chlorinated byproducts detected). Pd doping of the ZVI surface (1 mg Pd per m<sup>2</sup> Fe surface) increased the dechlorination rates only by a factor of about 3. This points to a minor role of active H\* because Pd is known as a very potent hydrogen activator. The authors discuss a sequence of possible reaction steps 4 to 8:



The high yield of methane is attributed to the rapid hydrogenation of CO (as shown in reaction 8). Surprisingly, the acceleration effect of Pd doping was found identical for CTC and TCE (factor of 3), although TCE is more affine to hydrogen species attack (due to its double bond). The pH value played a minor role only (increase in first-order rate constants by a factor of 2

between pH = 10 and 4). This was explained with the cathodic protection of the ZVI against corrosion under acidic conditions.

We would like in this study to accomplish the proposed reaction steps by the surface-mediated radical recombination as shown in reaction 9:

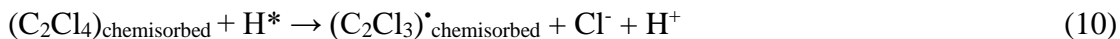


Different reaction conditions to generate active H\* at the surfaces of either Cu or Pd catalysts are investigated in this study and the product selectivity patterns during the dechlorination of CHCl<sub>3</sub> in water are presented.

In a subsequent study (Li and Farrell, 2001) with a rotating iron disk electrode (operated at the cathodic potentials in the range of -650 mV to -1200 mV versus SHE), the same authors confirmed their mechanistic conclusion that an outer-sphere electron-transfer step is rate-limiting for CTC reduction, whereas TCE reacts mainly with atomic hydrogen (from water). However, the main reaction byproduct from CTC was found to be CF (> 90 mol-% of the CTC converted and > 95 mol-% chloride yield normalized to one chloride from one CTC) rather than methane. The bulk phase reaction conditions (e.g. pH = 5.5 to 6.5) were pretty similar to the preceding study in Li and Farrell (2000). Surprisingly, the authors did not refer to their previous findings (methane instead of CF as the main CTC byproduct) nor did they explain the apparent difference. Again, TCE follows another rate-limiting step, which is the attack by surface-attached active H\*. The authors point to significantly different pre-conditions for an outer-sphere electron transfer and an active H\* attack on the adsorbed substrates: electron transfer is usually fast (only temporal approach of the substrate onto the surface). It requires therefore only physically adsorbed

substrates. Hydrogen attack proceeds through more complex transition states. Therefore, chemisorption of substrates is required. The different adsorption behaviors of saturated chlorinated alkanes (preferentially physisorption) and olefins (preferentially chemisorption, with di- $\sigma$ -bonds between carbons and surface) may be the key to understand their different reaction mechanisms.

A third study by Wang and Farrell (2003), investigated specifically the role of atomic hydrogen through electrochemical impedance spectroscopy and chronoamperometry. Unfortunately, these methods were applied only to the reduction of TCE and PCE, not to CTC or CF. Note that active hydrogen plays the role of a surface-mediated electron donor rather than a reactant which attacks directly the chemisorbed substrates (e.g. by addition to a double bond) as shown in reaction 10:



A significant contribution by active  $\text{H}^*$  to the conversion of TCE is indicated by its pH dependence. When the direct electron transfer dominates, the pH value is of minor importance. When CTC was dechlorinated on a nickel rotating disc electrode (instead of iron as investigated in (Li and Farrell, 2001), Wang et al. (2004) found methane ((95  $\pm$  4) mol-%) as the main product beside CF ((4.1  $\pm$  2.5) mol-%) and only traces of DCM. The rate-limiting step was again an outer-sphere transfer of the first electron to a physically adsorbed CTC molecule. The adsorption of CTC to electro-active sites of the Ni surface was important and fast enough (in comparison to the chemical conversion) to establish the adsorption-desorption equilibrium. Surprisingly, the overall conversion rate on Ni was a factor of 16 slower than on Fe, under similar reaction conditions. Therefore, Ni is not a good catalyst for the initial (and rate-determining) electron-transfer step but

may serve a catalytic role in the subsequent reaction steps. The authors did not specify these reactions.

Other than Ni, other hydrogenation-active metals such as Pd when applied as catalysts for dechlorination of CTC and CF produced CH<sub>4</sub> as the major product and only traces of chlorinated byproducts. For example, CH<sub>4</sub> accounted for more than 70 mol-% of CF transformed using Pd/Fe (Wang et al., 2009), Pd/Al<sub>2</sub>O<sub>3</sub> (Lowry and Reinhard, 1999), and PdAu/Al<sub>2</sub>O<sub>3</sub> catalysts (Velázquez et al., 2013). Similarly, gas-phase dechlorination of CTC and CF using metal catalysts in the presence of hydrogen was found to produce > 90 mol-% CH<sub>4</sub> (Ordóñez et al., 2000). In similar studies, the catalytic dechlorination of CTC using Pd/Fe/Al was also reported to produce about 38 mol-% CH<sub>4</sub> and 27 mol-% C<sub>2</sub>H<sub>6</sub> (Huang and Lien, 2010). Unfortunately, Huang and Lien (2010) did not explain the formation of a higher amount of C<sub>2</sub>H<sub>6</sub>. In summary, these studies show that similar dechlorination mechanisms are involved during the dechlorination of CTC and CF using the hydrogenation-active metals, Ni and Pd.

In similar studies, different reaction mechanisms were observed during the reduction of 1,1,1-TCA (an important water contaminant) using either metal reagents or catalysts. For example, hydrogenolysis was the main reaction mechanism during the dechlorination of 1,1,1-TCA by ZVI and the initial yield to 1,1-DCA was 67-69 mol-% (Fennelly and Roberts, 1998; Song and Carraway, 2005). The initial yield to 1,1-DCA as an intermediate during the dechlorination of 1,1,1-TCA was significantly decreased when ZVI was amended with metal catalysts (Cwiertny et al., 2006; Fennelly and Roberts, 1998). For example, the initial yields of 1,1-DCA were about 43 mol-% and 30 mol-% using Ni/Fe and Cu/Fe, respectively (Fennelly and Roberts, 1998). Metallic Fe serves as the source of active H\* for the catalytic dechlorination reaction at Ni and Cu surfaces.

The comparison between reagents (e.g. ZVI) and catalysts (e.g. Ni) demonstrates how the choice of the metal surface can control the reaction kinetics and product selectivity patterns. Pd and Ni are known as hydrogenation-active metals. Hence, the concentration of  $H^*_{\text{surface}}$  can be assumed higher on Pd and Ni than on ZVI. This  $H^*_{\text{surface}}$  may play two main roles: i) ‘hydrogenolysis’ of surface intermediates yielding stable chlorinated byproducts such as CF or DCM from CTC, and ii) ‘hydrogenation’ of the surface adsorbed intermediates yielding the fully dechlorinated product, e.g.  $CH_4$  from CTC and CF. The second role dominates at metal catalysts such as Pd and Ni surfaces. On the other hand, CTC conversion on the ZVI surface may lead to quite different product patterns ( $CH_4$  or CF from CTC), as demonstrated in (Li and Farrell, 2000) versus (Li and Farrell, 2001). The reason is still not clear.

In summary, the dechlorination of  $CCl_3-R$  compounds tends to produce fewer chlorinated byproducts where catalytically active metals are used in comparison to bare ZVI. Although catalysts e.g. Pd tend to produce fewer chlorinated byproducts during the dechlorination of CF and CTC, the accumulation of MCM and DCM as dead-end products is undesired. Ideally, a treatment system that can minimize the accumulation of the toxic chlorinated byproducts under ambient conditions will be a better alternative to ZVI and Pd. Hence in this work,  $Cu^0 + NaBH_4$  was investigated for the dechlorination of  $CCl_3-R$  compounds with a focus to determine the product yields, selectivity patterns and establish optimal reaction conditions that could minimize the accumulation of chlorinated byproducts.

#### *Chloroform as the target compound in this study*

As described earlier, the formation of chlorinated byproducts is inevitable during the dechlorination of chloroalkanes (especially  $CCl_3-R$  compounds) using metal reagents and metal catalysts. The questions of interest are i) what controls the product selectivity patterns? and ii) what

reaction conditions are optimal to prevent the accumulation of chlorinated byproducts? The solutions to these questions will be vital for the optimization of the treatment process for the subsequent reduction of chlorinated byproducts. In this study, CF was selected as the target compound to determine product yields and selectivity patterns during its dechlorination with  $\text{Cu}^0 + \text{NaBH}_4$  in water under different experimental conditions. Optimization of  $\text{Cu}^0 + \text{NaBH}_4$  to minimize DCM formation and accelerate its reduction during the dechlorination of CF was further investigated.

CF with a half-life of 3100 years under purely hydrolytic conditions at pH 7 is a heavy and volatile non-aqueous liquid whose environmental presence is highly undesired. It enters environmental compartments mainly due to its widespread application as a raw material or solvent in the manufacture of refrigerants, fluoropolymers, pesticides, fats, oils, rubber, alkaloids, resins, and cleaning agents (Harper, 2000; Mabey and Mill, 1978; Rosenthal, 1987). Besides, CF is a major disinfection byproduct arising from the reaction of chlorine or chlorine derivatives with organic matter in natural waters (Peters et al., 1980). Acute human exposure to CF is associated with systemic effects such as excitement, nausea, ataxia, dizziness, and drowsiness while chronic exposure results in hepatic damage (U.S. EPA, 2001). Being a potential human carcinogen, the recommended limit for CF in drinking water is 300  $\mu\text{g/L}$  (World Health Organization, 2005).

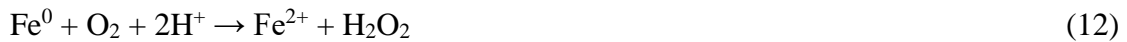
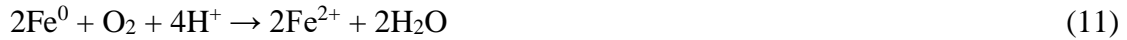
## ***2.4 Dehalogenation reactions using nZVI reagent***

### ***2.4.1 Synthesis and properties of nZVI***

Bare or amended ZVI can be used for the treatment of various water contaminants such as heavy metals, nitrate, nitrites, and HOCs (Liu et al., 2014; Ruangchainikom et al., 2006; Tibor and Krebsz, 2020; Zhang et al., 2017). In comparison to micro-scale ZVI, nanoscale zero-valent iron (nZVI) exhibits higher reactivity towards the reduction of HOCs due to its higher specific surface

area (Phenrat et al., 2009; Velimirovic et al., 2013). nZVI is also widely used for *in situ* groundwater treatment since its smaller dimensions ( $< 100$  nm) make it easier for injection into subsurface environments (Mueller et al., 2012; Tibor and Krebsz, 2020). Laboratory synthesis of nZVI is mostly done from  $\text{FeCl}_3 \cdot 6\text{H}_2\text{O}$  and stoichiometric excess  $\text{NaBH}_4$  at ambient conditions in an inert environment. Excess reductant ensures fast reduction reaction and uniform nanoparticle growth (Lin et al., 2010; Zhang, 2003). Commercial nZVI is synthesized by reduction of  $\text{Fe}_2\text{O}_3$  using hydrogen at  $> 450$  °C. Commercial nZVI includes reactive nanoscale iron particles (RNIP) from Toda Kogyo Corporation, Onoda, Japan, and nZVI (Nanofer) supplied by NANO IRON s.r.o (Rajhrad, Czech Republic) (Mueller et al., 2012).  $\text{NaBH}_4$  as a reductant is more expensive than hydrogen. Therefore, hydrogen as a reductant is more economical for the commercial synthesis of nZVI albeit the process requires high temperatures. Based on the reductant used,  $\text{nZVI}^{\text{BH}}$  and  $\text{nZVI}^{\text{H}}$  refer to nanoparticles synthesized using  $\text{NaBH}_4$  and  $\text{H}_2$ , respectively. The synthesis procedure determines the reactivity as well as crystallinity and magnetic properties of nZVI (Bae et al., 2018). Generally,  $\text{nZVI}^{\text{BH}}$  which is highly disordered (amorphous) exhibits higher reactivity for dehalogenation of HOCs than  $\text{nZVI}^{\text{H}}$  (Liu et al., 2005a; Liu et al., 2005b). Commercial  $\text{nZVI}^{\text{H}}$  has been used mostly for large-scale field treatment of various pollutants in European countries (Mueller et al., 2012).

As a result of van der Waals and magnetic forces, freshly prepared nZVI particles tend to quickly agglomerate in aqueous suspension. Reactivity of agglomerated particles decreases significantly due to a decrease in the available surface area. Freshly prepared nZVI particles readily undergo passivation in water or air (Bae et al., 2018). The passivation of ZVI due to oxidation may involve the transfer of either four or two electrons as shown in reactions 11 and 12, respectively (Joo et al., 2004).



Further oxidation of  $\text{Fe}^{2+}$  to  $\text{Fe}^{3+}$  occurs, depending on the availability of oxidants. The  $\text{Fe}^{3+}$  in the presence of water eventually precipitates to various hydroxides, e.g.  $\text{Fe}(\text{OH})_3$ ,  $\text{FeOOH}$ , and  $\text{Fe}_3\text{O}_4$  (Bae et al., 2018; Mackenzie et al., 1999; Noubactep, 2008). The oxide coating on the ZVI core provides a unique reactive surface for contaminant adsorption before their transformation via oxidative or reductive pathways. The transformation of contaminants continues even upon passivation of the ZVI-surface due to electrons conduction from the ZVI-core to the adsorbed contaminants. To minimize particle agglomeration and oxidation, nZVI is used under anaerobic conditions and in the presence of stabilizers (Lin et al., 2010). Common stabilizers include poly(acrylic acid) (PAA), poly(styrene sulfonate) (PSS), starch, carboxymethyl cellulose (CMC) and poly(vinylpyrrolidone) (PVP). The reactivity of various HOCs using nZVI depends on i) nZVI size, ii) presences or absence of stabilizers, iii) reaction pH iv) water matrix chemistry, and v) presence or absence of buffers.

Besides nanoparticle agglomeration, the other major drawbacks of nZVI for treatment of HOCs in groundwater include i) its poor wettability by organic solvents, ii) accelerated nZVI consumption at  $\text{pH} < 7$ , and iii) its low sorption affinity for HOCs. Therefore, controlling solution pH, oxygen and nitrate availability, particle sizes, and their stability are important parameters when designing a treatment system based on nZVI. Methods that can enhance the performance of nZVI include incorporation onto supports (Hildebrand et al., 2009a; Mackenzie et al., 2012), sulfidation to obtain sulfidated nZVI (S/nZVI) (Vogel et al., 2019), and surface modification with metal such

as Cu (Bransfield et al., 2006), Ni (Barnes et al., 2010) and Pd (Lien and Zhang, 2007; Wang et al., 2013). Amendment of nZVI with metals such as Pd significantly increases HOCs reactivity but comes at the expense of nZVI consumption due to enhanced galvanic corrosion (Cwiertny et al., 2007; Lin et al., 2004; Zhou et al., 2010). The use of Carbo-Iron<sup>®</sup> colloids (CIC) or sulfidated Carbo-Iron<sup>®</sup> colloids (S/CIC) provides a sorption active reagent that overcomes most of the challenges of bare nZVI. For these systems, 20-27 wt-% nZVI or S/nZVI are embedded onto activated carbon (AC) carrier (Bleyl et al., 2012; Vogel et al., 2019). Since most HOCs are usually present at very low concentrations in water, their adsorption onto the AC carrier brings them into close proximity to the embedded nZVI reagent. This generally increases the performance of the nZVI. In addition, the AC carrier minimizes nZVI agglomeration and facilitates the transport of reactive species (Kopinke et al., 2016). Sulfidation of nZVI slows the corrosion reaction which is important for increasing nZVI longevity. Therefore, CIC and S/CIC are viable alternatives to bare nZVI especially in the construction of permeable reactive barriers (PRBs) for the treatment of HOCs in groundwater.

#### 2.4.2 Reduction of HOCs using nZVI

Reductive dehalogenation using nZVI is a surface-mediated reaction and is facilitated by electron-transfer processes from the nZVI core. The consumption of nZVI in water and dehalogenation of HOCs can be described as shown in reaction 13:



Various R–X compounds (which are considered as electron sinks) with standard reduction potential greater than that of ZVI ( $E^\circ = -0.447$  V versus SHE) can be transformed. The product pattern depends on the chemical structure of the contaminant and the substitution of halogen atoms within the molecule. The formation of  $H_2$  due to  $Fe^0$  consumption is an undesired reaction that is dependent on  $H^+$  concentration. Hence it's accelerated at  $pH < 7$  (Liu and Lowry, 2006). For reduction of R–X, nZVI mainly acts as an electron transfer reagent and exhibits only low hydrogenation ability (Liu and Lowry, 2006). As described earlier, the performance of nZVI for reductive dehalogenation of HOCs varies depending on particle sizes, chemical composition, and reaction conditions. This makes it difficult sometimes to compare the performance of different nZVI particles used for the reduction of similar compounds. For various HOCs and different nZVI particles, a comparison on HOCs reactivity can be done based on nZVI surface area or mass of reagent supplied. In this case, the surface area-normalized rate constant ( $k_{SA}$  [ $L/(m^2 \cdot min)$ ]) or the specific nZVI activities ( $A_{nZVI}$  [ $L/(g \cdot min)$ ]) can be used to provide a solid comparison.

#### *2.4.3 HOC classes treatable by nZVI*

Several HOC classes have been tested for reductive dehalogenation by nZVI. Chlorinated compounds are the most studied contaminants. Other than nZVI properties and reaction conditions, reactivity and product distribution of HOCs depend on their chemical structure and the type of halogen atoms bound to the alkyl chain. Brominated HOCs undergo reduction much easier than their chlorinated counterparts due to the weaker C–Br bond (285 kJ/mol) than the C–Cl bond (337 kJ/mol). Chlorinated compound classes that have been studied using nZVI include mostly the olefins PCE and TCE. However, studies have also been reported for saturated aliphatic HOCs

which include chlorinated methanes and ethanes. The product yields and fate of halogenated intermediates depend mainly on the contaminant chemical structure and reaction conditions.

For chlorinated methanes, the reactivity decreases in the order: CTC > CF >> DCM (Song and Carraway, 2006). Similarly, the reactivity of chlorinated ethanes follows the order: HCA > PCA > 1,1,1,2-TeCA > 1,1,1-TCA > 1,1,2,2-TeCA > 1,1,2-TCA > 1,1-DCA (Song and Carraway, 2005). 1,2-DCA is stable against dechlorination using nZVI. Its transformation was only observed over a year when using nZVI in the presence of dithionite. By combining 5 g/L nZVI and dithionite (concentrations in the range of 22 to 44 mM), the rate constant ( $k_{\text{obs}}$ ) for dechlorination of 1,2-DCA ranges from  $3.8 \times 10^{-3}$  to  $7.8 \times 10^{-3}$  1/day which is not of practical significance for plume remediation (Garcia et al., 2016).

The order of reactivity of chlorinated methanes, ethanes, and ethylenes using nZVI provides knowledge about the rate-determining steps. This was achieved by establishing linear free energy relationships (LFERs) for various HOCs. LFERs take into account thermodynamics parameters, molecular characteristics, and HOCs reactivity. These include electronegativity of the leaving groups, bond dissociation energy (BDE), one-electron reduction potential ( $E_1$ ), two-electron reduction potential ( $E_2$ ), and energy of the lowest unoccupied molecular orbital ( $E_{\text{LUMO}}$ ). The use of BDE and  $E_1$  considers that the rate-determining step involves a single electron transfer (SET) process from nZVI to the surface adsorbed HOC molecules forming surface-bound alkyl radical species ( $\text{R-X} + \text{e}^- \rightarrow \text{R}\cdot + \text{X}^-$ ). Reactions via the  $E_2$  mechanism consider a two-electron transfer step as rate-determining to form hydrogenolysis products ( $\text{R-X} + \text{H}^+ + 2\text{e}^- \rightarrow \text{R-H} + \text{X}^-$ ). However, a two-electron transfer reaction being rate-determining is rare. In most cases, two fast successive one-electron transfer reactions are assumed to account for  $E_2$  reactions. Therefore,  $E_2$  is hardly used for correlation analysis since the first important step is always considered to involve

the direct transfer of one electron to the molecule (Jafvert and Lee Wolfe, 1987; Scherer et al., 1998; Totten and Roberts, 2001). Reaction steps involving  $E_2$  are observed mainly for compounds containing vicinal Cl-atoms. For chlorinated methanes and chlorinated ethanes, a strong correlation between reactivity was observed with  $E_1$  and  $E_{LUMO}$  (Scherer et al., 1998). Therefore, the rate-determining step was suggested to involve the transfer of a single electron from nZVI to the adsorbed contaminant. The electron transfer results in simultaneous cleavage of the weakest C–X bond. After the cleavage of the initial C–X bond, several reactions occur to produce the various products.

For chlorinated ethylenes, reactivity increases with an increase in halogenation degree and follows the order: VC (vinyl chloride) < DCEs (dichloroethylene isomers) < TCE < PCE. This order of reactivity shows that the rate-determining step does not involve SET processes, rather the formation of a di- $\delta$ -bond intermediate (Arnold and Roberts, 2000; Song and Carraway, 2008). Hence, at least two distinct rate-determining steps for HOCs are involved depending on the functional groups present next to the C–X bond. All these aforementioned correlations do not, however, consider explicitly the adsorption-desorption step of HOCs. Because this step and the corresponding sorption equilibria are inherent in any heterogeneous chemical reaction (e.g. electron transfer) doubts are allowed on the applied physical-chemical approaches.

The formation of halogenated intermediates from chlorinated ethanes varies depending on the degree of halogenation and presence of vicinal Cl-atoms. The higher chlorinated ethanes which contain vicinal Cl-atoms undergo dechlorination mainly via  $\beta$ -elimination to give predominantly the lower chlorinated olefins, PCE, TCE, and DCE isomers. These compounds do not remain but are further dechlorinated to produce ethylene ( $C_2H_4$ ),  $C_2H_6$ , and  $Cl^-$  (Song and Carraway, 2005). For the higher chlorinated olefins such as TCE and PCE, the dechlorination reaction results in the

formation of traces of the lower chlorinated byproducts such as VC (Arnold and Roberts, 2000; Li and Farrell, 2000; Orth and Gillham, 1996). Therefore, nZVI has been applied mainly for remediation of dense non-aqueous phase liquids (DNAPLs) containing TCE and PCE (Ahn et al., 2016; Mueller et al., 2012). Chlorinated ethanes with geminal chlorine atoms, i.e. 1,1,1-TCA and 1,1-DCA undergo dechlorination via hydrogenolysis which results in considerable accumulation of MCA as a dead-end byproduct (Song and Carraway, 2005). MCA accumulation makes the treatment process less efficient.

Even though the electron mediated cleavage of aromatic C–Cl bonds proceeds with much difficulty (Andrieux et al., 1986), there is information in the literature regarding the application of nZVI towards these compounds especially those with lower chlorination degree e.g. chlorobenzene (Poursaberi et al., 2012; Ševců et al., 2017; Shih et al., 2011; Wang and Zhang, 1997). However, these results are a matter of debate and could not be verified in our group. A possible explanation of the reported results could be due to the presence of catalytically active metal impurities during the synthesis of nZVI. Hydrogenation-active metals such as Ni, although present at trace levels are common impurities in commercial nZVI precursors. Therefore, nZVI in the absence of hydrogenation-active metals fails for cleavage of C–Cl bonds attached to aromatic structures (Balda and Kopinke, 2020; Kopinke et al., 2020).

## ***2.5 Reductive dechlorination using vitamin B12***

Vitamin B<sub>12</sub> or cyanocobalamin is a transition-metal complex occurring in all life forms. It consists of a Co<sup>+3</sup> metal center surrounded by a porphyrin-like structure of tetrapyrrole rings as shown in Figure 5.

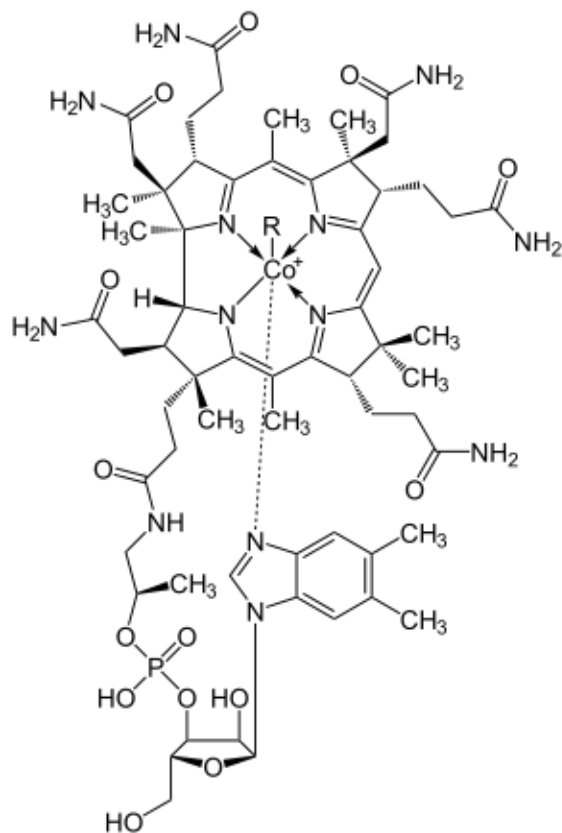


**Figure 5:** Chemical structure of vitamin B12 where R = CN (Silva et al., 2017).

Based on the oxidation state of the Co atom, the three forms of vitamin B12 are cyanocob(+3)alamin, cob(+2)alamin, and cob(+1)alamin. The reduced and super-reduced forms cob(+2)alamin and cob(+1)alamin are simply referred to as B<sub>12r</sub> and B<sub>12s</sub>, respectively. Common reductants used to generate B<sub>12r</sub> and B<sub>12s</sub> include titanium (III) citrate and NaBH<sub>4</sub>. Reductive dechlorination of compounds such as PCE and TCE only occurs in the presence of the reduced forms, B<sub>12r</sub> and B<sub>12s</sub>. The mechanism involves a two-electron transfer step involving Co<sup>+2</sup> or Co<sup>+1</sup> to the electrophilic carbon and formation of alkyl-cobalamin complexes (Co–R) (Burris et al., 1996; Schrauzer, 1976; Shey and van der Donk, 2000; Shimakoshi et al., 2005). These complexes then dissociate to regenerate vitamin B12 and formation of lower chlorinated byproducts and the fully dechlorinated hydrocarbons e.g. C<sub>2</sub>H<sub>4</sub>.

The combination of either Al or Cu with vitamin B12 has been found to significantly increase reaction rates for dechlorination of DCM (Huang et al., 2013, 2015). It is still unclear how the synergy between Cu and vitamin B12 in the presence of NaBH<sub>4</sub> works. The most important is that this synergy accelerates dechlorination reactions even for the compounds with lower chlorine substitution degrees such as DCM (Huang et al., 2013, 2015).

## ***2.6 Catalytic dechlorination***

### *2.6.1 Palladium catalysts*

Catalytic reduction of HOCs is another alternative that is superior to the electron-mediated reductive dehalogenation by nZVI reagent. In comparison to nZVI, which is consumed during the reduction reaction, catalysts are not depleted and can be reused. Furthermore, only small amounts of metal catalysts are necessary to treat huge volumes of contaminated waters. Among the noble metals, Rh is considered the most active but is the most susceptible to chloride poisoning (Benitez and Del Angel, 2000; Urbano and Marinas, 2001). Pd in comparison to Rh shows greater stability against chloride poisoning in water; hence it is widely used for HDC reactions (Chaplin et al., 2012; Lowry and Reinhard, 1999; Mackenzie et al., 2006). The combination of Pd with a reductant such as hydrogen gas or H-donors e.g. formic acid is necessary for the HDC reaction. Pd as a catalyst can adsorb and dissociate molecular hydrogen forming adsorbed surface hydrogen (Conrad et al., 1974; Coq et al., 1986; Teschner et al., 2010). The HDC reaction mechanism using Pd in the presence of H<sub>2</sub> involves the cleavage of the C–Cl bond and formation of C–H bonds as described by the reaction 14:



The dechlorination reaction occurs at the Pd surface between the chemisorbed H-atoms (i.e. active H\*) and the chlorinated compound. HDC using Pd occurs at a high rate and therefore offers the possibility of treating large amounts or flows of contaminated water within a short period. The HDC reaction can be carried out in the liquid phase using either suspended colloidal Pd nanoparticles or supported Pd catalysts. Pd is a precious and expensive metal. Hence only catalytic amounts are used by incorporation onto supports such as  $\gamma$ -Al<sub>2</sub>O<sub>3</sub> (Mackenzie et al., 2006), magnetite (Fe<sub>3</sub>O<sub>4</sub>) (Hildebrand et al., 2009b), and polymers (Fritsch et al., 2003; Munoz et al., 2017). Supported catalysts, e.g. Pd/ $\gamma$ -Al<sub>2</sub>O<sub>3</sub> offer the benefits such as higher dispersion, ease of handling, and the possibility to reuse and regenerate. Pd in comparison to nZVI can be used to dechlorinate various chlorinated organic contaminants and over a wide range of reaction pH (2-9) (Chaplin et al., 2012). However, the HDC reaction releases HCl which contributes to the deactivation of the catalyst (Aramendía et al., 2002; Aramendía et al., 2001; Coq et al., 1986). Hence the addition of a base, e.g. NaOH to neutralize HCl is sometimes necessary (Aramendía et al., 2002).

Under similar reaction conditions, specific Pd activities towards the reduction of HOCs are influenced by the nature of halogen atoms present, the number of geminal chlorine atoms, and the presence of  $\pi$ -electrons (Chaplin et al., 2012; Lowry and Reinhard, 1999; Mackenzie et al., 2006). Reactivity of chlorinated methanes and ethanes using Pd catalysts depends on the strength of the weakest C–Cl bond in the molecules. Hence cleavage of the weakest C–Cl bond is considered rate-determining and may involve homolytic dissociation of the C–Cl bond (Mackenzie et al., 2006; Rioux et al., 2000; Zhang et al., 2015; Zhou et al., 1999). The specific Pd activities for dechlorination of chlorinated methanes and ethanes decrease with a decrease in chlorination degree. The order of reactivity is CTC > CF >> DCM (Lowry and Reinhard, 1999; Mackenzie et

al., 2006) and  $1,1,1,2\text{-TeCA} > 1,1,1\text{-TeCA} > 1,1,2,2\text{-TeCA} \gg 1,2\text{-DCA}$  for chlorinated methanes and ethanes, respectively (Mackenzie et al., 2006). Under ambient conditions, dechlorination of compounds with lower chlorination degrees such as DCM, 1,1-DCA, and 1,2-DCA is more difficult using Pd (Lowry and Reinhard, 1999; Mackenzie et al., 2006). Other than HOCs reactivity, the amount and fate of chlorinated intermediates should also be considered to evaluate the efficiency of a treatment system. Dechlorination of higher chlorinated methanes and ethanes produces about 5-20 mol-% of chlorinated byproducts which remain more-or-less as dead-end byproducts (Mackenzie et al., 2006; Velázquez et al., 2013; Wang et al., 2009). These compounds such as DCM are toxic and their accumulation in the reactor as dead-end byproducts is a significant drawback where efficiency of the treatment system is considered.

Compared to chlorinated methanes and ethanes, chlorinated ethylenes are smoothly dechlorinated using Pd. Specific Pd activities are higher for the chlorinated ethylenes than those of chlorinated methanes and ethanes (Lowry and Reinhard, 1999; Mackenzie et al., 2006). Based on the specific Pd activity  $A_{\text{Pd}}$ , the order of reactivity of chlorinated ethylenes is  $\text{VC} > \text{DCE isomers} > \text{TCE} > \text{PCE}$ . This order of reactivity is opposite to that observed for chlorinated methanes and ethanes. Hence the reactivity of chlorinated ethylenes does not correlate with BDE due to a different rate-determining step. The higher reactivity of olefinic HOCs was considered to be due to their strong interaction with Pd surfaces via di- $\delta$ -bond intermediates followed by the addition of H-atoms to the double bond. Therefore, the rate-determining step for chlorinated ethylenes is the transfer of H-atoms to the double bond followed by the cleavage of the C-Cl bond (Mackenzie et al., 2006; Yuan and Keane, 2004). The hydrogenation of the double bond occurs later after the dechlorination step and produces ethane as the only product. Using Pd/ $\gamma\text{-Al}_2\text{O}_3$ , Mackenzie et al. (2006) showed that the specific Pd activity for the dechlorination of

VC ( $A_{Pd,VC} = 1180 \text{ L}/(\text{g}\cdot\text{min})$ ). In contrast to nZVI, lower chlorinated byproducts such as VC do not accumulate during the treatment of chlorinated ethylenes by Pd catalysts. Specific Pd activities for HDC of chlorinated benzenes decrease with an increase in chlorination degree and also differ depending on the chlorine-substitution pattern within the aromatic structures (Wiltschka et al., 2020; Zhu and Lim, 2007). The dechlorinated aromatic byproducts are followed by slow hydrogenation reactions to produce cycloalkanes, e.g. cyclohexane from the hydrogenation of benzene.

Despite the broad spectrum of compounds that can be dechlorinated, the field application of Pd is limited due to its susceptibility to deactivation by sulfite and sulfide. Sulfide when present even at small concentration results in deactivation of Pd (Angeles-Wedler et al., 2009). The formation of  $\text{H}_2\text{S}$  under anaerobic conditions in the presence of hydrogen can be facilitated by sulfate-reducing bacteria leading to Pd deactivation (Lowry and Reinhard, 1999). Hence protection of Pd against deactivation by sulfite and sulfide is important. This can be accomplished by pre-treatment of the contaminated water to remove the deactivating substances (Angeles-Wedler et al., 2008), using oxidants to regenerate fouled catalysts (Angeles-Wedler et al., 2009; Chaplin et al., 2007; Lowry and Reinhard, 2000), and embedding in non-porous, hydrophobic polymer coatings (Comandella et al., 2016; Fritsch et al., 2003; Kopinke et al., 2010; Navon et al., 2012). Protected Pd catalysts may be applied for the treatment of various HOCs in real water and wastewater effluents. However, the utilization of protected Pd catalysts will increase the cost of the catalyst which will subsequently increase the treatment costs. Hence metal cost, metal stability in water, and the yields and fate of chlorinated intermediates are equally important for consideration during decision making. Protected Pd can be of benefit for the cleavage of C–Cl bonds bound to aromatic compounds which are stable in the presence of bare nZVI.

### 2.6.2 Copper catalysts

In comparison to Pd, Cu is much less reactive in the activation of molecular hydrogen. Therefore, the combination of Cu with a more reactive reductant such as borohydride is essential for the dechlorination reactions. HDC reactions using  $\text{Cu}^0 + \text{NaBH}_4$  may be accomplished due to hydride species or chemisorbed H-atoms at the catalyst surfaces. The utilization of Cu catalysts in the presence of  $\text{NaBH}_4$  as reductant has so far been applied to dechlorinate DCM and 1,2-DCA (El-Sharnouby, 2016; Huang et al., 2012; Huang et al., 2011) and chlorinated aromatic compounds (Raut et al., 2016). 1,2-DCA and DCM are among the most common water contaminants which are rather inert in the presence of nZVI and Pd under ambient conditions. It has been shown that at temperatures  $> 350\text{ }^\circ\text{C}$ , DCM and 1,2-DCA can as well undergo dechlorination using Pd catalysts and hydrogen gas (Kopinke et al., 2003). However, stripping of these contaminants into the gas phase followed by dechlorination over solid Pd catalyst may be costly and therefore undesired. 1,2-DCA has also been shown to undergo dechlorination in water under ambient conditions using  $\text{Pd}^0 + \text{NaBH}_4$  (El-Sharnouby et al., 2018). A higher Pd dose (1-5 g/L) was used which is unsuitable for scale-up to field application if the metal cost is considered. The present market price for copper is about USD 0.009/g Cu (Copper Prices, 2021). Comparison of Pd and Cu prices shows that Pd (present cost USD 79/g Pd) cost more than Cu by a factor of about 8500. Therefore, Cu catalysts which are cheaper than Pd are attractive for application as catalysts in the treatment of HOCs. As a remediation system, the performance of  $\text{Cu}^0 + \text{NaBH}_4$  towards the treatment of saturated aliphatic HOCs, olefinic and aromatic HOCs containing F, Cl and Br need to be evaluated. Upon establishing the performance of  $\text{Cu}^0 + \text{NaBH}_4$ , it is also necessary to provide information regarding the application potential of Cu-, Pd- and nZVI-based systems for the treatment of various HOC classes frequently encountered in water.

The synthesis of Cu NPs can be done using bottom-up approaches which include chemical reduction, sonochemical reduction, micro-emulsion techniques, electrochemical reduction, hydrothermal or sol-gel synthesis, polyol, and microwave irradiation (Camacho-Flores et al., 2015; Gawande et al., 2016). Among these techniques, chemical reduction where a copper salt, oxide, or hydroxide is reduced with  $\text{BH}_4^-$ , hydrazine, starch, ascorbic acid, or cetyltrimethylammonium bromide (CTAB) can be used. When using hydrazine, ascorbic acid, and CTAB, the synthesis of Cu NPs requires refluxing at 60-85 °C for 30-120 min (Biçer and Şişman, 2010; Khan et al., 2016). Under ambient conditions the synthesis of Cu NPs by reduction with  $\text{NaBH}_4$  is the most common one due to its simplicity in operation and tendency to give nanoparticles with uniform sizes, narrow size distribution range, and uniform surface morphology (Huang et al., 2012; Huang et al., 2011). The procedure involves mixing an aqueous Cu salt solution with  $\text{NaBH}_4$ . The reaction is pH sensitive influenced by the stability of  $\text{NaBH}_4$ . At  $\text{pH} < 7$ , the rate of  $\text{NaBH}_4$  decomposition to hydrogen is fast with half-life  $< 4\text{s}$  (Kojima et al., 2002; Schlesinger et al., 1953; Wade, 1983). Controlled decomposition of  $\text{NaBH}_4$  occurs at  $\text{pH} \geq 10$  leading to uniform Cu NPs growth and development. Uniform nanoparticles are obtained by utilizing excess reductants where  $\text{Cu}^{2+}$  and  $\text{NaBH}_4$  in the molar ratio of 1:8 are essential. Lower molar ratios between  $\text{Cu}^{2+}$  and  $\text{NaBH}_4$  slow the reduction reaction producing non-uniform nanoparticles (Huang et al., 2012; Huang et al., 2011). Similar to the other nanoparticles such as Pd and nZVI, freshly prepared Cu NPs tend to oxidize when exposed to air (Huang et al., 2012). They also tend to agglomerate resulting in their sedimentation. Surface oxidation and particle agglomeration can be minimized through the addition of suitable stabilizers such as PVP, PAA, CMC, and other protective polymers.

## 2.7 Specific activities and performance of reagents and catalysts

The reductive dehalogenation of various HOCs at the surfaces of nZVI reagents and metal catalysts (e.g. Pd) in most cases can be described by pseudo-first-order kinetics as given in equation 15:

$$\frac{dc_i}{dt} = -k_{\text{obs}} \cdot c_i \quad (15)$$

where  $c_i$  refers to the concentration of HOCs (mg/L) and  $k_{\text{obs}}$  is the pseudo-first-order rate constant (1/min). For HOCs transformation using reagents and catalysts immobilized onto sorption active supports, there is usually a competition between contaminant transformation and adsorption. Since most HOCs are converted into less adsorbing gaseous products and halide formation, reaction rates can as well be determined from these products. Under conditions where the reaction rate is determined from the formation of products,  $k_{\text{obs}}$  can be approximately calculated using equation 16.

$$\ln\left(1 - \frac{c_{i,\text{product}}}{c_{\text{product,max}}}\right) = -k_{\text{obs}} \cdot t \quad (16)$$

where  $c_{i,\text{product}}$  is the concentration of product during dehalogenation reaction (mg/L),  $c_{\text{product,max}}$  represents the maximum concentration of product (mg/L) while  $t$  represents the reaction time (min). For comparison of reactivities of various HOCs,  $k_{\text{obs}}$  can be used for reaction conditions where identical metal dosing (metal concentrations and particle sizes) are used. Since in most cases these conditions may vary, normalization of  $k_{\text{obs}}$  values to metal surface areas is necessary. The

relationship between  $k_{\text{obs}}$  and the surface area-normalized rate constant for heterogeneous systems ( $k_{\text{SA}}$  in  $[\text{L}/(\text{m}^2 \cdot \text{min})]$ ) is given in equation 17:

$$k_{\text{SA}} = \frac{k_{\text{obs}}}{c_{\text{m}} \cdot a_{\text{s}}} \quad (17)$$

where  $c_{\text{m}}$  is the metal concentration (g/L) and  $a_{\text{s}}$  is the metal-specific surface area ( $\text{m}^2/\text{g}$ ). Equation 17 gives a direct relationship between  $k_{\text{SA}}$  and the two important parameters  $c_{\text{m}}$  and  $a_{\text{s}}$ .  $k_{\text{SA}}$  can be used for comparison purposes especially where the nanoparticles being studied vary in size. Generally,  $a_{\text{s}}$  increase with a decrease in nanoparticle sizes. For metal nanoparticles of similar mean particle sizes synthesized under identical conditions and in the absence of dispersity data (from CO chemisorption measurements), the specific metal activity ( $A_{\text{m}}$ ) calculated according to equation 18 can be used to provide a solid comparison.

$$A_{\text{m}} = \frac{V_{\text{w}}}{m \cdot \tau_{1/2}} = \frac{1}{c_{\text{m}} \cdot \tau_{1/2}} = \frac{\ln(c_{\text{t1}}/c_{\text{t2}})}{\ln 2 \cdot c_{\text{m}} (t_2 - t_1)} \quad [\text{L}/(\text{g} \cdot \text{min})] \quad (18)$$

where  $V_{\text{w}}$  is the volume of contaminated water (L),  $m$  is the metal mass (g),  $\tau_{1/2}$  is the HOCs half-life (min) obtained from the pseudo-first-order kinetics profile and  $c_{\text{m}}$  is the metal concentration (g/L). The variables  $c_{\text{t1}}$  and  $c_{\text{t2}}$  represent contaminant concentrations at two arbitrary sampling times  $t_1$  and  $t_2$ , respectively. The value of  $A_{\text{m}}$  can also be calculated from  $k_{\text{obs}}$  based on equation 19:

$$A_{\text{m}} = \frac{k_{\text{obs}}}{\ln 2 \cdot c_{\text{m}}} \quad (19)$$

The validity of equations 18 and 19 is limited to reaction conditions where mass transfer limitations are nonsignificant. For HOCs that undergo low dehalogenation rates and therefore a low degree of conversion, specific metal activities are preferably calculated from rates of product formation as described in equation 16. The advantages of using specific metal activities are that HOCs reactivity for systems with different degrees of catalyst dispersion preferably under similar experimental conditions can be determined when comparing materials of similar particle sizes. The specific metal activity  $A_m$  is also a measure of the amount of metal required to treat a given volume of contaminated water over a given period which is an important criterion of a treatment system in terms of technical and economical points of view. The value of  $A_m$  is also a reflection of the intrinsic dehalogenation ability of the metal and is independent of the initial HOCs concentration. In general, both the specific metal activities  $A_m$  and the surface area-normalized rate constants  $k_{SA}$  for various HOCs are valuable decision tools required in the design of a field-scale treatment system using metal reagents and catalysts.

### 3 Research Methodology

#### 3.1. Chemicals, reagents, and materials

##### 3.1.1 Chemicals, reagents, and gases

Analytical grade chemicals, reagents, and gases were obtained from different suppliers and used without further purification. The specifications for chemicals and reagents are presented in Table 1 while specifications for gases are presented in Table 2.

**Table 1:** Specifications for chemicals and reagents and suppliers

Chemical or reagent	Purity (%) or concentration	Supplier
$\text{Cu}(\text{C}_2\text{H}_3\text{O}_2)_2 \cdot \text{H}_2\text{O}$	99	Merck, Germany
$\text{Pd}(\text{C}_2\text{H}_3\text{O}_2)_2$	97	
$\text{CuSO}_4 \cdot 5\text{H}_2\text{O}$	99	
$\text{Na}_2\text{SO}_4$	99	
$\text{Na}_2\text{SO}_3$	99	
$\text{NaHCO}_3$	99.7	
$\text{NaNO}_3$	99.5	
$\text{NaNO}_2$	99	
$\text{MgSO}_4 \cdot 7\text{H}_2\text{O}$	98	
$\text{CaCl}_2 \cdot 2\text{H}_2\text{O}$	99	
$\text{FeSO}_4 \cdot 7\text{H}_2\text{O}$	99	
$\text{NaOH}$	99	
$\text{KOH}$	99.95	
$\text{NaBH}_4$	98	
$\text{KCl}$	99	
Methyl tert-butyl ether (MTBE)	99.8	
Methanol (MeOH)	99.95	
CTC, $\text{CCl}_4$	99.5	

CF, CHCl <sub>3</sub>	99.8	Sigma-Aldrich, Germany
DCM, CH <sub>2</sub> Cl <sub>2</sub>	99.8	
HCA, CCl <sub>3</sub> -CCl <sub>3</sub>	99	
MCM, CH <sub>3</sub> Cl	(200 mg/L in MeOH)	
1,2-DCA, CH <sub>2</sub> Cl-CH <sub>2</sub> Cl	99.8	
MCA, CH <sub>2</sub> Cl-CH <sub>3</sub>	(1000 mg/L MeOH)	
1,1,1-TCA, CCl <sub>3</sub> -CH <sub>3</sub>	97	
1,1,1,2-TeCA, CCl <sub>3</sub> -CH <sub>2</sub> Cl	99	
1,1,2,2-TeCA, CHCl <sub>2</sub> -CHCl <sub>2</sub>	97	
VC, CHCl=CH <sub>2</sub>	(200 mg/L MeOH)	
1,1-DCE, CCl <sub>2</sub> =CH <sub>2</sub>	99	
<i>trans</i> -dichloroethylene ( <i>trans</i> -DCE)	98	
<i>cis</i> -dichloroethylene ( <i>cis</i> -DCE)	97	
TCE, CCl <sub>2</sub> =CHCl	99.5	
PCE, CCl <sub>2</sub> =CCl <sub>2</sub>	99	
1,2-dichloropropane (1,2-DCP), CH <sub>2</sub> Cl-CHCl-CH <sub>3</sub>	99	
1,2,3-trichloropropane (1,2,3-TCP), CH <sub>2</sub> Cl-CHCl-CH <sub>2</sub> Cl	99	
1,2-dichlorobutane (1,2-DCB), CH <sub>2</sub> Cl-CHCl-CH <sub>2</sub> -CH <sub>3</sub>	98	
Dibromomethane (DBM), CH <sub>2</sub> Br <sub>2</sub>	99	
Bromoform (BF), CHBr <sub>3</sub>	99	
Vinyl bromide (VB), CHBr=CH <sub>2</sub>	98	
1,1,2-trichloro-1,2,2-trifluoroethane (CFC-113), CCl <sub>2</sub> F-CClF <sub>2</sub>	99.8	
Trichlorofluoromethane (CFC-11), CFCl <sub>3</sub>	99.5	
Chlorobenzene (CB)	99.5	

Bromobenzene (BB)	99.5	
CMC (molecular weight 2000)	- <sup>a</sup>	
NaF	99	
Na <sub>2</sub> CO <sub>3</sub>	99.5	
NH <sub>3</sub> OH (28 % NH <sub>3</sub> in H <sub>2</sub> O)	99.9	
HNO <sub>3</sub>	65	
H <sub>2</sub> SO <sub>4</sub>	99.9	
HCl	37	
CaCO <sub>3</sub>	99	
Monobromomethane (MBM), CH <sub>3</sub> Br	(100 mg/L MeOH)	Dr. Ehrenstorfer, Germany
1,1,2-TCA, CHCl <sub>2</sub> -CH <sub>2</sub> Cl	98	J & K Scientific, Belgium
1,1-DCA, CHCl <sub>2</sub> -CH <sub>3</sub>	99	Supelco-Germany
KBr	99	Fluka Analytics, Germany
NaCl	99.5	
Bromotrichloromethane, CBrCl <sub>3</sub>	98	
Ethanol	99.5	CHEMSOLUTE <sup>®</sup> , Germany
Na <sub>2</sub> S·H <sub>2</sub> O	60	Carl-Roth, Germany
MnSO <sub>4</sub> ·H <sub>2</sub> O	99	Alfa Aesar, Germany
Suwannee River Humic Acid (SRHA) reference number 2R101N	- <sup>a</sup>	International Humic Substances Society (IHSS)

<sup>a</sup> No information provided.

**Table 2:** Specifications for gases and suppliers

Gaseous substance	Purity (%)	Supplier
CH <sub>4</sub>	99.9	SIAD S.p.A, Italy
C <sub>2</sub> H <sub>6</sub>	99	
C <sub>2</sub> H <sub>4</sub>	99.9	
Propane (C <sub>3</sub> H <sub>8</sub> )	99.5	Linde AG, Germany
H <sub>2</sub>	5.0 grade	
N <sub>2</sub>		
Ar		
He		

### 3.1.2 Materials

**Table 3:** List of materials purchased and their key specifications

Material	Manufacturer	Manufacturer's designation	Particle sizes	BET surface area (m <sup>2</sup> /g)
MFI 90 zeolite	Clariant, Germany	T-4480	5 μm <sup>a</sup>	420 <sup>b</sup>
MFI 24 zeolite	Tosoh Corporation, Japan	HSZ-822	5 μm <sup>a</sup>	350 <sup>b</sup>
Activated carbon	Hosokawa Alpine, Germany	SAS	$d_{50} = 0.8 \mu\text{m}^a$ , $d_{90} = 1.6 \mu\text{m}^a$	1100 <sup>b</sup>
Activated carbon felt (ACF)	Jacobi CARBONS, Sweden	Actitex FC 1501C, JSR-10273	- <sup>c</sup>	1600 <sup>b</sup>
Amberlite cation exchange resin	Aldrich, Germany	IRP-69	100-500 wet mesh size <sup>s</sup>	- <sup>c</sup>

<sup>a</sup> Particle size as provided by the manufacturer.

<sup>b</sup> Brunauer-Emmett-Teller (BET) surface area determined by N<sub>2</sub>-adsorption-desorption measurements.

<sup>c</sup> No information provided.

### *Laboratory supplied materials*

Carbo-Iron<sup>®</sup> and sulfidated Carbo-Iron colloids were received as laboratory samples and the details regarding their synthesis and properties are presented elsewhere (Bleyl et al., 2012; Vogel et al., 2019).

### *Synthesis of Cu NPs*

The procedure was modified from the one described elsewhere (Huang et al., 2011). Using a stock solution of  $\text{CuSO}_4 \cdot 5\text{H}_2\text{O}$  ( $c_{\text{Cu}^{2+},\text{stock}} = 60 \text{ mg/L}$ ), 60 mL dilute solutions in 120 mL glass vials were prepared with  $c_{\text{Cu}^{2+}} = 0.2$  to 10 mg/L in deionized water. For the preparation of 100 mg/L of  $\text{Cu}^{2+}$ , 24 mg  $\text{CuSO}_4 \cdot 5\text{H}_2\text{O}$  was dissolved in 60 mL deionized water. The pH was then adjusted to 10 using 1 M NaOH to form  $\text{Cu}(\text{OH})_2$  as an intermediate. After pH adjustment,  $\text{N}_2$  was purged into the solution for 20 min followed by the addition of an aqueous solution of  $\text{NaBH}_4$  ( $c_{0,\text{NaBH}_4} = 300 \text{ mg/L}$ ) to form the Cu NPs.  $\text{N}_2$  flow through the Cu NPs was maintained for another 20 min and the glass vial was sealed with butyl rubber septa. The Cu NPs were dispersed in an ultrasonic bath before use. A sample of the nanoparticles was taken from the suspension, diluted, and transferred to a glass slide where the particle size distribution was determined by Nano tracking analysis (NTA) coupled with NTA software.

### *Synthesis of bimetallic Ag/Cu particles*

Four different procedures were used to prepare bimetallic Ag/Cu particles. A stock solution containing 1000 mg/L  $\text{Ag}^+$  was prepared using  $\text{AgNO}_3$  in deionized water. Ag/Cu (co-red) particles were prepared by mixing 0.5 mg/L  $\text{Ag}^+$  (from the stock solution) and 1.5 mg/L  $\text{Cu}^{2+}$  (from the stock solution) in one batch reactor. The solution pH was adjusted to 10 using 1 M NaOH

followed by the addition of  $\text{NaBH}_4$  ( $c_{0,\text{NaBH}_4} = 300 \text{ mg/L}$ ). The mixture of nanoparticles was shaken for 120 min at 130 rpm and used in subsequent CF dechlorination experiments.

Ag/Cu (mix) nanoparticles were prepared as follows. From the stock solution, 0.5 mg/L  $\text{Ag}^+$  solutions at pH 10 were prepared in 30 mL deionized water purged with  $\text{N}_2$ . Ag nanoparticles were then synthesized by reduction of  $\text{Ag}^+$  with  $\text{NaBH}_4$  ( $c_{0,\text{NaBH}_4} = 150 \text{ mg/L}$ ). In another batch reactor, 1.5 mg/L  $\text{Cu}^{2+}$  solutions at pH 10 were prepared in 30 mL deionized water and the solution was purged with  $\text{N}_2$ . The formation of Cu NPs was carried out by reduction of  $\text{Cu}^{2+}$  with  $\text{NaBH}_4$  ( $c_{0,\text{NaBH}_4} = 150 \text{ mg/L}$ ). The Ag and Cu nanoparticles were then transferred into a 120 mL glass vial under  $\text{N}_2$  flow. The mixture of nanoparticles in the vial was placed onto an orbital shaker preset at 130 rpm for 120 min and used for dechlorination of CF.

Ag/Cu (sep) particles were prepared as follows. Cu NPs ( $c_{\text{Cu}} = 1.5 \text{ mg/L}$ ) were prepared by reduction using  $\text{NaBH}_4$  in an Ar-purged solution. By maintaining argon flow into the Cu NPs suspension, 6 M HCl was added dropwise to accelerate the decomposition of  $\text{NaBH}_4$ . When gas evolution ceased indicating that  $\text{NaBH}_4$  was decomposed, an Ar-purged  $\text{Ag}^+$  solution ( $c_{\text{Ag}^+} = 0.5 \text{ mg/L}$ ) was spiked into the solution containing the Cu NPs. The vial was placed onto an orbital shaker preset at 130 rpm for 120 min and used in subsequent CF dechlorination experiments.

Ag/Cu ( $\text{H}_2$ -red) was prepared by first mixing 500 mg  $\text{AgNO}_3$  and 1500 mg  $\text{Cu}(\text{NO}_3)_2$  in 20 mL deionized water. The water was removed by heating at 100 °C to obtain a solid mixture of Ag- and Cu-precipitates (mostly oxides). The solid mixture was transferred into a thermostat oven and heated at 500 °C for 30 min in the presence of 5 vol. %  $\text{H}_2$  in  $\text{N}_2$  mixture whose flow rate was maintained at 5 mL/min. After heating, the solid was let to cool for 60 min under 5 vol. %  $\text{H}_2$  in

N<sub>2</sub> gas flow maintained at 5 mL/min. The coarse particles were stored under argon gas for subsequent use.

#### *Synthesis of Pd nanoparticles (Pd NPs)*

The synthesis of Pd NPs was done using a similar method as described elsewhere (Hildebrand et al., 2009a). A stock solution containing 1000 mg/L Pd<sup>2+</sup> was prepared by first dissolving 220 mg Pd(C<sub>2</sub>H<sub>3</sub>O<sub>2</sub>)<sub>2</sub> in 5 mL tetrahydrofuran and dilution to 100 mL using deionized water. Using this stock solution, 0.5-500 mg/L Pd<sup>2+</sup> were prepared by adding appropriate amounts of the stock solution into 120 mL glass. The volume of the Pd<sup>2+</sup> solution was adjusted to 60 mL using deionized water and its pH was then adjusted to 10 using 1 M NaOH. The formation of Pd NPs through the reduction of Pd<sup>2+</sup> was done by purging the solution with H<sub>2</sub> for 60 min. The particles were then dispersed in an ultrasonic bath and used for subsequent experiments. The size of Pd NPs was determined by nanoparticle tracking analysis after dilution of the suspension.

#### *Synthesis of nZVI*

10 g FeSO<sub>4</sub>·7H<sub>2</sub>O was dissolved in 2 L deionized water in a three-necked round bottom flask and the solution purged with argon. 3 g NaBH<sub>4</sub> was first dissolved in 100 mL Ar-purged deionized water and then transferred to the solution to precipitate Fe<sup>0</sup> as shown in the reaction 20 (Feng and Lim, 2007):



The nZVI suspension was maintained under Ar flow and was agitated with KPG stirrer for 60 min. The nZVI particles were immobilized by placing a magnet below the flask and the solvent

drained. The immobilized nZVI particles were rinsed with Ar-purged deionized water, followed by ethanol, and then dried under Ar flow.

#### *Preparation of Cu-modified activated carbons (Cu/AC)*

10 g activated carbon powder was added to 15 mL deionized water and then evacuated to remove air. It was immediately impregnated with 15 mL of 0.1 M  $\text{CuSO}_4 \cdot 5\text{H}_2\text{O}$  in a 20 cm long tube and left for 120 min. The excess solution was sucked out. A vacuum was created by sucking the air out of the tube. Opening the tube was done to introduce air. The air pressure was to push the  $\text{Cu}^{2+}$  into the pores of the AC matrix. This procedure was repeated five times to get more  $\text{Cu}^{2+}$  into the pores of the AC matrix. After impregnation, excess solution was filtered and the sample dried at ambient conditions. An aqueous solution of  $\text{NaBH}_4$  ( $c_{0,\text{NaBH}_4} = 100 \text{ mg/L}$ ) was added and the mixture was left for 180 min. The Cu/AC material was further cleaned by Ar-purged deionized water and then dried at 120 °C to constant weight.

#### *Preparation of Cu-modified activated carbon felts (Cu/ACF)*

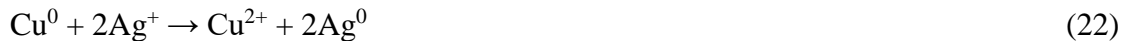
1.2 g ACF was cleaned with a 1:1 mixture of Millipore water and methanol and then rinsed with Millipore water. The cleaned ACF was impregnated with 200 mL of 0.1 M  $\text{CuSO}_4 \cdot 5\text{H}_2\text{O}$  and filtered to remove excess solution. The  $\text{Cu}^{2+}$  ions were pushed into the pores of ACF by creating a vacuum in the system and introducing air pressure as described earlier for Cu/AC. 300 mg/L  $\text{NaBH}_4$  was dissolved in 10 mL Millipore water and then introduced into the Cu/ACF and suspended for 15 h. The Cu/ACF was then cleaned with Ar-purged Millipore water and dried at 120 °C to constant weight. 0.5 wt-% copper content in the ACF material (method of analysis of Cu content presented later in this chapter) was obtained.

*Preparation of Cu- and Ag-modified Carbo-Iron<sup>®</sup> and sulfidated Carbo-Iron*

CIC and S/CIC colloids were used as received without further modification. The Fe<sup>0</sup> content in the laboratory samples for CIC and S/CIC were 26 and 24 wt-%, respectively. The synthesis of copper-modified CIC and S/CIC (Cu/CIC and Cu/S/CIC) was done in a 1 L two-necked flask maintained under Ar flow. 5 g CIC were added into a 1 L two-necked flask containing 150 mL Millipore water that was being purged with Ar. A 10 mL solution of CuSO<sub>4</sub>·5H<sub>2</sub>O (c<sub>Cu2+</sub> = 2200 mg/L) was purged with Ar and then added dropwise into the Ar-purged CIC suspension. This procedure was to deposit about 2 wt-% metallic Cu onto nZVI according to reaction 21 (Shubair et al., 2018):



The prepared Cu/CIC was stored under Ar for subsequent use. To produce Ag modified Cu/CIC, desired aqueous solution of Ag<sup>+</sup> (from the 1000 mg/L Ag<sup>+</sup> stock solution) was added into an Ar-purged suspension of Cu/CIC and shaken for 60 min. The deposition of metallic Ag onto metallic Cu proceeds as shown in the reaction 22 (Rosbero and Camacho, 2017):



The amount of Ag was varied from 0.02-1.0 wt-% calculated based on copper content within the Cu/CIC material. The deposition of 2 wt-% metallic Cu onto S/nZVI in S/CIC was done using the same procedure as described for Cu/CIC. Similarly, 1.0 wt-% Ag based on Cu was also deposited on Cu/S/CIC to form 1.0 wt-% Ag/Cu/S/CIC.

### *Preparation of Cu-modified zeolites*

The MFI 24 zeolite was used as received. MFI denotes the zeolite pentasil family and 24 is the module indicating the Si/Al ratio. The copper species were introduced into the zeolite by i) incipient wetness impregnation or ii) ion-exchange. The incipient wetness impregnation method was carried out at pH 4 where 10 g of the zeolite powder was added in 200 mL of 0.01 M  $\text{Cu}(\text{C}_2\text{H}_3\text{O}_2)_2 \cdot \text{H}_2\text{O}$  and equilibrated for 12 h at 130 rpm. Although any copper salt can be used, previous studies showed that using 0.01-0.05 M  $\text{Cu}(\text{C}_2\text{H}_3\text{O}_2)_2 \cdot \text{H}_2\text{O}$  led to higher Cu loading (Beznis et al., 2010). After equilibration, the zeolite was separated by filtration and then dried at 100 °C. The impregnation step with fresh 0.01 M  $\text{Cu}(\text{C}_2\text{H}_3\text{O}_2)_2 \cdot \text{H}_2\text{O}$  and drying steps were repeated two times. The dried Cu-modified zeolite was then suspended in aqueous  $\text{NaBH}_4$  at pH 10 for 24 h. The solid was cleaned several times with Ar-purged deionized water and then dried at 120 °C. The composite prepared by this method was labeled Cu/MFI 24 (w).

The ion-exchange procedure was carried out by mixing the 10 g of the zeolite powder with 1 M  $\text{NaNO}_3$  and equilibration for 6 h at 130 rpm. After each ion-exchange step, the zeolite was separated by filtration and then dried at 100 °C. This procedure was to exchange any  $\text{H}^+$  sites in the zeolite with  $\text{Na}^+$ . The ion-exchange procedure was repeated two times. The exchange of  $\text{Na}^+$  with  $\text{Cu}^{2+}$  was done using 0.01 M  $\text{Cu}(\text{C}_2\text{H}_3\text{O}_2)_2 \cdot \text{H}_2\text{O}$ . After Cu-exchange, the material was then suspended in aqueous  $\text{NaBH}_4$  at pH 10 for 24 h. The prepared Cu-modified zeolite was also cleaned several times with Ar-purged deionized water and dried at 120 °C to constant weight. The composite was labeled Cu/MFI 24 (i).

Since the Si/Al ratio for zeolites greatly influences its ability for contaminant adsorption and metal uptake, another MFI zeolite with higher Si/Al was selected. The zeolite MFI 90 was modified with Cu according to the two procedures as described for MFI 24 zeolite. Based on the Si/Al content and synthesis procedure, the Cu-modified MFI 90 zeolites were labeled as

Cu/MFI 90 (w) and Cu/MFI 90 (i). Excess or loosely bound Cu-species in the Cu-modified MFI 24 and MFI 90 zeolites were removed by suspending the samples in Ar-purged deionized water for 14-16 h followed by filtration and drying at 120 °C. The cleaning step was done several times until  $\text{Cu}^{2+}$  could not be detected in the effluent upon analysis by UV/VIS spectrophotometry. The filtrates were further evaluated for dechlorination of CF in the presence of  $\text{NaBH}_4$ . At the point where CF was stable for 600 min (i.e. no  $\text{CH}_4$  detected), the filtrate was considered to contain no Cu-species. The cleaned Cu-modified zeolite samples were then dried at 120 °C to constant weight and stored for subsequent experiments. The copper content in the prepared samples was determined by inductively coupled plasma mass spectrometry (ICP-MS).

#### *Preparation of Copper-doped cation-exchange resin (Cu/resin)*

10 g amberlite IRP-69 cation exchange resin was cleaned with Millipore water then soaked for 60 min in a 1:1 mixture of Millipore water and methanol. The resin was dried at 100 °C to constant weight and left to swell in methanol for 24 h. The swollen resin was further cleaned three times with 200 mL Millipore water and then impregnated with  $\text{Cu}^{2+}$  using 200 mL of 0.01 M  $\text{Cu}(\text{C}_2\text{H}_3\text{O}_2)_2 \cdot \text{H}_2\text{O}$  at pH 4. The Cu/resin was cleaned with Millipore water and suspended in a 200 mL solution containing 300 mg/L of  $\text{NaBH}_4$  at pH 10 for 24 h. It was further cleaned with Ar-purged Millipore water and dried at 120 °C to constant weight. 1.4 wt-% copper content in the resin was obtained as determined by ICP-MS (procedure for analysis of Cu presented later in this chapter).

#### *3.1.3 Preparation of synthetic freshwater*

Synthetic freshwater was prepared following the modified protocol for standard synthetic freshwater described in the United States Environmental Protection Report, EPA-821-R-02-012

(U.S. EPA, 2002). Synthetic freshwater with moderate hardness and alkalinity of 80-100 and 57-64 mg CaCO<sub>3</sub>/L, respectively was prepared as follows. Approximately 96, 60, and 4 mg/L of NaHCO<sub>3</sub>, MgSO<sub>4</sub>, and KCl were dissolved in 600 mL Millipore water. The solution was adjusted from 600 to 900 mL. 60 mg/L of CaSO<sub>4</sub>·2H<sub>2</sub>O was added into the 900 mL solution and mixed thoroughly. Air was purged into the solution for 24 h. The air-purged solution was adjusted from 900 to 1000 mL using Millipore water and its final pH was 7.2. Similarly, synthetic freshwater with hardness and alkalinity in the range of 280-320 and 225-245 mg CaCO<sub>3</sub>/L, respectively was prepared using the same procedure as described for moderately hard water. However, the amount of NaHCO<sub>3</sub>, MgSO<sub>4</sub>, KCl, and CaSO<sub>4</sub>·2H<sub>2</sub>O were adjusted to 384, 240, 16, and 240 mg/L, respectively. The resultant solution pH was 8.3.

#### *3.1.4 Preparation of SRHA solution*

SRHA was used as a surrogate for natural organic matter (NOM). SRHA was used as obtained without further purification. SRHA stock solution was prepared by dissolving 4 mg of the dry sample in 20 mL Millipore water and adjusting the solution pH to 10 using 1 M NaOH. The solution was stirred for 24 h and then stored at 4 °C for subsequent use.

### ***3.2 Electrodes characterization and CF dechlorination experiments***

#### *3.2.1 Characterization of Cu and Cu/ACF electrodes by cyclic voltammetry (CV)*

A two-necked electrochemical cell with a total volume of 500 mL was used as shown in the appendix Figure A1-1. The counter electrode (C.E.) and the working electrode (W.E.) were Pt plate and Cu mesh, respectively. Manufacturer details for Cu mesh, Pt plate, and Pt wires are presented in the appendix Table A1-2. Ag/AgCl ( $E^\circ = 0.197$  V versus SHE) was used as the

reference electrode (R.E.). The Pt- and Cu-electrodes were first cleaned by soaking in aqua regia (a mixture of 1 part concentrated  $\text{HNO}_3$  and 3 parts concentrated  $\text{HCl}$ ), then rinsed with Millipore water and dried at  $100\text{ }^\circ\text{C}$ . The Cu-, Pt- and Ag/AgCl-electrodes were connected to the EG & G potentiostat (OGS100, OrigaLys Electrochem SAS, France) using Pt wires. The distance between the C.E. and W.E. was maintained at 6 cm while the distance between the W.E. and R.E. was 0.5 cm. All three electrodes were dipped into the same electrolyte without any separation between them.

The characterization of the Cu electrode was done by CV and the profiles were determined separately in 0.1 M NaOH and 0.1 M  $\text{Na}_2\text{SO}_4$ . The electrolytes were not stirred to allow migration of electroactive species only by diffusion. Before the CV scan, the electrolytes were purged with Ar to remove dissolved oxygen. The CV profiles were obtained using an EG & G potentiostat interfaced to a personal computer. Charge transfer processes were then measured at a scan rate of 25 mV/s. ACF as a conductive material was modified with Cu as described earlier. The CV profiles for Cu/ACF were done using the same electrochemical setup as used for the Cu electrode under similar reaction conditions. Before CV analysis, the Cu/ACF was immersed into the electrolyte for 60 min and the solution purged with argon.

### *3.2.2 Electrochemical dechlorination of CF*

The same electrochemical setup as described in 3.2.1 was applied. 400 mL of 0.1 M  $\text{Na}_2\text{SO}_4$  were used as the electrolyte where the C.E., W.E., and R.E. were dipped into the electrolyte without any barrier between them. The electrolyte was purged with Ar for 30 min to remove dissolved oxygen. CF ( $c_{0,\text{CF}} = 5\text{ mg/L}$ ) as a methanolic solution was added to the electrolyte and the contents were mixed using a magnetic stirrer for 180 min. The potential was

applied and NaBH<sub>4</sub> ( $c_{0,\text{NaBH}_4} = 300 \text{ mg/L}$ ) was spiked to initiate the reaction. The applied potentials at the W.E. were set at -0.8 V and -1.0 V and maintained throughout the experiments. A similar setup was used where H<sub>2</sub> was purged into the electrochemical cell as a substitute for NaBH<sub>4</sub> and the potential was set to -0.5 and -0.8 V. Control experiments at -0.5 V and -0.8 V without the addition of NaBH<sub>4</sub> or H<sub>2</sub> were done under similar reaction conditions. Another experiment for dechlorination of CF was done without application of potential using the same Cu electrode and 300 mg/L of NaBH<sub>4</sub>. For comparison purposes, electrochemical dechlorination of CF using the same Cu electrode was carried out at a cathodic potential of -1.1 V and without NaBH<sub>4</sub>.

As a conductive material ACF modified with copper was also used as an electrode for dechlorination of CF. A methanolic solution of CF was spiked into the electrochemical reactor and the contents were mixed for 24 h to allow 30-40 % CF adsorption onto the Cu/ACF electrode. After 15 h, the potential was set at -0.8 V and NaBH<sub>4</sub> ( $c_{0,\text{NaBH}_4} = 300 \text{ mg/L}$ ) was added to initiate the reaction.

### *3.2.3 Dehalogenation of HOCs using Cu NPs*

Dehalogenation experiments for HOCs were carried out at an ambient temperature in 120 mL serum bottles sealed with poly(tetrafluoroethylene) (PTFE) lined butyl rubber septa and aluminum crimp caps. 60 mL aqueous solution and 60 mL of headspace volumes were used throughout the experiment. For dehalogenation of CH<sub>2</sub>Cl-CH<sub>3</sub>, CCl<sub>4</sub>, CFCl<sub>3</sub>, and CCl<sub>2</sub>F-CClF<sub>2</sub>, the aqueous suspensions and headspace volumes were adjusted to 100 and 20 mL, respectively. Cu NPs were prepared using NaBH<sub>4</sub> ( $c_{0,\text{NaBH}_4} = 300 \text{ mg/L}$ ) and then purged with N<sub>2</sub> to remove dissolved oxygen. The nanoparticles were dispersed by ultra-sonication. Suitable internal standards (CH<sub>4</sub>, C<sub>2</sub>H<sub>6</sub>, MTBE, and toluene) were added to the batch reactors. Methanol solutions

of HOCs were spiked into the reactors to give the desired initial concentrations and initiate the reaction. The batch reactors were placed onto an orbital shaker and shaken horizontally at 130 rpm. For volatile substances, the reaction progress was followed by headspace analysis. For the less volatile substances, liquid-phase extraction was used. The initial reaction conditions were maintained at pH = 10 using aqueous 1 M NaOH. The addition of buffers to reaction media was avoided to prevent interference with the catalyst surface. Control experiments were done using either Cu NPs + H<sub>2</sub> or NaBH<sub>4</sub> under similar conditions as that applied for Cu<sup>0</sup> + NaBH<sub>4</sub>.

#### *3.2.4 Dehalogenation of HOCs using Pd NPs*

120 mL batch reactors were used for the dehalogenation of HOCs using Pd NPs. Aqueous suspensions of Pd NPs of desired concentration from a stock solution were transferred into a 100 mL aqueous solution. The pH of the solution was adjusted to 10 using 1 M NaOH and then purged with N<sub>2</sub> for 20 min to remove dissolved oxygen. The Pd NPs were formed by the reduction of Pd<sup>2+</sup> with H<sub>2</sub>. Hydrogen was purged for 60 min and the batch reactors were placed onto an orbital shaker preset at 130 rpm for 24 h. Suitable internal standards (MTBE, CH<sub>4</sub>, C<sub>2</sub>H<sub>6</sub>, and toluene) were added and methanolic solutions of HOCs were spiked to initiate the reaction.

#### *3.2.5 Dehalogenation of HOCs using nZVI*

The dehalogenation reactions of HOCs were done in 250 mL glass vials. nZVI was added into Ar-purged 125 mL deionized water to give the desired concentration of nanoparticles,  $c_{nZVI} = 0.4\text{-}5$  g/L. CMC was added as a stabilizer for nZVI. The CMC-nZVI suspension was dispersed by ultrasonication and the HOC of interest was spiked as a methanolic solution into the reactor to obtain the desired concentration ( $c_{0,HOC} = 10\text{-}20$  mg/L) and initiate the reaction.

### *3.2.6 Dechlorination of CF using Cu-modified materials*

This procedure was used for Cu-modified AC, ACF, resin, and zeolites. All experiments were carried out in 120 mL glass vials. The appropriate mass of Cu-modified material was added into Ar-purged 60 mL deionized water and the solution pH was adjusted to 10 using 1 M NaOH. Mass of the Cu-modified material was adjusted so that approximately 40-50 % of CF was adsorbed. A methanolic CF solution was added to give the desired concentration  $c_{0,CF} = 10$  mg/L. 200  $\mu$ L of  $C_2H_6$  was added as internal standard and the reactor was placed onto an orbital shaker preset at 130 rpm for 120 min. A solution of  $NaBH_4$  ( $c_{0,NaBH_4} = 300$  mg/L) was spiked into the reactor to initiate the reaction. For dechlorination of CF using CIC, S/CIC, and their metal modified forms, the material was introduced into Ar-purged 60 mL deionized water.  $C_2H_6$  was added as internal standard and CF ( $c_{0,CF} = 10$  mg/L) as a methanolic solution was spiked to initiate the reaction.

### *3.2.7 Evaluation of Cu stability for dechlorination of CF*

The stability of Cu as a catalyst in the presence of co-solutes was done using CF as the probe compound. The specific Cu activities in the presence of the co-solutes were then compared to the baseline of Cu in deionized water. 60 mL of deionized water containing 1 mg/L of freshly prepared Cu NPs and 300 mg/L  $NaBH_4$  was degassed by purging with nitrogen for 20 min. Stock solutions for the various co-solutes (with each stock solution containing 100 mg/L of co-solute of interest) were prepared. The co-solute of interest e.g. NaF from the stock solution was spiked into the freshly prepared Cu NPs suspension to give the desired concentration. The mixture of co-solute and Cu NPs was purged with  $N_2$  for 20 min and then placed onto an orbital shaker preset at 130 rpm for 120 min. A methanolic solution of CF ( $c_{0,CF} = 10$  mg/L) was spiked into the reactor to initiate

the reaction. The CF dechlorination reaction was monitored to evaluate the performance of Cu as a catalyst in the presence of the common water co-solutes  $\text{Na}_2\text{SO}_4$ ,  $\text{Na}_2\text{SO}_3$ ,  $\text{NaHCO}_3$ ,  $\text{Na}_2\text{CO}_3$ ,  $\text{NaNO}_3$ ,  $\text{NaNO}_2$ ,  $\text{MgSO}_4$ ,  $\text{CaCl}_2$ ,  $\text{FeSO}_4$ ,  $\text{NaF}$ ,  $\text{NaCl}$ ,  $\text{KBr}$ ,  $\text{MnSO}_4$ ,  $\text{Na}_2\text{S}$ , and SRHA. The performance of Cu as a catalyst towards the dechlorination of CF was further evaluated by replacing deionized water with either synthetic freshwaters (prepared by a standard protocol described in 3.1.3) or laboratory-supplied tap water (characteristic details presented in the appendix Table A1-1).

### *3.2.8 Lifetime and regeneration of Cu-doped cation-exchange resin*

To determine the lifetime and reusability of Cu as a catalyst, the Cu/resin catalyst was selected and was repeatedly used for dechlorination of CF ( $c_{0,\text{CF}} = 10 \text{ mg/L}$ ) in 9 consecutive reaction cycles. After each reaction cycle which lasted 120 min and the conversion of CF was  $\geq 95 \%$ , the Cu/resin catalyst was removed from the reactor, rinsed with deionized water, and dried at  $120 \text{ }^\circ\text{C}$  to constant weight. To determine  $\text{Cu}^{2+}$  bleeding or dissolution from the resin during the CF dechlorination reaction and after each cleaning step, the aqueous samples were analyzed for  $\text{Cu}^{2+}$  by UV/VIS spectrophotometry. Also, the effluent was tested for dechlorination of CF by addition of borohydride ( $c_{0,\text{NaBH}_4} = 300 \text{ mg/L}$ ) and mixing at 130 rpm for 600 min. The dried Cu/resin was reused for dechlorination of CF ( $c_{0,\text{CF}} = 10 \text{ mg/L}$ ) after the addition of  $\text{NaBH}_4$ .

To evaluate the regeneration of the Cu/resin catalyst, the catalyst was added into batch reactors containing different concentrations of  $\text{Na}_2\text{S}$  (1 and 20 mg/L). Based on the concentration of  $\text{Na}_2\text{S}$  fed, the catalysts were labeled as Cu/resin (1 mg/L  $\text{Na}_2\text{S}$ ) and Cu/resin (20 mg/L  $\text{Na}_2\text{S}$ ). The suspensions were purged with  $\text{N}_2$  and then placed onto an orbital shaker preset at 130 rpm for 120 min. CF ( $c_{0,\text{CF}} = 10 \text{ mg/L}$ ) and the batch reactors containing the catalysts were equilibrated at

130 rpm for 120 min. NaBH<sub>4</sub> ( $c_{0,\text{NaBH}_4} = 300$  mg/L) was added to initiate the reaction. The reaction was terminated when CF conversion was  $\geq 95$  %. The sulfide-deactivated Cu/resin catalysts were isolated from the reactors, rinsed with deionized water, and dried at 120 °C to constant weight. The washed Cu/resin catalysts were then reused for the dechlorination of CF ( $c_{0,\text{CF}} = 10$  mg/L) as described earlier by the addition of fresh NaBH<sub>4</sub> ( $c_{0,\text{NaBH}_4} = 300$  mg/L). Based on the concentration of Na<sub>2</sub>S used, the regenerated catalysts after sulfide-deactivation were labeled as wCu/resin (1 mg/L Na<sub>2</sub>S) and wCu/resin (20 mg/L Na<sub>2</sub>S).

### ***3.3 Analytical techniques***

#### *3.3.1 Determination of surface area*

The surface areas of the Cu-modified materials were determined with a BELSORP MINI II (MicrotracBEL, Japan) via N<sub>2</sub>-adsorption-desorption measurements using a Micromeritics ASAP 2010 instrument. Before BET surface area measurement of the materials, the samples were pretreated at 100-300 °C under vacuum (< 5 Pa).

#### *3.3.2 Determination of Fe<sup>0</sup> content*

20-25 mg of nZVI were added into Ar-purged deionized water to obtain the metal suspensions. Anaerobic corrosion of nZVI was done in an Ar-purged system through the addition of 2 mL of concentrated HCl (6 M) in the glass vials. The addition of concentrated HCl led to the digestion of nZVI and generation of H<sub>2</sub> according to the redox reaction 23:



The amount of H<sub>2</sub> evolved was measured by gas chromatography (GC) coupled with a thermal conductivity detector (TCD). The amount of H<sub>2</sub> from nZVI digestion was analyzed by the sampling of the headspace using a 50 µL gas-tight syringe and injecting it into a GC (HP 6850) coupled with TCD. The GC was fitted with a porous layer open tubular HP PLOT column whose dimensions were 30 m × 0.32 mm × 12 µm. The temperatures for the injector port, detector, and oven were set at 50, 155, and 30 °C, respectively. An external calibration curve for H<sub>2</sub> was prepared and was used to measure the H<sub>2</sub>. The amount of H<sub>2</sub> measured was used to calculate the amount of Fe<sup>0</sup> in the prepared samples according to reaction 23. The Fe<sup>0</sup> content in the CIC and S/CIC samples was also determined using the same procedure as described for nZVI.

### 3.3.3 Analysis of Cu<sup>2+</sup> in prepared samples

#### *Analysis of Cu<sup>2+</sup> by UV/VIS-spectrophotometry*

The amounts of Cu<sup>2+</sup> in the AC and the ACF frameworks were evaluated by acid digestion of the samples at pH 1. About 2-3 g of the dried Cu/AC were mixed with 50 mL of 1 M HNO<sub>3</sub> and shaken for 180 min at 130 rpm. The samples were filtered through cellulose acetate membrane filters (0.45 µm pore size) to remove the solids. The pH of the filtrate was adjusted to 7 using 6 M NaOH. After pH adjustment the filtrate was then mixed with 1 mL of 6 M NH<sub>3</sub>OH to form tetraamine copper (II) complexes according to reaction 24 (Byrd and Ohrenberg, 2017):



The absorbance of the tetraamine copper (II) complex was measured using a UV/VIS spectrophotometer (photolab 6600) at the wavelength,  $\lambda_{\text{max}} = 600$  nm to determine the

Cu<sup>2+</sup> concentration. An external calibration curve was used to calculate the Cu<sup>2+</sup> amount in the samples. A 500 mg Cu/ACF strip was treated as described for Cu/AC to determine the amount of Cu<sup>2+</sup>.

*Analysis of Cu<sup>2+</sup> by ICP-MS*

The amount of Cu<sup>2+</sup> in zeolites and amberlite resin was determined by ICP coupled with MS (Thermo Fisher Scientific iCAP QS). The concentration of Cu<sup>2+</sup> was determined by ICP-MS in the normal mode of operation using external calibration curves against concentrated HNO<sub>3</sub>. Concentrated HNO<sub>3</sub> was used for digesting the samples while 2 % w/w HNO<sub>3</sub> was used as a background solution during analysis. HNO<sub>3</sub> was introduced into the sample during analysis to minimize background interference while <sup>103</sup>Rh was used as the internal standard. The operating parameters for the ICP-MS are presented in Table 4.

**Table 4:** ICP-MS parameters for the determination of Cu

<b>Parameter</b>	<b>Value</b>
Analyte monitored	<sup>63</sup> Cu
Nebulizer	PFA-ST MicroFlow
Spray chamber	Micro Mist quartz cyclonic
Nebulizer gas flow	0.95 L/min
Carrier gas	Ar
RF power	1550 W
RF frequency	35 MHz
Sample flow	0.34 mL/min
Collision gas flow	5 mL/min
Dwell time	5 ms
Measurement time	60 s

### 3.3.4 Measurement of HOCs and dehalogenation products

All experiments were performed either in duplicate or triplicate to give reproducible data. Analysis of HOCs was done by GC (GC2010, Shimadzu) coupled with MS (GCMS-QP2010, Shimadzu) detector. The GC was fitted with a DB1-MS capillary column (J & W, 60 m  $\times$  0.25 mm  $\times$  0.25  $\mu$ m). Temperature conditions for the injector port, oven, interface, and ion source were set at 180, 40, 200, and 250  $^{\circ}$ C, respectively. A 25  $\mu$ L gastight syringe was used for headspace sampling of aliquots for GC analysis where the split ratio was set to 5. The analysis of gaseous products such as CH<sub>4</sub> and C<sub>2</sub>H<sub>6</sub> was done by GC (GC2010 Plus, Shimadzu) equipped with a flame ionization detector (FID). The GC was fitted with a wide-bore column (GS-Q, 30 m  $\times$  0.53 mm  $\times$  1.0  $\mu$ m) whose temperature conditions were set at 200, 40, and 280  $^{\circ}$ C for the injector, oven, and ion source, respectively. A 25  $\mu$ L gastight glass syringe was used for headspace sampling for GC analysis and the split ratio was also set to 5.

The concentrations of the educts and products were determined by the external standard method using calibration curves. Since identical solution/headspace volume ratios between calibration and batch reaction systems were maintained throughout, concentrations determined from calibration curves account for vapor/water partitioning. The GC retention times from standard samples were used to identify dehalogenation products in the GC-FID and GC-MS. For systems that result in the production of H<sub>2</sub> which results in expansion of the headspace volume, MTBE, CH<sub>4</sub>, C<sub>2</sub>H<sub>6</sub>, and toluene were used as internal standards. Obtained data were corrected to the change in internal standard at each sampling point.

The reaction progress was monitored by headspace analysis of the educts and products. The reaction kinetics were followed from contaminant disappearance profile in experiments without an adsorbent present. For HOCs with lower conversion degrees and adsorption overlaid

reaction, the reaction kinetics were followed from the product formation profiles. The reason is that products are usually less prone to adsorption than educts. For the less volatile substances in adsorbent-free solutions, solvent extraction was chosen for following the reaction progress. The extraction solvent comprised 99 mL hexane and 1 mL toluene. For reactions carried out in the presence of adsorbent, residual chlorinated compounds were analyzed by liquid phase analysis. The extraction solvent for liquid phase analysis was constituted by mixing 2 mL benzene, 9 mL ethanol, and 89 mL toluene. Benzene was applied as internal standard. About 1 mL aqueous phase extracted from the batch reactor was mixed with 10  $\mu$ L of 6 M HCl to decompose  $\text{NaBH}_4$  and stop the dehalogenation reaction. The solution was then mixed with 1 mL of the extraction solvent and shaken for 60 min. The extraction solvent (organic phase) was separated from the aqueous phase and mixed with anhydrous  $\text{Na}_2\text{SO}_4$  to remove traces of water. The organic phase was then subjected to analysis by GCMS. For liquid phase analysis, the temperature conditions for the injector port, interface, and detector were set at 180, 200, and 250  $^\circ\text{C}$ , respectively. The oven temperature was maintained at 60  $^\circ\text{C}$  for 4 min then ramped up at the rate of 10  $^\circ\text{C}/\text{min}$  to 100  $^\circ\text{C}$  and maintained at this temperature for another 5 min. A 1  $\mu$ L gastight syringe was used for sampling of the organic phase for GC analysis where the split ratio was set to 50.

Raw data from replica experiments were processed to obtain the mean and standard deviation values. For kinetic analysis of experimental data with larger headspace volumes compared to the aqueous phase volumes, the  $k_{\text{obs}}$  values (equation 15) were processed to give corrected  $k_{\text{obs,corr}}$  which is given as shown in equations 25 and 26:

$$k_{\text{obs,corr}} = \frac{k_{\text{obs}}}{\text{HOC}_{\text{S}_w}} \quad (25)$$

$$HOCs_w = \frac{V_w}{V_w + (K_H \times V_h)} \quad (26)$$

where  $HOCs_w$  refers to the fraction of contaminant in water,  $K_H$  is the dimensionless Henry's law constant while  $V_w$  and  $V_h$  are the aqueous and headspace volumes (L), respectively. This correction takes into account that the gas phase fraction of the HOCs is not in direct contact with the catalyst particles and acts as a reservoir to the delayed reaction. The reactivities of the different HOCs using catalysts and reagents were done by calculating the specific metal activities as given in equations 18 and 19. Mass transfer limitations were assumed negligible at the high reactor shaking speed (130 rpm) and the small nanoparticle sizes. For nZVI,  $k_{obs}$  values for some HOCs were obtained from literature and further processed using equations 18 and 19 taking the initial nZVI mass supplied into account.

During the dehalogenation reaction, it is important to know the fraction of the contaminant transformed at a given time. The conversion of educt was calculated as shown in equation 27:

$$X_{HOC} = \left(1 - \frac{n_{HOC,t}}{n_{HOC,0}}\right) \times 100 \% \quad (27)$$

where  $X_{HOC}$  is the conversion of the HOC (%),  $n_{HOC,t}$  refers to moles of educt at a given time (mol) and  $n_{HOC,0}$  refers to the moles of educt fed into the batch reactor at time  $t = 0$  (mol). To determine the efficiency of the dehalogenation process, the product yields were calculated according to equation 28:

$$Y_{i,product} = \frac{n_{i,product}}{n_{HOC,0}} \times 100 (\%) \quad (28)$$

where  $Y_{i,\text{product}}$  is the yield of a given product  $i$  (mol-%),  $n_{i,\text{product}}$  refers to the moles of product  $i$  obtained at a given time (mol) and  $n_{\text{HOC},0}$  refers to the moles of educt fed into the reactor at time  $t = 0$  (mol).

For the dehalogenation of  $\text{CCl}_3\text{-R}$  compounds, the product selectivities were calculated using equation 29:

$$S_{i,\text{product}} = \frac{n_{i,\text{product}}}{n_{\text{converted HOC}}} \times 100 \% \quad (29)$$

where  $S_{i,\text{product}}$  is the selectivity to a given product  $i$  (mol-%),  $n_{i,\text{product}}$  refers to the moles of the considered product  $i$  at the given time (mol) and  $n_{\text{converted,HOC}}$  refers to the moles of educt converted at the given time (mol).

### 3.3.5 Analysis of halide ions by ion chromatography (IC)

2 mL aqueous aliquot was taken from the batch reactor and then filtered through cellulose acetate membrane filters (0.45  $\mu\text{m}$  pore size). 1 mL of the filtrate was used for the analysis of  $\text{F}^-$ ,  $\text{Cl}^-$ , and  $\text{Br}^-$  by IC (ICDX 500 instrument, Dionex, US). The IC instrument comprised of an anion exchange column (IonPac AS11-HC, Dionex, US), a 4 mm suppressor (ASRS 300), an eluent generator (E650), autosampler (A550), and a conductivity detector (IC-25, Dionex, US). The eluent was a mixture of KOH solution and Millipore water. The eluent flow rate was maintained at 1 mL/min and the KOH gradient was adjusted as follows: 0-2 min, 7 mM; 2-8 min, 8 mM; 10-12 min, 8-45 mM; 12-17 min, 45 mM; 17-19 min, 45-7 mM. External calibration curves were used to determine the concentrations of  $\text{F}^-$ ,  $\text{Cl}^-$ , and  $\text{Br}^-$ . The halide balance was determined by

measuring the moles of halide ions released in the bulk aqueous phase to the total moles of halogen in the parent compound.

## 4 Results and Discussion

### 4.1 Dehalogenation of $\text{CCl}_3\text{-R}$ compounds using the $\text{Cu}^0 + \text{NaBH}_4$

$\text{Cu}^0 + \text{NaBH}_4$  was used in this study as a short description for the system comprising Cu NPs and  $\text{NaBH}_4$ . The system was used for the dehalogenation of HOCs in water. Compounds with the general formula  $\text{CCl}_3\text{-R}$  are a unique class of substances frequently occurring as water pollutants. These compounds are also of relevance as a target in environmental catalysis. As prominent representatives  $\text{CHCl}_3$ ,  $\text{CCl}_4$ ,  $\text{CBrCl}_3$ ,  $\text{CFCl}_3$ , and 1,1,1-TCA were chosen as probe substances in the present study. The dehalogenation of these compounds using ZVI-containing reagents and Pd catalysts are in most cases characterized by the accumulation of compounds with lower chlorine substitution and their lower reaction rates. The reaction pathways to account for the formation of the different products are  $\alpha$ -elimination and hydrogenolysis. In this study, the selectivities during the dehalogenation of these compounds were investigated to identify which of the two reaction pathways was dominant when using  $\text{Cu}^0 + \text{NaBH}_4$ . First, the dechlorination of CF using  $\text{Cu}^0 + \text{NaBH}_4$  was investigated to identify product yields, selectivity patterns, and the reaction pathways for the formation of the different products. Selectivities were then investigated under different reaction conditions and also with suitable catalyst combinations where DCM accumulation could be minimized.  $\text{Cu}^0 + \text{NaBH}_4$  was then applied for dehalogenation of  $\text{CCl}_4$ ,  $\text{CBrCl}_3$ ,  $\text{CFCl}_3$ , and 1,1,1-TCA and the influence of the R-substituent on selectivities is reported.

#### 4.1.1 Dechlorination of CF using $\text{Cu}^0 + \text{NaBH}_4$

The dechlorination of CF by  $\text{Cu}^0 + \text{NaBH}_4$  (Figure 6 (a)) follows pseudo-first-order kinetics with a half-time of  $\tau_{1/2} = 7$  min using 1 mg/L Cu NPs and  $c_{0,\text{NaBH}_4} = 300$  mg/L at pH = 10. Control experiments showed that CF was stable for at least 120 min in the presence of i) only 300 mg/L  $\text{NaBH}_4$  and ii) 1 mg/L Cu NPs where the solution and headspace were purged with  $\text{H}_2$

before the introduction of CF. The reaction conditions for the controls were chosen as applied for  $\text{Cu}^0 + \text{NaBH}_4$ .

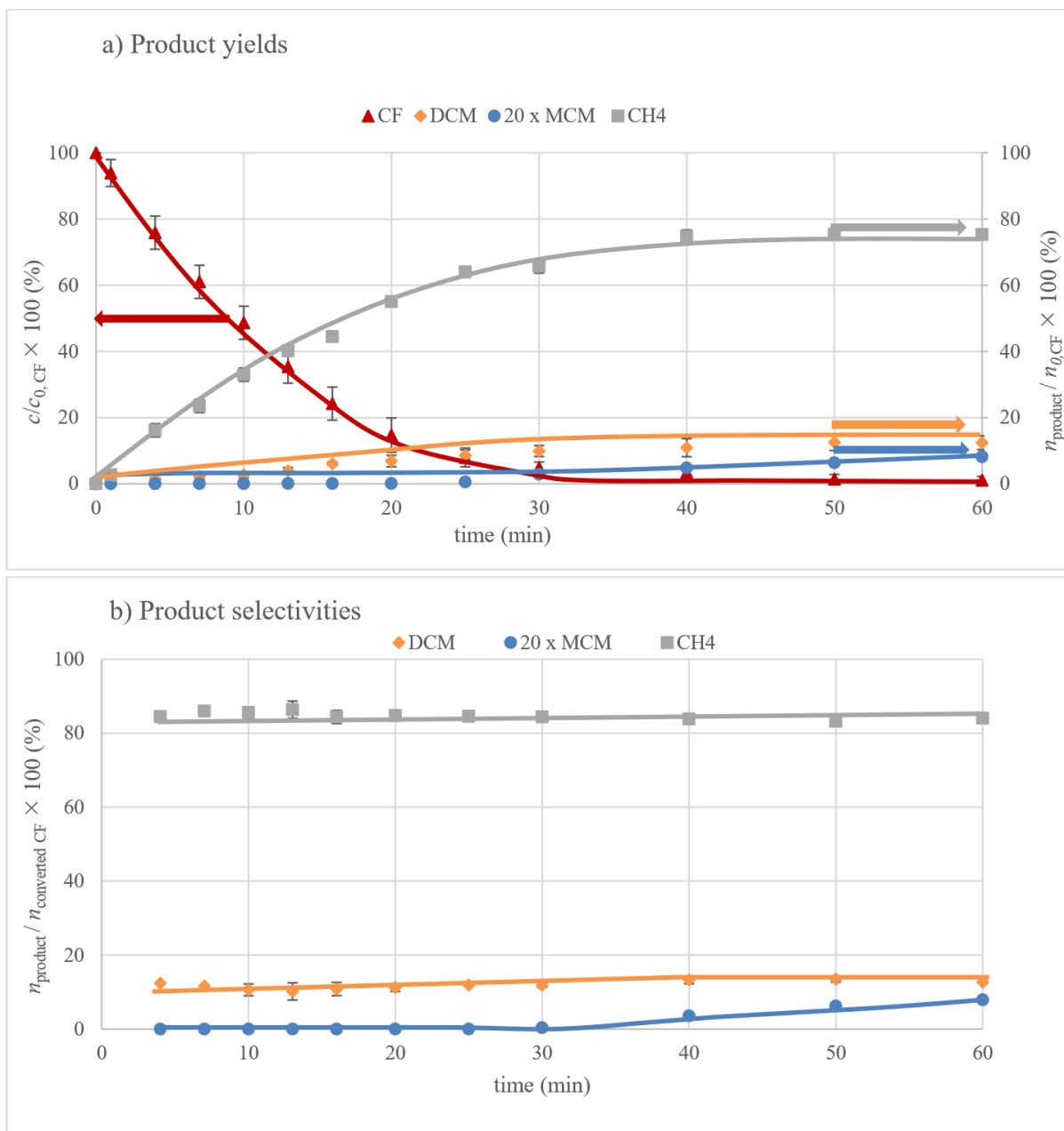


**Figure 6:** Reaction progress during the dechlorination of CF in water using  $\text{Cu}^0 + \text{NaBH}_4$  a) Product yields and b) Product selectivities ( $c_{\text{Cu}} = 1 \text{ mg/L}$ ;  $c_{0,\text{NaBH}_4} = 300 \text{ mg/L}$ ;  $c_{0,\text{CF}} = 10 \text{ mg/L}$ ;  $\text{pH} = 10$ ). Note that for MCM, the values in both graphs are multiplied by a factor of 20.

As shown in Figure 6 (a), the dechlorination of CF by  $\text{Cu}^0 + \text{NaBH}_4$  produces  $\text{CH}_4$ , DCM, and MCM from the beginning of the reaction. The product yields at  $t = 40$  min where CF conversion was  $\geq 95\%$  divided to  $(76 \pm 1)\%$ ,  $(12 \pm 1)\%$ , and  $(0.5 \pm 0.2)\%$  for  $\text{CH}_4$ , DCM, and MCM, respectively. The scattering ranges result from three parallel experiments. To obtain a better understanding of the CF dechlorination reaction in terms of product partitioning, the selectivities towards each product were evaluated as shown in Figure 6 (b). The selectivities to MCM, DCM, and  $\text{CH}_4$  were  $(0.3 \pm 0.2)\%$ ,  $(13 \pm 2)\%$ , and  $(84 \pm 2)\%$ , respectively. These selectivities are nearly constant over the entire CF conversion range. Hence the CF dechlorination follows three main parallel pathways to form the various products. Consecutive reaction pathways do not play a significant role in this time scale. The sum of  $\text{C}_2\text{H}_6$  and  $\text{C}_2\text{H}_4$  account for  $< 0.5\%$  of CF converted while  $\text{Cl}^-$  yield was  $(80 \pm 2)\%$ , which conforms with the chlorine amounts released from the detected products ( $76\% + 12\% \times 1/3 + 0.5\% \times 2/3 = 80.0\%$ ).

The detection of small quantities of  $\text{C}_2\text{H}_6$  and  $\text{C}_2\text{H}_4$  indicates that radical coupling reactions play a minor role but take place. Radical coupling products have also been reported by other authors to account for the formation of  $\text{C}_2\text{H}_6$ , PCE, and TCE during the dechlorination of CTC and CF (Feng and Lim, 2007; McCormick and Adriaens, 2004; Velázquez et al., 2013). In the current study, TCE and PCE were not detected. Considering the product balance, it remains a balanced gap of about  $100 - 76 - 12 - 0.5 = 11.5\%$  which is small and possibly insignificant. Considering the chlorine balance and the hydrocarbon balance together this indicates a fraction of  $\leq 11.5\%$  of non-detected (non-identified) chlorinated reaction products. However, similar gaps in the carbon balance and the chlorine balance would result from loss of CF due to gas

leakage. Having in mind the formation of hydrogen gas from borohydride such gas losses cannot be ruled out.

For evaluation of kinetic data the decomposition rate of  $\text{BH}_4^-$  may become significant. Its half-time was about 10-12 h under standard reaction conditions (pH 10, 1 mg/L Cu NPs). This means,  $c_{\text{BH}_4^-}$  can be approximated as constant during the CF degradation periods. Based on the products detected, the possible reaction pathways for the dechlorination of CF using  $\text{Cu}^0 + \text{NaBH}_4$  are presented in Figure 7.

The specific Cu activities  $A_{\text{Cu}}$  for the dechlorination of the educts and the formation of a particular product are presented in Table 5. The data in Table 5 are derived from additional experiments presented later in this chapter.

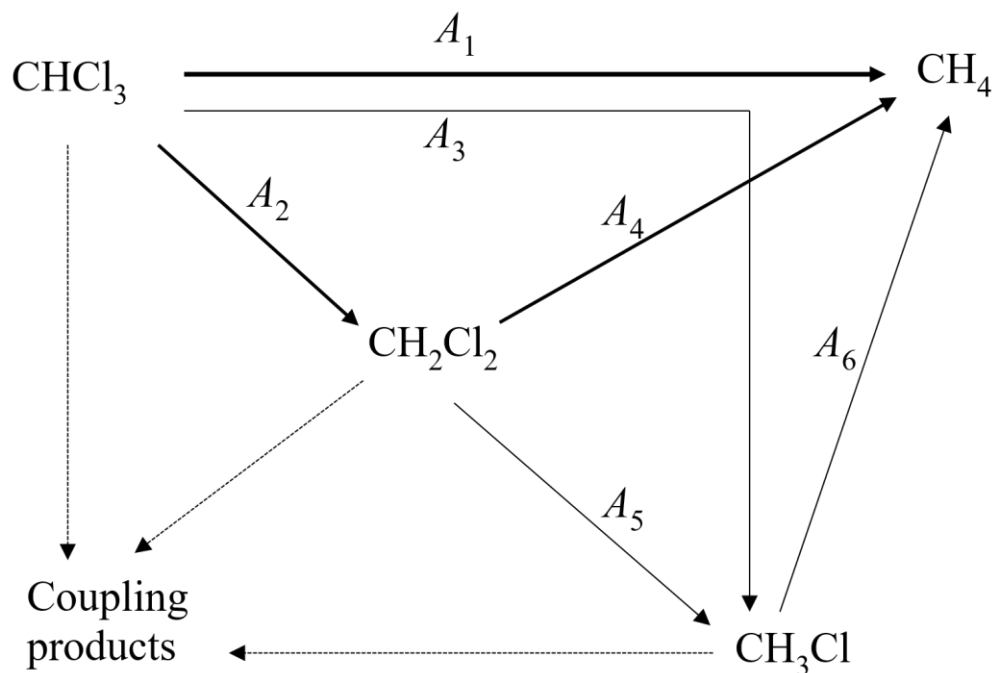


**Figure 7:** Proposed reaction pathways for the dechlorination of CF in water using  $\text{Cu}^0 + \text{NaBH}_4$ . ( $c_{\text{Cu}} = 1-100$  mg/L;  $c_{0,\text{NaBH}_4} = 300$  mg/L;  $c_{0,\text{HOCs}} = 2-10$  mg/L; pH = 10). (Based on the product selectivity patterns in Figure 6, different arrow designs are used in this scheme to show which reaction is significant).

**Table 5:** Calculated specific Cu activities  $A_{Cu}$  for the dechlorination of CF, DCM, and MCM and to account for the formation of products during dechlorination of CF and DCM using  $Cu^0 + NaBH_4$  ( $C_{Cu} = 1-100$  mg/L;  $C_{0,NaBH_4} = 300$  mg/L;  $p_{H_2} = 100$  kPa; pH = 10)

Specific Cu activity	$A_{CF}$	$A_1$	$A_2$	$A_3$	$A_{DCM}$	$A_4$	$A_5$	$A_6$
$A_{Cu}$ [L/(g·min)]	$130 \pm$	110	17	$0.6 \pm$	$0.22 \pm$	$0.19 \pm$	$0.029 \pm$	$0.0020 \pm$
	$10^a$	$\pm 5^b$	$\pm 5^b$	$0.2^b$	$0.02^c$	$0.01^d$	$0.002^d$	$0.0002^e$

<sup>a</sup>  $A_{CF}$  represents the overall specific Cu activity for the dechlorination of CF.

<sup>b</sup> Value calculated from CF as the educt.

<sup>c</sup>  $A_{DCM}$  represents the overall specific Cu activity for dechlorination of DCM.

<sup>d</sup> Value calculated from experiments with DCM as educt.

<sup>e</sup> Value calculated from experiments with MCM as educt.

Since the sum of  $C_2H_6$  and  $C_2H_4$  accounts for < 0.5 mol-% of the CF transformed, it shows that radical coupling reactions were of minor importance. As described earlier (Figure 3), DCM is formed when a second electron is transferred to  $\bullet CHCl_2$  followed by protonation. To determine whether DCM and MCM are ‘free’ intermediates on the pathway from CF to  $CH_4$ , separate studies were done for the dechlorination of DCM and MCM using  $Cu^0 + NaBH_4$ . As shown in Table 5, the specific Cu activities  $A_{Cu}$  for the dechlorination of DCM and MCM were  $(0.22 \pm 0.02)$  L/(g·min) and  $(0.0020 \pm 0.0002)$  L/(g·min), respectively. Hence  $CH_4$  formation occurred directly from the dechlorination of CF but not through hydrogenolysis via DCM and MCM. Therefore, reactions **4**, **5**, and **6** are negligible and stepwise hydrogenolysis of CF to  $CH_4$  is unlikely. Thus the dechlorination of CF through  $\alpha$ -elimination (-HCl) pathways via dichlorocarbene intermediates may account for the formation of  $CH_4$  (McCormick and Adriaens, 2004; Song and Carraway, 2006). Based on the product patterns (Figure 6), the dechlorination of CF can be described mainly by three parallel reactions **1**, **2**, and **3** (Figure 7). Reaction **1** leading to  $CH_4$  is dominant followed by reaction **2** which leads to DCM. Reaction **3** leading to MCM is minor.

### Effect of Cu NPs concentration on selectivity patterns

As described earlier, DCM is the major chlorinated product whose formation selectivity was  $(13 \pm 2)$  mol-%. The DCM persists even after the CF dechlorination reaction shown in Figure 6 (a) was continued for 20 h, ( $c_{20h,NaBH_4} = 75$  mg/L). Hence DCM can be considered more-or-less a dead-end product under the experimental conditions ( $c_{Cu} = 1$  mg/L). From a remediation perspective, DCM is an undesired byproduct since it is a water contaminant of a public health concern due to its carcinogenic potential (Dekant et al., 2021; Schlosser et al., 2015). Thus its accumulation in the system should be minimized. Further experiments were performed to determine DCM and MCM selectivity patterns under different experimental conditions. First, the selectivity patterns were determined by varying Cu NPs concentration from 0.1 to 100 mg/L at  $c_{0,NaBH_4} = 300$  mg/L as shown in Figure 8.

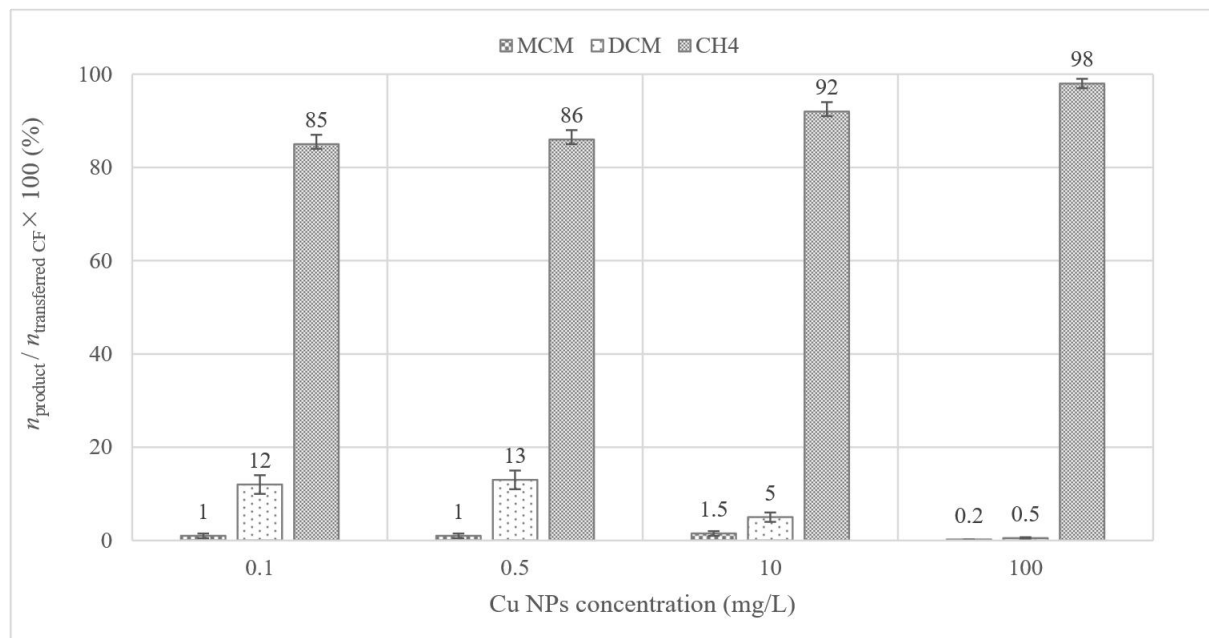


**Figure 8:** Effect of Cu NPs concentration on the selectivity patterns during the dechlorination of CF ( $c_{0,NaBH_4} = 300$  mg/L;  $c_{0,CF} = 10$  mg/L; pH = 10). Selectivity patterns were determined at the termination of reaction after 60 min where CF conversion  $\geq 95$  %.

As shown in Figure 8, the selectivity towards DCM decreased with an increase in Cu NPs concentration. When the Cu NPs concentration was maximized to  $c_{\text{Cu}} = 100 \text{ mg/L}$ , selectivity towards DCM was  $(0.5 \pm 0.2) \text{ mol-\%}$ . This was not a ‘true’ selectivity effect in the CF conversion but was due to subsequent dechlorination of DCM. This approach prevents the release of the intermediate DCM but at the expense of a much higher catalyst concentration.

#### *Comparison of Cu-, Pd- and nZVI<sup>BH</sup>-based systems for dechlorination of CF*

As described earlier, the dechlorination of CF using  $\text{Cu}^0 + \text{NaBH}_4$  produces DCM and  $\text{CH}_4$  as the major products. The question remains, is borohydride as the reducing agent responsible for this selectivity pattern? Therefore, for comparison purposes, the dechlorination of CF was done using  $\text{Pd} + \text{H}_2$ ,  $\text{Pd}^0 + \text{NaBH}_4$ , and nZVI<sup>BH</sup> as reduction systems. Using literature data and own experimental data, the product selectivity patterns during the dechlorination of CF were determined for Cu-, Pd- and nZVI-based systems. The results are presented in Table 6.

**Table 6:** Selectivity patterns during the dechlorination of CF in water using  $\text{Cu}^0 + \text{NaBH}_4$ ,  $\text{Pd}^0 + \text{NaBH}_4$ ,  $\text{Pd} + \text{H}_2$ , and  $\text{nZVI}^{\text{BH}}$  remediation systems under ambient conditions ( $c_{\text{Cu}} = 1 \text{ mg/L}$ ;  $c_{\text{Pd}} = 3\text{-}5 \text{ mg/L}$ ;  $c_{\text{NaBH}_4} = 300 \text{ mg/L}$ ;  $c_{\text{nZVI}} = 5 \text{ g/L}$ )

Reduction system	$n_{\text{product}} / n_{\text{converted CF}} \times 100 (\%)$			Specific metal activities $A_m$ [L/(g·min)]	Cl <sup>-</sup> yield (mol-%)
	CH <sub>4</sub>	DCM	MCM		
$\text{Cu}^0 + \text{NaBH}_4$	84 ± 2	13 ± 2	0.3 ± 0.2	130 ± 10	80 ± 2
$\text{Pd}^0 + \text{NaBH}_4$	78 ± 4	15 ± 3	5 ± 2	10 ± 2	75 ± 3
$\text{Pd} + \text{H}_2$	80 ± 3	11 ± 2	8 ± 2	5 ± 1	78 ± 3
$\text{Pd}/\text{Al}_2\text{O}_3 + \text{H}_2$ (Velázquez et al., 2013)	90	10	n.a.	n.a.	n.a.
$\text{PdAu}/\text{Al}_2\text{O}_3 + \text{H}_2$ (Velázquez et al., 2013)	94.4	5.5	0.1	n.a.	n.a.
$\text{Pd}/\text{Al}_2\text{O}_3 + \text{H}_2$ (Lowry and Reinhard, 1999)	80	n.a.	n.a.	n.a.	n.a.
$\text{nZVI}^{\text{BH}}$	24 ± 2	40 ± 5	35 ± 5	0.003 ± 0.001	50 ± 5

n.a. = not analyzed

Selectivities were calculated at 25-35 % CF conversion;  $\text{pH}_0$  for  $\text{nZVI}^{\text{BH}}$  was 8.3 which increased to 9 at the termination of the reaction; no  $\text{BH}_4^-$  or  $\text{H}_2$  was added into the reactor during CF dechlorination by  $\text{nZVI}^{\text{BH}}$ ;  $\text{pH}$  for the systems  $\text{Pd}^0 + \text{NaBH}_4$ ,  $\text{Pd} + \text{H}_2$ , and  $\text{Cu}^0 + \text{NaBH}_4$  remains about 10; chloride yield measured at termination of reaction where CF conversion was  $\geq 95\%$ ; Selectivities for the systems  $\text{Pd}/\text{Al}_2\text{O}_3 + \text{H}_2$  and  $\text{PdAu}/\text{Al}_2\text{O}_3 + \text{H}_2$  were obtained from literature; for the remediation systems which were tested in this study, the sum of  $\text{C}_2\text{H}_6$  and  $\text{C}_2\text{H}_4$  accounts for 0.5-2 mol-% of CF converted; the specific metal activities  $A_m$  were calculated using nanoparticles of comparable sizes i.e.  $d_{50,\text{Cu NPs}} = 50 \text{ nm}$ ,  $d_{50,\text{Pd NPs}} = 60 \text{ nm}$  and  $d_{50,\text{nZVI}} = 75 \text{ nm}$  (further details on particle sizes are presented in the appendix Table A2-3).

Metallic Pd and Cu are true catalysts while  $\text{nZVI}$  is a reagent, possibly with catalytic properties. Hence different dechlorination mechanisms are involved. For Cu and Pd catalysts and in the presence of a reductant, the dechlorination process may involve the transfer of H-species (active  $\text{H}^*$ ) in the form of either chemisorbed H-atoms or hydrides. As shown in Table 6, the selectivity to  $\text{CH}_4$ ,  $\text{DCM}$ , and  $\text{MCM}$  during the dechlorination of CF changes depending on which catalyst or reagent was used. Since  $\text{CH}_4$ ,  $\text{DCM}$  and  $\text{MCM}$  selectivities were nearly the same using

the systems  $\text{Cu}^0 + \text{NaBH}_4$ ,  $\text{Pd} + \text{H}_2$ ,  $\text{Pd}^0 + \text{NaBH}_4$ , and  $\text{Pd}/\text{Al}_2\text{O}_3 + \text{H}_2$ , one can speculate that the dechlorination of CF follows a similar mechanism, despite the quite different catalysts and reductants ( $\text{NaBH}_4$  or  $\text{H}_2$ ). For the Pd-based catalysts, the  $\text{H}_2$  source has no marked effect on selectivities but affects the specific catalyst activity. From experimental data which were used to determine product selectivities as shown in Table 6, the specific Pd activities  $A_{\text{Pd}}$  for the dechlorination of CF using  $\text{Pd} + \text{H}_2$  and  $\text{Pd}^0 + \text{NaBH}_4$  were  $(5 \pm 1) \text{ L}/(\text{g}\cdot\text{min})$  and  $(10 \pm 2) \text{ L}/(\text{g}\cdot\text{min})$ , respectively. This difference in activities is rather small, indicating that  $\text{NaBH}_4$  plays the role of a hydrogen source only, rather than participating directly in the dechlorination reaction. DCM selectivity was lower for  $\text{PdAu}/\text{Al}_2\text{O}_3 + \text{H}_2$  compared to  $\text{Pd}/\text{Al}_2\text{O}_3 + \text{H}_2$  systems by a factor of 2. As will be discussed later in this work, Ag which is in the same group as Au in the periodic table also has a marked effect on the product selectivities. Hence the choice of metal or metal combinations may be necessary to achieve the desired selectivity towards lower DCM. Since the selectivities were nearly the same for  $\text{Pd}/\text{Al}_2\text{O}_3 + \text{H}_2$ ,  $\text{Pd} + \text{H}_2$ , and  $\text{Pd}^0 + \text{NaBH}_4$ , one can conclude that borohydride as a reductant has no marked influence on the product selectivities. Remarkably, Pd favors the formation of MCM much more than Cu (by factor 17) which might be due to the higher availability of active  $\text{H}^*$  at the Pd surface, necessary for stepwise hydrogenolysis of adsorbed intermediates.

As shown in Table 6, the selectivities to  $\text{CH}_4$ , DCM, and MCM were  $(24 \pm 2) \text{ mol}\%$ ,  $(40 \pm 5) \text{ mol}\%$ , and  $(35 \pm 5) \text{ mol}\%$ , respectively during the dechlorination of CF through electron transfer processes using  $n\text{ZVI}^{\text{BH}}$  as a reagent. Since DCM is rather stable in the presence of monometallic  $n\text{ZVI}$ , stepwise hydrogenolysis of CF via DCM to  $\text{CH}_4$  was ruled out. Another major product was MCM whose selectivity was nearly 7 to 117 times higher for  $n\text{ZVI}$  than for the catalytic systems based on Pd and Cu. Hence stepwise hydrogenolysis was the main reaction

pathway for the dechlorination of CF using nZVI. The specific nZVI activity  $A_{nZVI}$  for dechlorination of CF was  $(0.003 \pm 0.001) \text{ L}/(\text{g}\cdot\text{min})$ , which is by far the lowest among the investigated systems.

Mackenzie et al. (2006) have determined specific activities for HDC of various chlorinated hydrocarbons, among them CF and DCM, under identical reaction conditions with a  $\text{Pd}/\gamma\text{-Al}_2\text{O}_3$  catalyst +  $\text{H}_2$ . The obtained values  $A_{\text{Pd,CF}} = 0.8 \text{ L}/(\text{g}\cdot\text{min})$  and  $A_{\text{Pd,DCM}} = 0.0015 \text{ L}/(\text{g}\cdot\text{min})$  yield a ratio  $A_{\text{Pd,CF}}/A_{\text{Pd,DCM}} = 533$ . The corresponding ratio for the  $\text{Cu}^0 + \text{NaBH}_4$  system is  $A_{\text{Cu,CF}}/A_{\text{Cu,DCM}} = 591$  (data from Table 5). Surprisingly, the two ratios are quite similar despite the different catalysts and reductants. This may be an accident or a hint to similar rate-controlling steps. From the remediation point of view, it means that  $\text{Pd} + \text{H}_2$  and  $\text{Cu}^0 + \text{NaBH}_4$  both have similar problems concerning the formation of DCM as a recalcitrant byproduct and intermediate during the dechlorination of CF. Copper is by far the cheaper metal (cheaper on a mass basis by a factor of 8500 compared to Pd), but  $\text{NaBH}_4$  is the more expensive reductant and the aqueous suspension must be alkaline. As discussed later in chapter 4.2.4, comparison based on reduction equivalents show that  $\text{NaBH}_4$  costs more than  $\text{H}_2$  by a factor of 12. Considering both reductant and metal costs,  $\text{Cu}^0 + \text{NaBH}_4$  is cheaper than  $\text{Pd} + \text{H}_2$  for HDC reactions.

#### *Effect of initial $\text{NaBH}_4$ concentration on product selectivities and catalyst activities*

Although the dechlorination of CF using  $\text{Cu}^0 + \text{NaBH}_4$  can mitigate the accumulation of DCM when  $c_{\text{Cu}} = 100 \text{ mg}/\text{L}$  was used, the question remains what controls the ‘true’ DCM selectivity? By maintaining  $c_{\text{Cu}} = 1 \text{ mg}/\text{L}$ , the dechlorination of CF was investigated under different experimental conditions. First, the initial  $\text{NaBH}_4$  concentration was varied from 25 to 500 mg/L at the same catalyst concentration. Product selectivity patterns and the corresponding

specific Cu activities  $A_{Cu}$  under these conditions were investigated. The results are presented in Figures 9 and 10, respectively.

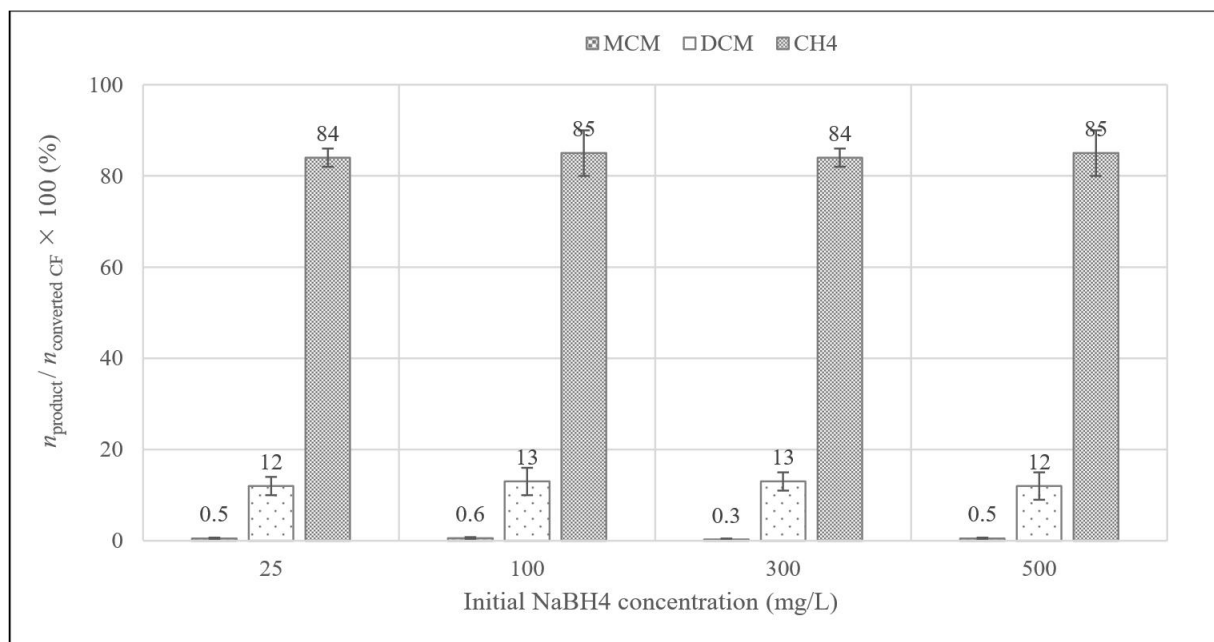


**Figure 9:** Effect of initial NaBH<sub>4</sub> concentration on the selectivity patterns during the dechlorination of CF using Cu NPs ( $c_{Cu} = 1$  mg/L;  $c_{0,CF} = 10$  mg/L; pH = 10). Selectivities determined at CF conversion  $\geq 95$  %.

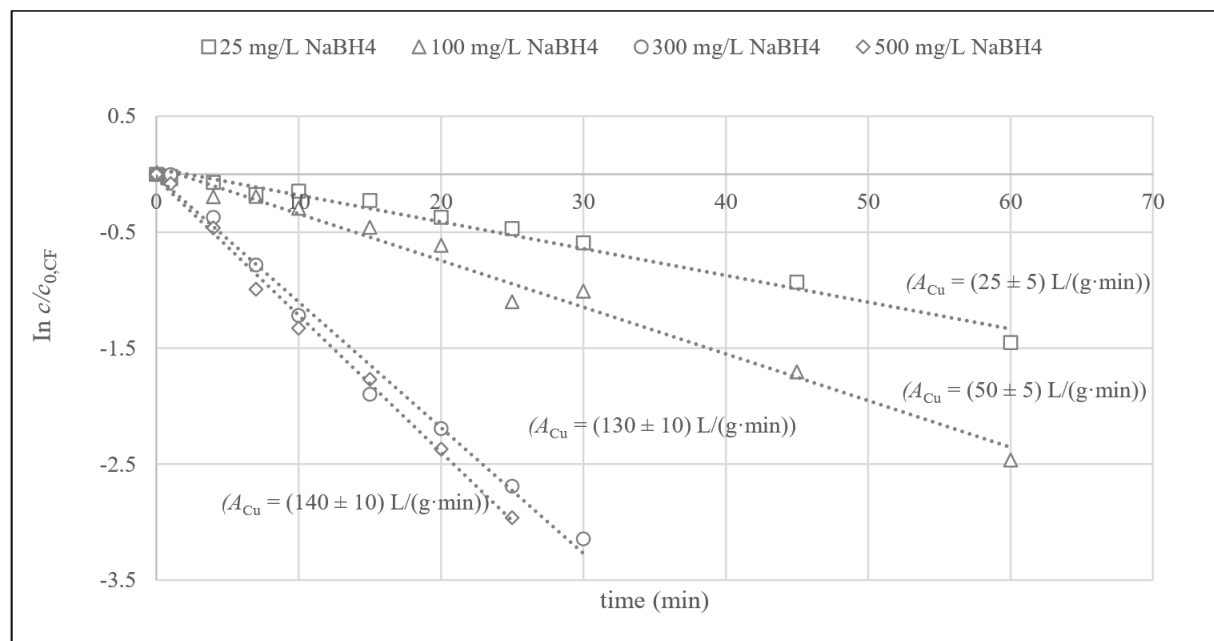


**Figure 10:** Effect of initial NaBH<sub>4</sub> concentration on the specific Cu activities during the dechlorination of CF ( $c_{Cu} = 1$  mg/L;  $c_{0,CF} = 10$  mg/L; pH = 10).

As shown in Figure 9, the initial concentration of NaBH<sub>4</sub> supplied has no marked effect on the selectivities. Hence, the dechlorination of CF using Cu<sup>0</sup> + NaBH<sub>4</sub> can be considered to follow the same reaction pathways independent of the concentration of reducing species present (active H\* or hydrides). As shown in Figure 10, specific Cu activities increased almost linearly with an increase in initial NaBH<sub>4</sub> concentration between 25 and 300 mg/L NaBH<sub>4</sub>. Above 300 mg/L NaBH<sub>4</sub>, a plateau in reaction rates appears which may be due to surface saturation. Similar studies have shown that during the dechlorination of DCM and 1,2-DCA, low oxidation-reduction potential (ORP) conditions (as a result of increased NaBH<sub>4</sub> concentrations) were attributed to increased reaction rates (Huang et al., 2012; Huang et al., 2011).

*Effect of initial CF concentrations on product selectivities and catalyst activities*

Other than the concentration of reducing species, the concentration of CF molecules on the surface of the catalyst was investigated to determine product selectivity patterns. The initial CF concentration was varied from 1 to 40 mg/L while maintaining  $c_{\text{Cu}} = 1 \text{ mg/L}$  and  $c_{0,\text{NaBH}_4} = 300 \text{ mg/L}$ . Under these reaction conditions, the selectivity patterns and the corresponding specific Cu activities  $A_{\text{Cu}}$  were determined and the results are presented in Figures 11 and 12, respectively.

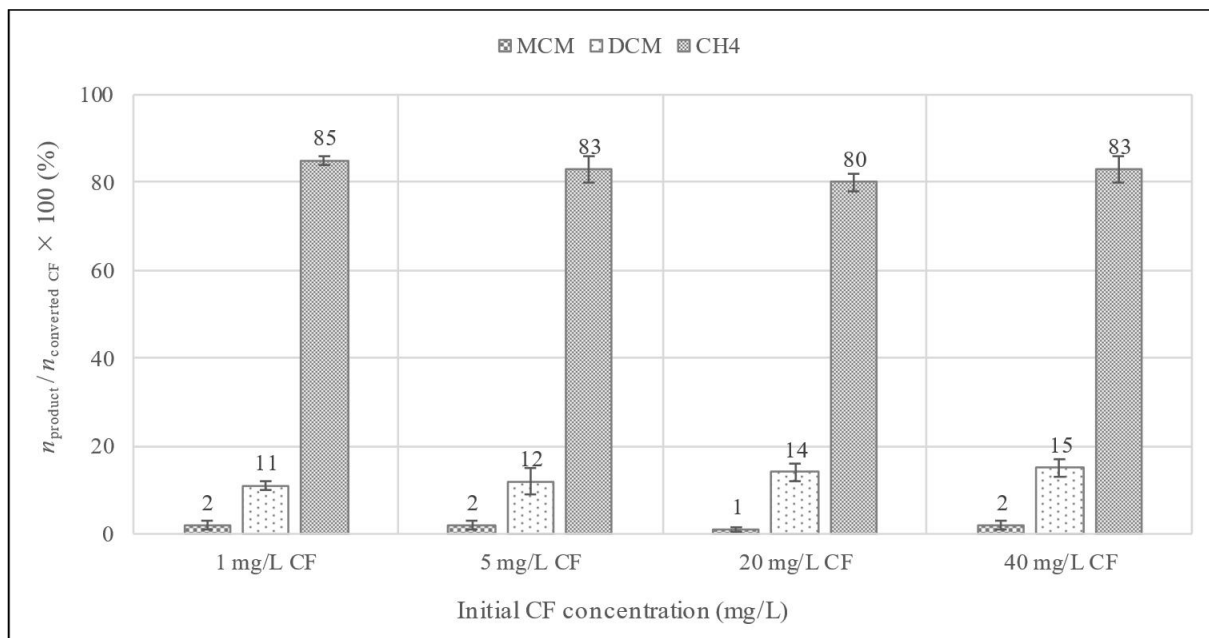


**Figure 11:** Effect of initial CF concentration on the selectivity patterns during the dechlorination reactions using  $\text{Cu}^0 + \text{NaBH}_4$  ( $c_{\text{Cu}} = 1 \text{ mg/L}$ ;  $c_{0,\text{NaBH}_4} = 300 \text{ mg/L}$ ;  $\text{pH} = 10$ ). Selectivities determined at CF conversion  $\geq 95\%$ .

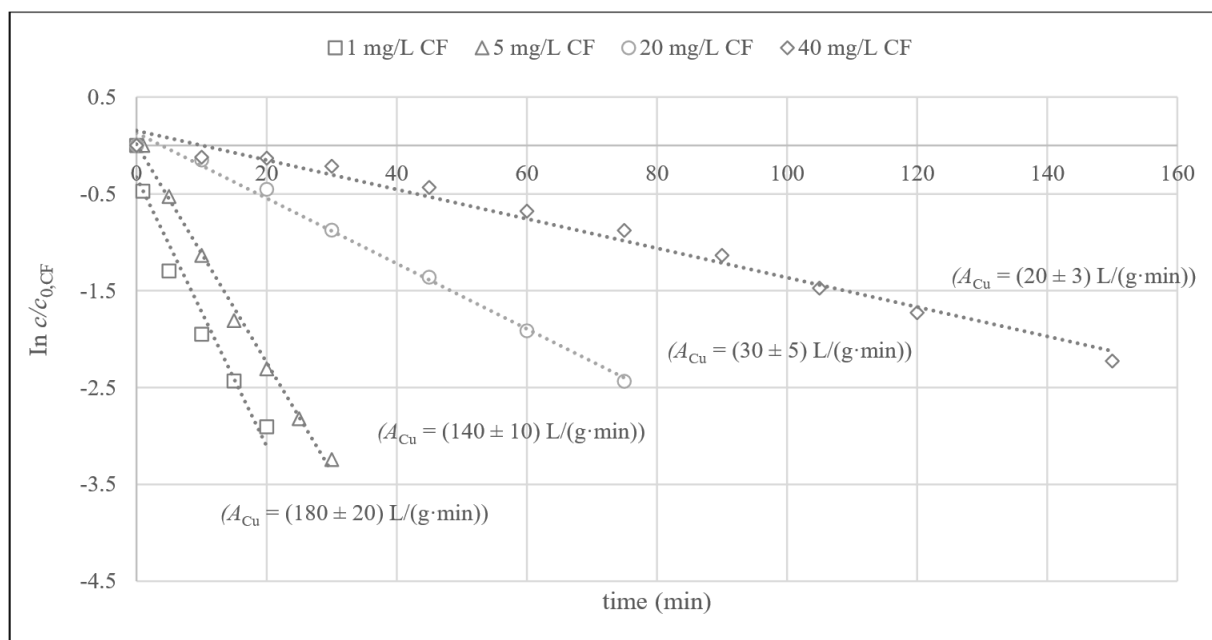


**Figure 12:** Effect of initial CF concentration on the specific Cu activities during the dechlorination reactions using  $\text{Cu}^0 + \text{NaBH}_4$  ( $c_{\text{Cu}} = 1 \text{ mg/L}$ ;  $c_{0,\text{NaBH}_4} = 300 \text{ mg/L}$ ;  $\text{pH} = 10$ ).

As shown in Figure 11, the selectivity patterns were nearly the same at the different initial CF concentrations. However, the concentration of CF affects the reaction rate constants (regression line slopes in Figure 12) and hence the specific Cu activities: the higher the initial CF concentration, the lower the apparent catalyst activity. These findings are, however, in contrast to constant catalyst activities along with the conversion progress, proved by the linear regression lines in Figure 12 (i.e. constant slopes = constant catalyst activities). These two findings,  $A_{Cu} = f(c_{0,CF})$  and apparent first-order kinetics between and up to  $\geq 90$  % CF conversion are not easily compatible. One possible explanation is a product inhibition, e.g. by chloride, which appears already from the early stages of the dechlorination experiment. The data for the highest CF concentration ( $c_{0,CF} = 40$  mg/L, violet curve) show a significantly curved course in semi-logarithmic coordinates. This is equivalent to an increasing rate constant (specific catalyst activity) along with the reaction progress. It is in line with the observed dependence  $A_{Cu} = f(c_{CF})$ .

#### *Effect of water constituents and metal additives on CF dechlorination*

The influence of co-solutes and metal additives on product selectivity patterns during the dechlorination of CF using  $Cu^0 + NaBH_4$  was extensively studied. The co-solutes were mixed with freshly prepared Cu NPs at 130 rpm for 120 min. CF was then introduced to initiate the reaction. The product selectivity patterns in the presence of co-solutes were compared to the baseline for Cu without co-solute (i.e. in deionized water). As benchmarks, laboratory tap water was used. The results are shown in Figure 13. SRHA as co-solute was used as a surrogate for organic matter.

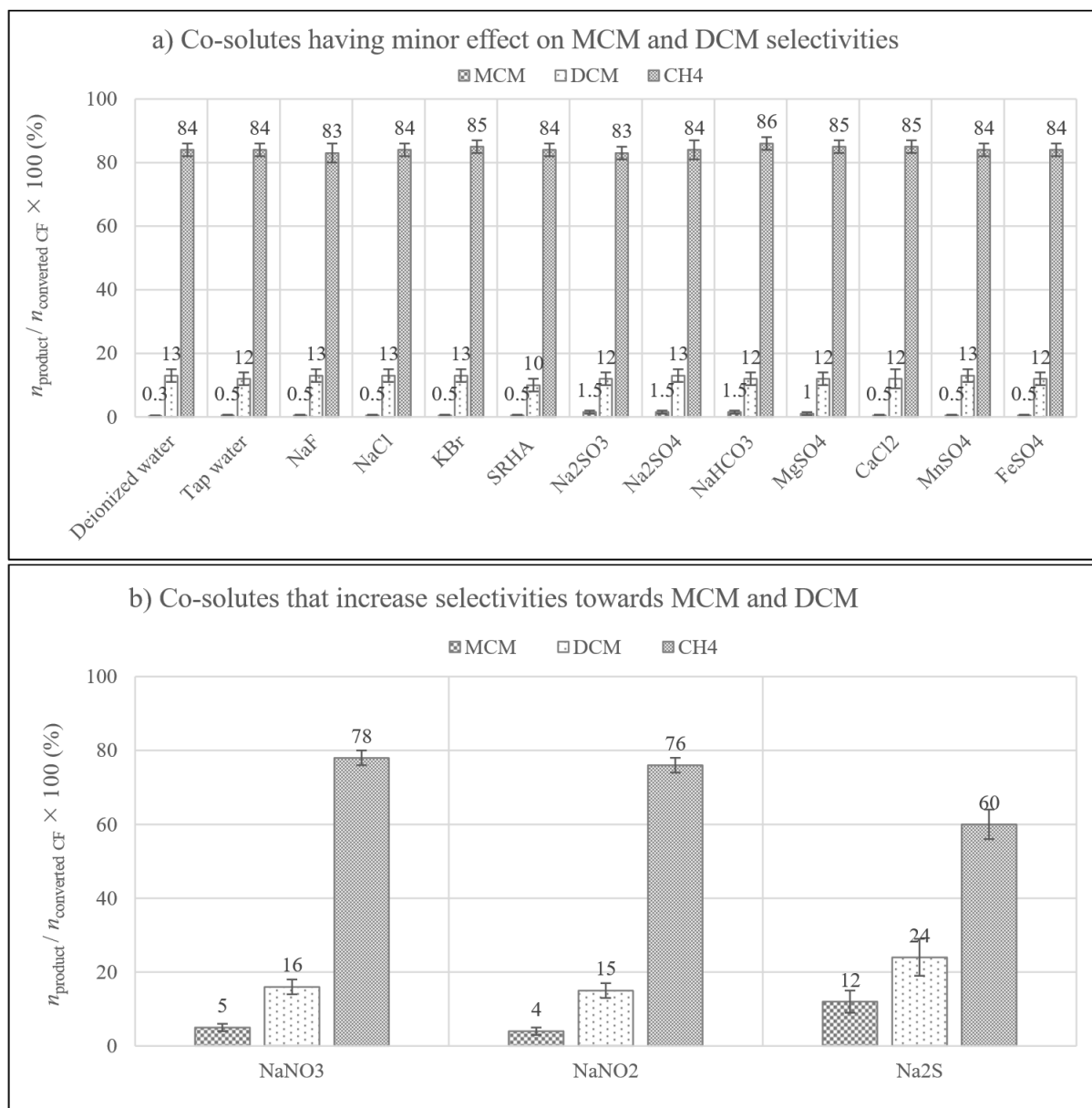


**Figure 13:** Product selectivity patterns for the dechlorination of CF using  $\text{Cu}^0 + \text{NaBH}_4$  a) Co-solutes that have minor effects towards MCM and DCM selectivities and b) Co-solutes that increase selectivities towards MCM and DCM ( $c_{\text{Cu}} = 1 \text{ mg/L}$ ;  $c_{0,\text{NaBH}_4} = 300 \text{ mg/L}$ ;  $c_{0,\text{CF}} = 10 \text{ mg/L}$ ;  $\text{pH} = 10$ ;  $\text{pH}_{\text{NaHCO}_3} = 8$ ;  $c_{\text{solute}} = 10 \text{ mg/L}$ ;  $c_{\text{Na}_2\text{S}} = 1 \text{ mg/L}$ ). Selectivities determined at CF conversion  $\geq 95 \%$ .

As shown in Figure 13 (a), the selectivity towards DCM was nearly the same in deionized water, tap water, and in the presence of 10 mg/L each of NaF, NaCl, KBr, SRHA, Na<sub>2</sub>SO<sub>3</sub>, Na<sub>2</sub>SO<sub>4</sub>, NaHCO<sub>3</sub>, MgSO<sub>4</sub>, CaCl<sub>2</sub>, MnSO<sub>4</sub>, and FeSO<sub>4</sub>. These ions may be considered to compete not to a

large extent for active sites or reduction equivalents with CF molecules. The product selectivities were not only affected by matrix composition but in some cases also the specific catalyst activities. A deeper discussion of the influence of co-solutes on the specific Cu activities is presented later in this thesis (chapter 4.2.2). The presence of NaF, NaCl, KBr, SRHA, Na<sub>2</sub>SO<sub>3</sub>, and Na<sub>2</sub>SO<sub>4</sub> had no marked effect on specific Cu activities, NaHCO<sub>3</sub> had a positive effect while MgSO<sub>4</sub>, MnSO<sub>4</sub>, CaCl<sub>2</sub>, and FeSO<sub>4</sub> had negative effects on the catalyst activity (discussion presented in chapter 4.2.2).

Co-solutes with inhibition and deactivation effect on the catalyst (data and discussion in chapter 4.2.2) led to undesired selectivities (i.e. increased selectivities to chlorinated byproducts). As shown in Figure 13 (b), NaNO<sub>3</sub> and NaNO<sub>2</sub> led to a slight increase in selectivities towards MCM and DCM. The presence of 10 mg/L NaNO<sub>3</sub> and 10 mg/L NaNO<sub>2</sub> decreased the catalyst activities from (130 ± 10) to (100 ± 10) L/(g·min), which is not significant. The most significant effects on product selectivity patterns and specific Cu activity ( $A_{Cu} = (13 \pm 2) \text{ L/(g}\cdot\text{min)}$ ) were observed in the presence of 1 mg/L Na<sub>2</sub>S. Under the experimental conditions (pH = 10), bisulfide (HS<sup>-</sup>) is the dominant species. Due to the strong interaction between bisulfide with Cu catalysts, the surface of the catalyst is modified (formation of CuS). This modification supports stepwise hydrogenolysis as a dechlorination mechanism.

Next, bimetallic mixtures of particles were prepared by reduction of the metals in the same batch reactor with NaBH<sub>4</sub>. The speciation of metals in the resulting particles was not analyzed. For bimetallic Ag/Cu particles, four methods of preparation were used as described earlier in chapter 3.1.2. Since vitamin B12 (with its Co center) in the presence of Cu has been found to accelerate dechlorination of DCM (Huang et al., 2013, 2015), Cu<sup>0</sup> + NaBH<sub>4</sub> was also used together with vitamin B12 for dechlorination of CF. The product selectivity patterns and specific metal activities

$A_m$  are shown in Figures 14 and 15, respectively. The corresponding chloride yields are presented in the appendix Table A3-1.

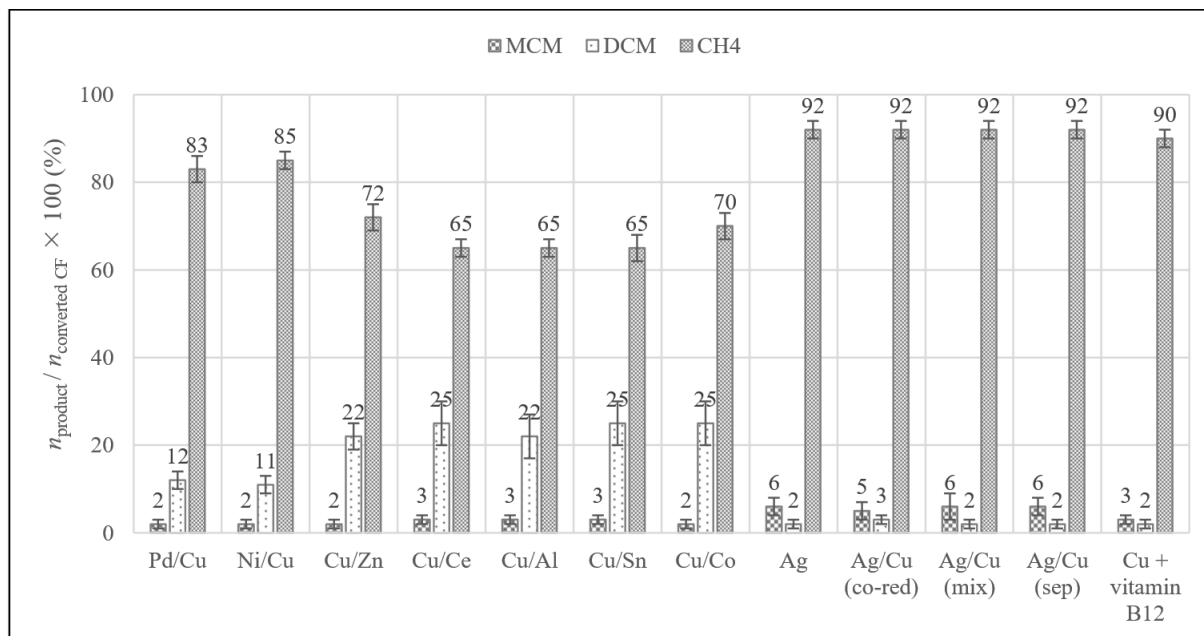


**Figure 14:** Selectivity patterns during the dechlorination of CF using  $Ag^0 + NaBH_4$  and  $Cu^0 + NaBH_4$  in the presence of metal additives and vitamin B12 ( $c_{metal\ catalyst, total} = 2\ mg/L$ ;  $c_{0, NaBH_4} = 300\ mg/L$ ;  $c_{vitamin\ B12} = 5\ mg/L$ ;  $c_{0, CF} = 10\ mg/L$ ;  $pH = 10$ ). Selectivities determined at CF conversion  $\geq 95\%$ ; 25 wt-% Ag on Cu used for bimetallic Ag/Cu particles. For Cu + vitamin B12 ‘apparent selectivities’ results from subsequent dechlorination of DCM intermediate.

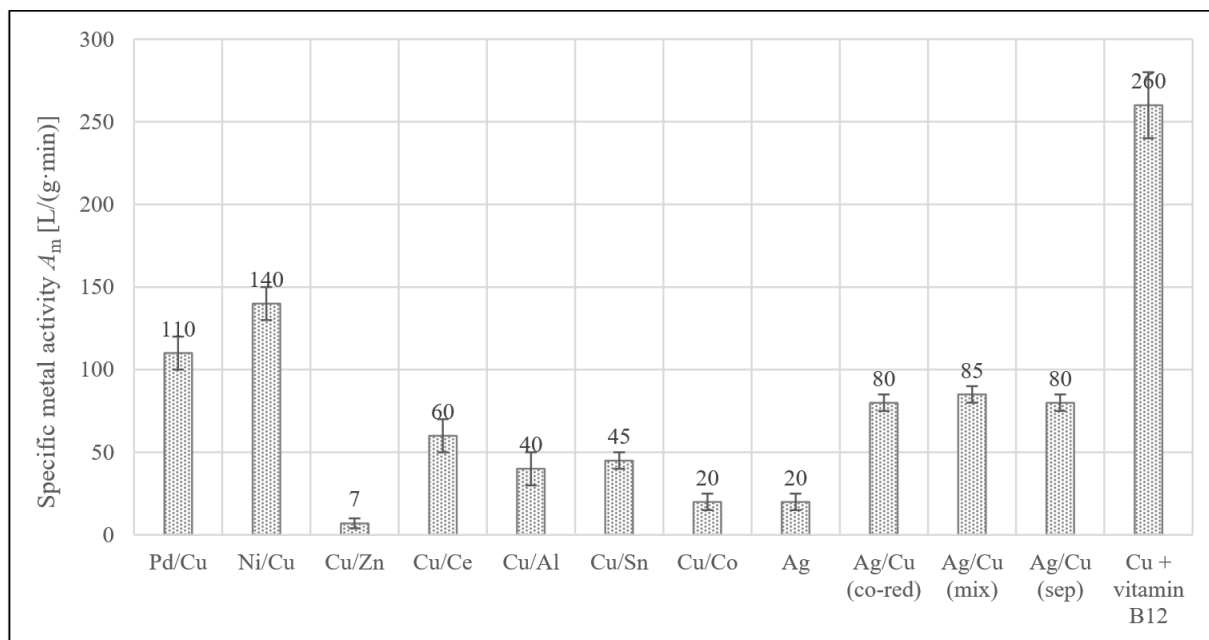


**Figure 15:** Specific metal activities for dechlorination CF using  $\text{Ag}^0 + \text{NaBH}_4$  and  $\text{Cu}^0 + \text{NaBH}_4$  in the presence of metal additives and vitamin B12 ( $c_{\text{metal catalyst, total}} = 2 \text{ mg/L}$ ;  $c_{0, \text{NaBH}_4} = 300 \text{ mg/L}$ ;  $c_{\text{vitamin B12}} = 5 \text{ mg/L}$ ;  $c_{0, \text{CF}} = 10 \text{ mg/L}$ ;  $\text{pH} = 10$ ). Specific metal activities for Pd/Cu, Ni/Cu, Zn/Cu, Ce/Cu, Al/Cu, Sn/Cu, Co/Cu, and Cu + vitamin B12 were calculated based on the total metal concentration; 25 wt-% Ag on Cu used for the bimetallic Ag/Cu particles.

As shown in Figure 14, the combination of Cu catalysts with the hydrogenation-active metals Pd and Ni had no marked effects on dechlorination selectivity nor activity. As shown in Figure 15, the metallic-mixture-systems comprised of Cu/Zn, Cu/Ce, Cu/Al, Cu/Sn, and Cu/Co show lower specific metal activities  $A_m$  than the baseline activity for monometallic Cu ( $A_{\text{Cu}} = (130 \pm 10) \text{ L/(g·min)}$ ). These metals act as inhibitors for the dechlorination reaction by the Cu catalyst and hence the increased selectivity towards DCM. Although for the systems Cu/Zn, Cu/Ce, Cu/Al, Cu/Sn, and Cu/Co, selectivity towards  $\text{CH}_4$  was lower than Pd/Cu and Ni/Cu, the chloride yields were comparable (details are presented in the appendix Table A3-1). Hence radical coupling reactions could be considered to be more pronounced for these metal combinations.

As shown in Figure 14, the selectivity towards DCM was 2-3 mol-% for Ag, Ag/Cu (co-red), Ag/Cu (mix), and Ag/Cu (sep) systems while the selectivity towards  $\text{CH}_4$  was 92 mol-%. The

DCM selectivity for Ag-containing catalysts was nearly 6.5 times lower than the baseline for Cu ( $S_{\text{DCM}} = (13 \pm 2)$  mol-%). However, the MCM selectivity 5-6 mol-%, was nearly 17 times higher than for Cu ( $S_{\text{MCM}} = (0.3 \pm 0.2)$  mol-%). The MCM for Ag/Cu systems remained when the reaction was continued for 20 h ( $c_{20\text{h}, \text{NaBH}_4} = 75$  mg/L) implying it is more-or-less a dead-end product. As shown in Figure 15, the synthesis procedure for the bimetallic Ag/Cu particles has no significant effect on the product selectivity patterns and specific metal activities. For the powdered Ag/Cu (H<sub>2</sub>-red), the product selectivity patterns (data presented in the appendix Table A3-3) were similar to those of the three bimetallic Ag/Cu particles. However, the specific metal activity for the dechlorination of CF using Ag/Cu (H<sub>2</sub>-red) was ( $A_m = (3 \pm 1)$  L/(g·min)) which was lower by a factor of about 27 in comparison to the other three bimetallic Ag/Cu particles. Further assessment to explain the lower specific metal activity of the Ag/Cu (H<sub>2</sub>-red) was not done.

The further advantage of the Ag-containing catalysts is that the DCM does not accumulate but is subsequently dechlorinated in a second step. The specific activity for dechlorination of DCM using Ag/Cu (co-red) ( $A_{\text{Ag/Cu,DCM}} = (1.0 \pm 0.5)$  L/(g·min)) was higher by a factor of 4.5 than for monometallic Cu ( $A_{\text{Cu,DCM}} = (0.22 \pm 0.02)$  L/(g·min)). Ag<sup>0</sup> + NaBH<sub>4</sub> was also more potent for the dechlorination of DCM with the specific Ag activity ( $A_{\text{Ag,DCM}} = (2.1 \pm 0.5)$  L/(g·min)) being higher by a factor of 9.5 compared to the baseline for monometallic Cu ( $A_{\text{Cu,DCM}} = (0.22 \pm 0.02)$  L/(g·min)). The ratio of specific Ag activities for dechlorination of CF and DCM is  $A_{\text{Ag,CF}}/A_{\text{Ag,DCM}} = 9.5$ . Similarly, for Ag/Cu (co-red), the ratio of the specific metal activities for dechlorination of CF and DCM  $A_{m,\text{CF}}/A_{m,\text{DCM}} = 80$ . These ratios in comparison to the ratios  $A_{\text{Cu,CF}}/A_{\text{Cu,DCM}} = 591$  and  $A_{\text{Pd,CF}}/A_{\text{Pd,DCM}} = 533$ , show that DCM dechlorination is better handled when Ag is present.

Although selectivity towards DCM was lower for  $\text{Ag}^0 + \text{NaBH}_4$ , the specific Ag activity  $A_{\text{Ag}}$  for dechlorination of CF was  $(25 \pm 5) \text{ L}/(\text{g}\cdot\text{min})$  which was lower by a factor of 6 and 4 than the baseline activity for Cu ( $A_{\text{Cu}} = (130 \pm 10) \text{ L}/(\text{g}\cdot\text{min})$ ) and Ag/Cu (co-red) ( $A_{\text{m}} = (80 \pm 5) \text{ L}/(\text{g}\cdot\text{min})$ ), respectively. Metallic Ag might be subject to self-poisoning when it comes into contact with chloride due to the possible formation of AgCl coatings. Surprisingly, this deactivation did not happen since the specific Ag activity for dechlorination of CF increased slightly through the addition of NaCl at the start of the reaction. The specific Ag activities  $A_{\text{Ag}}$  were  $(20 \pm 5) \text{ L}/(\text{g}\cdot\text{min})$ ,  $(30 \pm 5) \text{ L}/(\text{g}\cdot\text{min})$  and  $(40 \pm 5) \text{ L}/(\text{g}\cdot\text{min})$  in the presence of 5, 20 and 500 mg/L NaCl, respectively.

It was demonstrated earlier in this work that the concentration of the catalyst  $c_{\text{Cu}} = 100 \text{ mg/L}$  was essential to avoid the accumulation of DCM in the system. As could be demonstrated, a second alternative to mitigate DCM accumulation in the reactors during the dechlorination of CF is to use either Ag or bimetallic Ag/Cu particles. However, Ag (whose cost is about USD 0.84/g Ag) (Silver Prices, 2021) costs more than Cu (USD 0.009/g Cu) by a factor of about 90 on a mass basis. Since Ag is expensive and also a lower specific Ag activity, bimetallic Ag/Cu particles are recommended for dechlorination of CF. For the bimetallic systems, about 25 wt-% Ag onto Cu could achieve similar product selectivity patterns as monometallic Ag. Therefore, only catalytic amounts of metallic Ag onto Cu are necessary. Nevertheless, it cannot be disregarded that the selectivities of MCM are an order of magnitude higher with Ag-containing catalysts (5 mol-% compared to 0.3 mol-% with monometallic Cu).

A third alternative to eliminate the accumulation of DCM in the reactor during the dechlorination of CF is to combine  $\text{Cu}^0 + \text{NaBH}_4$  with vitamin B12. As shown in Figure 14, the combination of  $\text{Cu}^0 + \text{NaBH}_4$  and vitamin B12 decreased selectivity towards DCM from

( $13 \pm 2$ ) mol-% to ( $2 \pm 1$ ) mol-%. This was due to the accelerated dechlorination of DCM. Hence it is not a true selectivity. The specific metal activity  $A_m$  for dechlorination of DCM as educt using  $\text{Cu}^0 + \text{NaBH}_4 + \text{vitamin B12}$  was ( $15 \pm 3$ ) L/(g·min) which was higher by a factor of 68 than for Cu ( $A_{\text{Cu,DCM}} = (0.22 \pm 0.02)$  L/(g·min)). The selectivity to MCM using  $\text{Cu}^0 + \text{NaBH}_4 + \text{vitamin B12}$  was ( $3 \pm 1$ ) mol-%, which was higher by a factor of 10 than for Cu ( $S_{\text{MCM}} = (0.3 \pm 0.2)$  mol-%). Nevertheless, the MCM was not a dead-end product but further dechlorinated in a second step when the reaction was continued for 120 min.

The specific metal activity  $A_m$  for the dechlorination of CF ( $A_{m,\text{CF}} = (260 \pm 20)$  L/(g·min)) was higher by a factor of 2 than for monometallic Cu ( $A_{\text{Cu,CF}} = (130 \pm 10)$  L/(g·min)). Therefore, the system comprising  $\text{Cu}^0 + \text{NaBH}_4 + \text{vitamin B12}$  accelerates dechlorination reactions for both CF and DCM. As shown in Figure 14, the system comprised of Cu/Co +  $\text{NaBH}_4$  increases selectivity towards DCM ( $S_{\text{DCM}} = (25 \pm 5)$  mol-%) and also as shown in Figure 15, has a lower specific metal activity ( $A_m = (20 \pm 5)$  L/(g·min)). In separate experiments for dechlorination of CF, the selectivity to DCM using vitamin B12 +  $\text{NaBH}_4$  was ( $40 \pm 5$ ) mol-%. Therefore, a kind of synergy between  $\text{Cu}^0 + \text{NaBH}_4$  and vitamin B12 exists that accelerates the dechlorination of CF and DCM. Thus vitamin B12 as a chelating agent or redox molecule provides an electronic environment that is beneficial for the dechlorination reactions. As described earlier in chapter 2.5, reductive dehalogenation of HOCs by vitamin B12 in the presence of reducing agents such as titanium (III) acetate and  $\text{NaBH}_4$  has been considered to involve two-electron transfer processes to the electrophilic carbon by the super-reduced form of vitamin B12 ( $\text{Co}^{1+}$ , assigned B12s) (Burriss et al., 1996; Huang et al., 2013, 2015; Shey and van der Donk, 2000; Shimakoshi et al., 2005). In the presence of  $\text{Cu}^0 + \text{NaBH}_4$ , vitamin B12 was considered to act as an electron mediator for dechlorination of DCM (Huang et al., 2013, 2015). Therefore, two-electron transfer processes

could be responsible for the accelerated dechlorination of CF and DCM by  $\text{Cu}^0 + \text{NaBH}_4 + \text{vitamin B12}$ .

For the system comprising  $\text{Cu}^0 + \text{NaBH}_4 + \text{vitamin B12}$ , the ratio of the specific metal activities for dechlorination of CF and DCM is  $A_{\text{m,CF}}/A_{\text{m,DCM}} = 17$  which is more-or-less comparable to  $A_{\text{Ag,CF}}/A_{\text{Ag,DCM}} = 9.5$ . Due to the higher specific metal activities for the dechlorination of both CF and DCM by  $\text{Cu}^0 + \text{NaBH}_4 + \text{vitamin B12}$ , vitamin B12 provides a better alternative to Ag. In conclusion, the system  $\text{Cu}^0 + \text{NaBH}_4 + \text{vitamin B12}$  can be considered as an optimal catalysts combination for the dechlorination of CF in water. Nevertheless, the high cost of vitamin B12 as a fine chemical (currently USD 96/g) must be put into consideration during the decision making process.

#### *Dechlorination of CF using CIC, S/CIC, Cu/CIC, and Cu/S/CIC*

As described earlier for  $\text{Pd} + \text{H}_2$  and  $\text{Pd}^0 + \text{NaBH}_4$ , the type of reductant had no marked effect on product selectivity patterns during the dechlorination of CF. As stated earlier, Cu is unable to activate molecular hydrogen into active  $\text{H}^*$  under ambient conditions. Therefore, it was combined with ZVI as a source of activated hydrogen with the intention to allow nascent hydrogen to interact with the Cu surface. ZVI-containing composite colloids (Carbo-Iron<sup>®</sup>) with and without sulfide doping for corrosion protection (CIC and S/CIC) were applied as sorption active reagents and additionally modified by 2 wt-% Cu to obtain Cu/CIC and Cu/S/CIC. CIC consists of colloidal activated carbon and embedded nZVI structures (Bleyl et al., 2012; Mackenzie et al., 2012). The product selectivity patterns for the dechlorination of CF using CIC, Cu/CIC, S/CIC, and Cu/S/CIC are presented in Figure 16. The corresponding chloride yields and  $k_{\text{obs}}$  data are presented in the appendix Table A3-2.

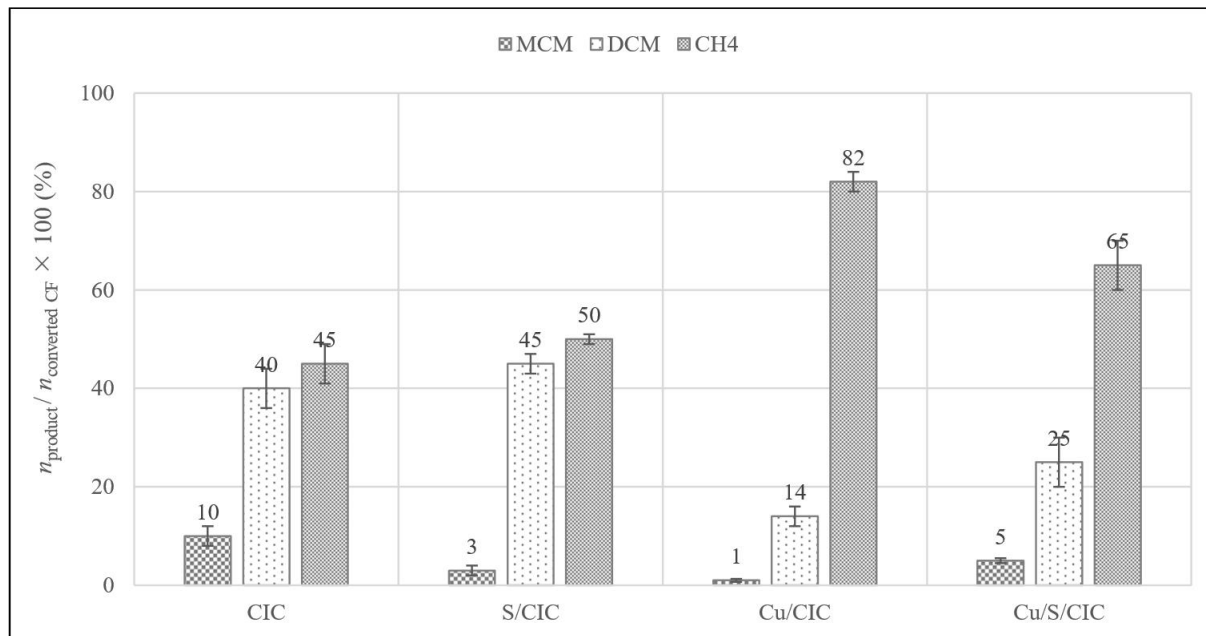


**Figure 16:** Product selectivity patterns during the dechlorination of CF using CIC, S/CIC, Cu/CIC, and Cu/S/CIC ( $c_{\text{CIC}} = c_{\text{Cu/CIC}} = c_{\text{Cu/S/CIC}} = 500 \text{ mg/L}$ ;  $c_{0,\text{CF}} = 10 \text{ mg/L}$ ;  $\text{pH} = 8$ ). Selectivities determined at CF conversion  $\geq 95 \%$ .

The dechlorination of CF using CIC and S/CIC combines both adsorptions onto the AC carriers and electron transfer from the embedded nZVI reagent. As shown in Figure 16, the dechlorination of CF using CIC and S/CIC shows that selectivities towards MCM, DCM, and CH<sub>4</sub> were in the range 3-10, 40-45, and 45-50 mol-%, respectively. The sum of C<sub>2</sub>H<sub>6</sub> and C<sub>2</sub>H<sub>4</sub> was about 2-3 mol-% of the CF converted, an indication of the formation of higher chlorinated compounds due to radical coupling reactions. Higher molecular weight substances were not detected by headspace analysis. Solvent extraction was not performed. Thus their formation cannot be fully ruled out. The selectivity towards DCM and CH<sub>4</sub> during the dechlorination of CF using CIC and S/CIC were similar to the other iron metal reagents, such as nZVI<sup>BH</sup> (data presented earlier

in Table 6). Thus adsorption of CF onto the AC carrier and sulfidation of the embedded ZVI has no marked effects on the product selectivity patterns.

The deposition of metallic Cu onto nZVI led to the formation of galvanic elements. During nZVI corrosion, adsorbed  $H^+$  ions can gain electrons and are then transformed to nascent hydrogen on the Cu surface. The catalytic dechlorination of CF then occurs at the Cu surface mediated by active  $H^*$ . Note that no borohydride was used as a reductant for all the systems in Figure 16. As shown in Figure 16, for Cu/CIC, selectivities to DCM and  $CH_4$  were  $(14 \pm 2)$  mol-% and  $(82 \pm 2)$  mol-%, respectively. The product selectivities were comparable to those observed by  $Cu^0 + NaBH_4$ . Hence the AC carrier and nZVI as a source for nascent hydrogen have no marked effect on the selectivity patterns. For Cu/S/CIC, selectivities towards DCM and  $CH_4$  were  $(25 \pm 5)$  mol-% and  $(65 \pm 5)$  mol-%, respectively. As described earlier, for  $Cu^0 + NaBH_4$  in the presence of  $Na_2S$  (Figure 13 (b)), the formation of CuS may explain the increased selectivity towards DCM for Cu/S/CIC. For Cu/CIC and Cu/S/CIC, DCM was not a dead-end product but was subsequently dechlorinated when the reaction was continued for 72-100 h, and the final selectivities towards MCM, DCM, and  $CH_4$  were in the range 1-2, 1-3, and 95-96 mol-%, respectively.

As carried out for pure Cu NPs, further modification of Cu/CIC and Cu/S/CIC was done using Pd, Ni, and Ag to evaluate product selectivity patterns during the dechlorination of CF in water as shown in Figure 17. The corresponding chloride yields and  $k_{obs}$  data are presented in the appendix Table A3-2.

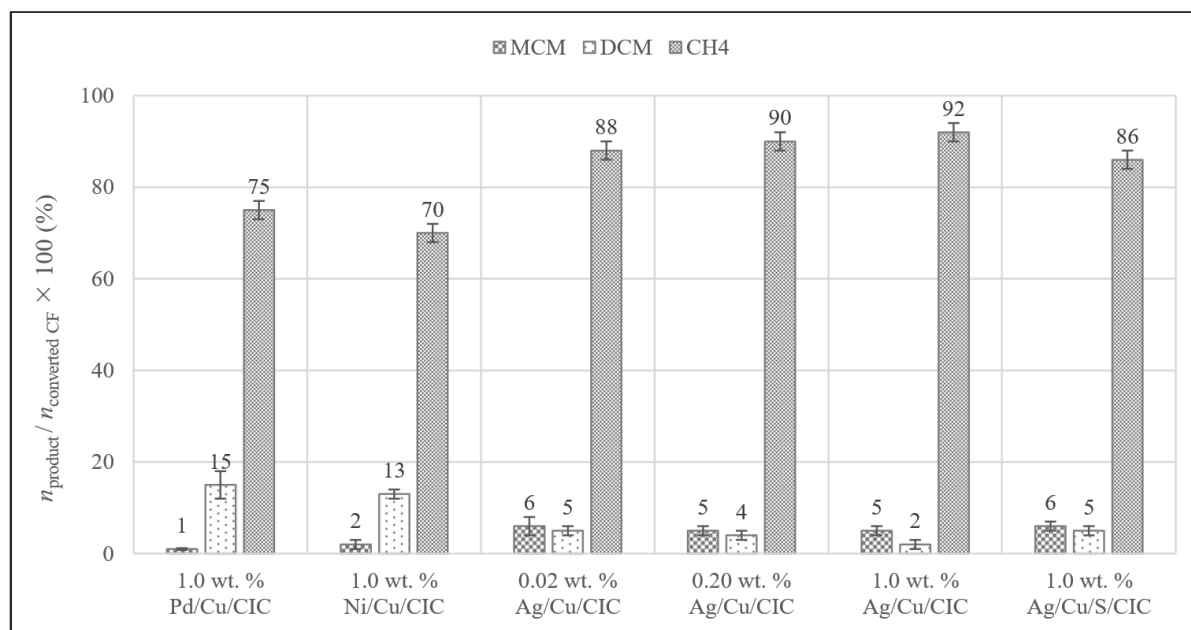


**Figure 17:** Product selectivity patterns during the dechlorination of CF using metal-modified Cu/CIC and Cu/S/CIC ( $c_{\text{Pd/Cu/CIC}} = c_{\text{Ni/Cu/CIC}} = c_{\text{Ag/Cu/CIC}} = c_{\text{Ag/Cu/S/CIC}} = 500 \text{ mg/L}$ ;  $c_{0,\text{CF}} = 10 \text{ mg/L}$ ;  $\text{pH}_0 = 6.5$ ). Selectivities determined at CF conversion  $\geq 95 \%$ .

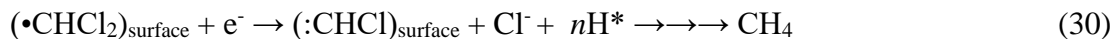
As shown in Figure 17, the metals Pd and Ni have no marked effects on the selectivity towards DCM. Similar to the bimetallic Ag/Cu particles in the presence of  $\text{NaBH}_4$  (Figure 14), upon deposition of Ag onto Cu/CIC and Cu/S/CIC, the selectivities to  $\text{CH}_4$ , DCM and MCM were in the range 86-92, 2-5, and 5-6 mol-%, respectively. The product selectivity patterns were independent of Ag loading on the Cu/CIC. This suggests that only catalytic amounts of Ag are required. Since the product selectivities during dechlorination of CF using Cu/CIC, Cu/S/CIC and their Ag-modified materials were comparable to those of  $\text{Cu}^0 + \text{NaBH}_4$  and bimetallic Ag/Cu particles, the nature of the primary reductant, i.e.  $\text{NaBH}_4$  or ZVI, when used with Cu or Ag catalysts has no marked effect on the product selectivities. From the mechanistic point of view, this is a very significant finding. Apparently, the various primary reductants generate the same reactive species (electrons or active  $\text{H}^*$ ) which are responsible for the initial surface-mediated (catalytic) dechlorination steps. Hydride species are less likely to be involved therein.

### *Dechlorination of CF using Cu/AC, Cu/ACF, Cu/zeolites, and Cu/resin*

As it was demonstrated earlier for Cu/CIC and Cu/S/CIC, the AC carrier does not bring any benefit in the product selectivities during the dechlorination of CF. Nevertheless, Cu-modified AC, ACF, zeolites, and amberlite resin were also tested for the dechlorination of CF in the presence of NaBH<sub>4</sub>. The Cu-modified materials were cleaned to ensure that CF dechlorination was due to copper within the material but not due to copper-leached into the aqueous phase. For Cu/AC, Cu/ACF, Cu/resin, and Cu/zeolites, the selectivities to MCM, DCM, and CH<sub>4</sub> were in the range 0.5-1, 12-14, and 81-86 mol-% (details are presented in the appendix Table A3-3). The product selectivity patterns were within the same range as that for Cu<sup>0</sup> + NaBH<sub>4</sub> which shows that all these carriers for the Cu metal present no marked benefit in terms of dechlorination selectivities.

### *Dechlorination of CF under the influence of external electric potentials*

The product selectivity patterns from the dechlorination of CF can as well be considered to be controlled by the competition between i) a second electron-transfer step and ii) a saturation of surface intermediates by active H\* as shown in reactions 30 and 31. In reaction 30, *n* refers to the moles transferred.



The dual role of surface-bound hydrogen species becomes obvious: they are necessary for the formation of methane from all intermediates (reaction 30) and they are responsible for the stabilization (and afterward release) of chlorinated intermediates (reaction 31). Therefore, two

hypothetical strategies were considered: i) are the two hydrogen species in reactions 30 and 31 identical or different? If different, can one favor the 'right' hydrogen? and ii) an optimal interplay between electron delivery, hydrogen availability, and adsorption state (physisorption versus chemisorption) is the key.

A possible smart way to control one of these parameters independently was by application of cathodic potential on Cu electrodes. The electrochemical setups are presented in the appendix Figure A1-1. Cu mesh and Cu/ACF were used as the working electrodes for electrochemical dechlorination of CF. Since Cu metal acts as a catalyst, the experimental conditions were adjusted such that Cu exists in its oxidation state 0 (details are presented in the appendix Figure A1-3). ACF as conductive support material for Cu was applied at potentials where water electrolysis was minimized (details are presented in the appendix Figure A1-4).

For comparison purposes, the selectivity patterns during the dechlorination of CF were also investigated in the absence of applied potential (open-circuit system) and the presence of cathodic potential and NaBH<sub>4</sub> as shown in Table 7. For further comparison, electrochemical dechlorination of CF was carried out using the Cu electrode at a cathodic potential of -1.1 V.

**Table 7:** Product selectivity patterns during the dechlorination of CF in water using Cu- and Cu/ACF-electrodes under an external electric potential and in the presence or absence of NaBH<sub>4</sub> ( $m_{\text{Cu-electrode}} = 370 \text{ mg}$ ;  $m_{0.5 \text{ wt-\% Cu/AC}} = 6.3 \text{ mg}$ ;  $c_{0,\text{CF}} = 5 \text{ mg/L}$ ;  $c_{0,\text{NaBH}_4} = 300 \text{ mg/L}$ ;  $\text{pH}_0 = 7$ ;  $V_{\text{electrolyte}} = 400 \text{ mL}$  of  $0.1 \text{ M Na}_2\text{SO}_4$ ;  $V_{\text{h}} = 100 \text{ mL}$ )

Electrode type and reaction conditions	$n_{\text{product}} / n_{\text{transferred CF}} \times 100$ (%)			Cl <sup>-</sup> yield (mol-%)
	MCM	DCM	CH <sub>4</sub>	
Cu electrode + NaBH <sub>4</sub> (open circuit system)	5 ± 1	14 ± 2	82 ± 2	84 ± 3
-1.1 V <sup>a</sup> + Cu electrode (electrochemical dechlorination of CF)	2 ± 1	13 ± 2	82 ± 2	85 ± 2
-0.8 V <sup>a</sup> + Cu electrode + NaBH <sub>4</sub>	3 ± 1	11 ± 3	84 ± 3	84 ± 2
-1.0 V <sup>a</sup> + Cu electrode + NaBH <sub>4</sub>	4 ± 2	12 ± 3	85 ± 2	85 ± 3
-0.8 V <sup>a</sup> + Cu/ACF electrode + NaBH <sub>4</sub>	3 ± 1	10 ± 2	85 ± 2	88 ± 2

<sup>a</sup> Applied potential of the working electrode measured against Ag/AgCl.

Product selectivities were determined at 30-40 % CF conversion.

The chloride yields were determined at a CF conversion of  $\geq 95$  %.

For all CF dechlorination reactions, the sum of C<sub>2</sub>H<sub>4</sub> and C<sub>2</sub>H<sub>6</sub> accounts for 1-2 mol-% measured at CF conversion  $\geq 95$  %.

Control experiments showed that CF was stable for at least 12 h when the applied potential was maintained at -0.5 and -0.8 V versus Ag/AgCl and the electrolyte and headspace having been purged with H<sub>2</sub> gas before the addition of CF. Thus it shows that activation of dissolved H<sub>2</sub> at the Cu electrode to form active H\* due to the applied potential did not occur. As shown in Table 7, there was no marked change in selectivity patterns during the dechlorination of CF at the different electrodes in the presence or absence of applied potentials. Also, the combination of NaBH<sub>4</sub> and applied potential had no significant effect on the selectivity patterns. From the mechanistic point of view, these results indicate that the electron-transfer steps to CF adsorbed at the surfaces of Cu and Cu/ACF are not driven by the potential of free electrons (in the conduction band) but more likely by reactive hydrogen species, resulting from BH<sub>4</sub><sup>-</sup> decomposition (possibly hydride species). Surprisingly, similar product selectivity patterns were obtained for the i) borohydride-assisted

dechlorination of CF and ii) electrochemical dechlorination reaction at cathodic potential of -1.1 V (data in Table 7). A similar study for the electrochemical dechlorination of CF in water using a graphite electrode showed that an increase in cathodic potential from -0.75 to -1.3 V had no marked effect on the selectivity patterns (Battke, 2006). Apparently, these results (Table 7) show that both reactive species (active H<sup>\*</sup> or electrons) are responsible for the initial surface-mediated (catalytic) dechlorination steps. The advantage of the cathodic potential of -1.1 V at the Cu electrode was that DCM was not a dead-end product but was subsequently dechlorinated when the reaction was continued for 50 h (i.e.  $S_{\text{DCM},50\text{h}} = (2 \pm 1) \text{ mol-\%}$ ).

In conclusion, the results presented in this chapter with CHCl<sub>3</sub> as the substrate show that similar selectivity patterns (ratio of CH<sub>2</sub>Cl<sub>2</sub>: CH<sub>4</sub>) are observed for very different reduction systems. This is the opposite in comparison to the findings of Farrell et al (Li and Farrell, 2000, 2001; Wang et al., 2004; Wang and Farrell, 2003). Nevertheless, it supports the view that presently we are not in a position to explain or even predict initial product selectivity patterns in heterogeneous reductive dechlorination of CHCl<sub>3</sub> in aqueous suspensions.

#### 4.1.2 Dehalogenation of CCl<sub>4</sub>, CFCl<sub>3</sub>, CBrCl<sub>3</sub> and CCl<sub>3</sub>-CH<sub>3</sub> using Cu<sup>0</sup> + NaBH<sub>4</sub>

As presented earlier, selectivities towards CH<sub>4</sub>, DCM, and MCM were (84 ± 2) mol-%, (13 ± 2) mol-%, and (0.3 ± 0.2) mol-%, respectively for the dechlorination of CF using Cu<sup>0</sup> + NaBH<sub>4</sub>. The influence of the R-substituent on selectivity patterns for the dehalogenation of CCl<sub>4</sub>, CFCl<sub>3</sub>, CBrCl<sub>3</sub>, and 1,1,1-TCA was investigated. The selectivities were determined at the point where the educt conversion was ≥ 95 % and at the point where the conversion of the immediate first intermediates CHCl<sub>3</sub>, CHCl<sub>2</sub>F, and CHCl<sub>2</sub>-CH<sub>3</sub> was ≥ 95 %. The data for the product selectivity patterns during the dehalogenation of the halogenated methanes and their first

daughter products are presented in Figure 18. The corresponding chloride yield data are presented in the appendix Table A3-4.

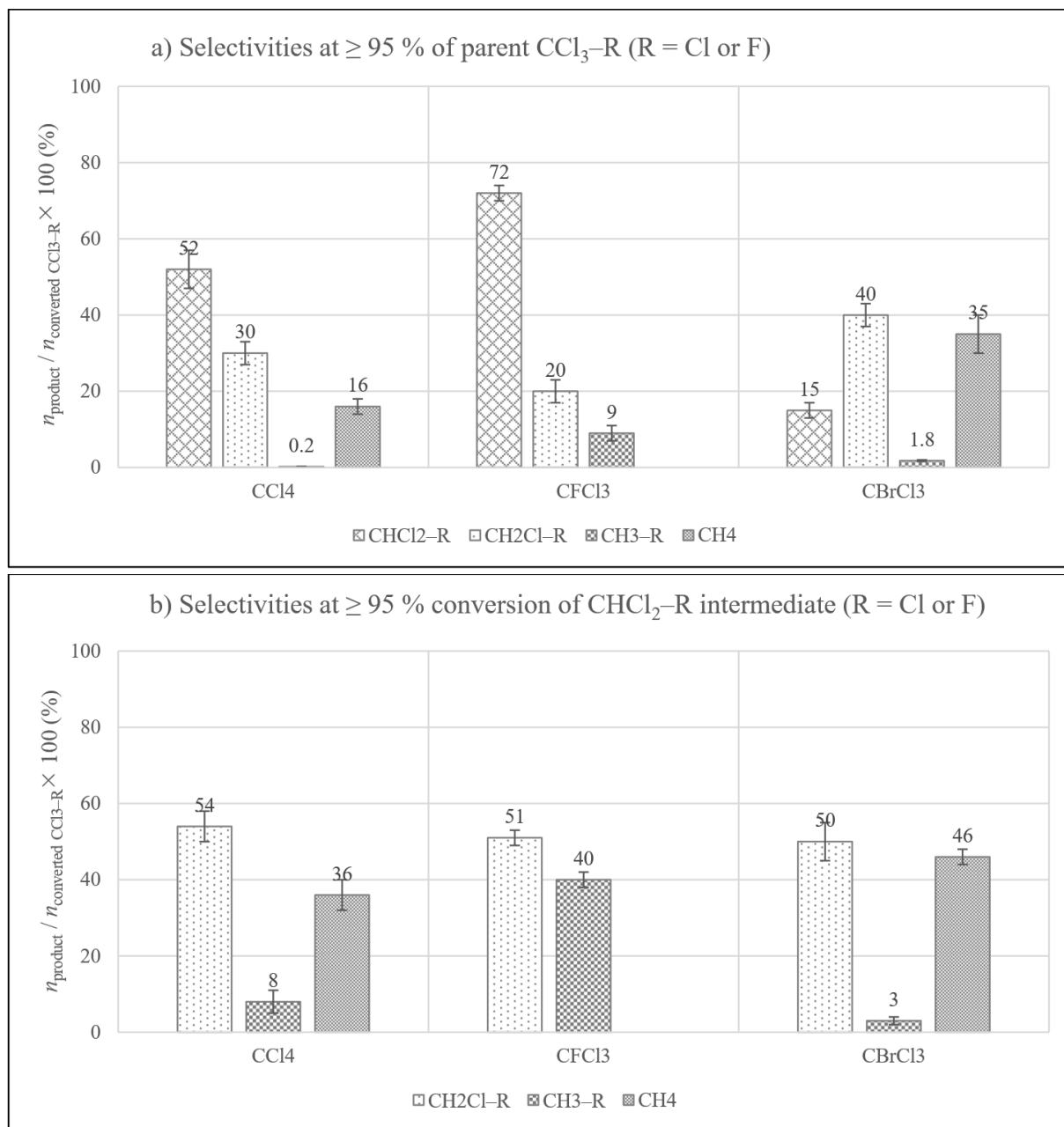


**Figure 18:** Product selectivity patterns during the dehalogenation of  $\text{CCl}_4$ ,  $\text{CFCl}_3$  and  $\text{CBrCl}_3$  using  $\text{Cu}^0 + \text{NaBH}_4$  a) Selectivities at  $\geq 95\%$  conversion of the parent  $\text{CCl}_3\text{-R}$  compound and b) Selectivities at  $\geq 95\%$  conversion of the immediate  $\text{CHCl}_2\text{-R}$  intermediate ( $c_{\text{Cu}} = 0.2\text{-}2 \text{ mg/L}$ ;  $c_{0,\text{educt}} = 20 \text{ mg/L}$ ;  $c_{0,\text{NaBH}_4} = 300 \text{ mg/L}$ ;  $\text{pH} = 10$ ).

The product selectivity patterns at  $\geq 95\%$  conversion of  $\text{CCl}_4$ ,  $\text{CFCl}_3$ , and  $\text{CBrCl}_3$  are as shown in Figure 18 (a). For  $\text{CCl}_4$  and  $\text{CFCl}_3$ ,  $\text{CF}$  and  $\text{CHCl}_2\text{F}$  were the major intermediates, respectively, and accounted for 52-72 mol-% of the educt converted. The selectivity to  $\text{CF}$  was about 15 mol-% of  $\text{CBrCl}_3$  converted. A slightly higher  $\text{DCM}$  selectivity of 40 mol-% was observed for  $\text{CBrCl}_3$  than that for  $\text{CCl}_4$  and  $\text{CH}_2\text{CIF}$  from  $\text{CFCl}_3$ . That means the second dehalogenation step is not as preferred as we could observe for the reduction of the C–Br bond. For  $\text{CCl}_4$  and  $\text{CBrCl}_3$ , the selectivities to  $\text{CH}_4$  were 16 and 35 mol-%, respectively. Both  $\text{CH}_4$  and  $\text{F}^-$  were not detected during the dehalogenation of  $\text{CFCl}_3$  implying that cleavage of the C–F bond using  $\text{Cu}^0 + \text{NaBH}_4$  did not occur. Therefore, the dehalogenation reaction occurred preferably via hydrogenolysis which led to the high selectivities of the halogenated intermediates during the dehalogenation of  $\text{CCl}_4$ ,  $\text{CFCl}_3$ , and  $\text{CBrCl}_3$ .

The intermediates  $\text{CF}$  and  $\text{CHCl}_2\text{F}$  did not accumulate but were further transformed as can be seen in Figure 18 (b) by the further generation of  $\text{MCM}$ ,  $\text{DCM}$ , and  $\text{CH}_4$ . Similarly, the further transformation of  $\text{CHCl}_2\text{F}$  led to an increase in the daughter products  $\text{CH}_2\text{CIF}$  and  $\text{CH}_3\text{–F}$ .  $\text{MCM}$ ,  $\text{DCM}$ ,  $\text{CH}_2\text{CIF}$ , and  $\text{CH}_3\text{–F}$  persisted when the reaction was continued for 30 h ( $C_{30\text{h},\text{NaBH}_4} = 38 \text{ mg/L}$ ), hence they were considered more-or-less as dead-end byproducts under the chosen reaction conditions with low  $\text{Cu}$  concentrations. Therefore, when  $\text{F}$ ,  $\text{Cl}$ , and  $\text{Br}$  replace the chloroform's H-substituent, there was a shift in selectivities which may be due to the electron-withdrawing and steric effects at the electrophilic carbon.

To simulate steric effects, dechlorination of 1,1,1-TCA, where the chloroform's H-substituent was replaced by the more bulky methyl group, was investigated using  $\text{Cu}^0 + \text{NaBH}_4$  to evaluate the product selectivity patterns as shown in Figure 19.

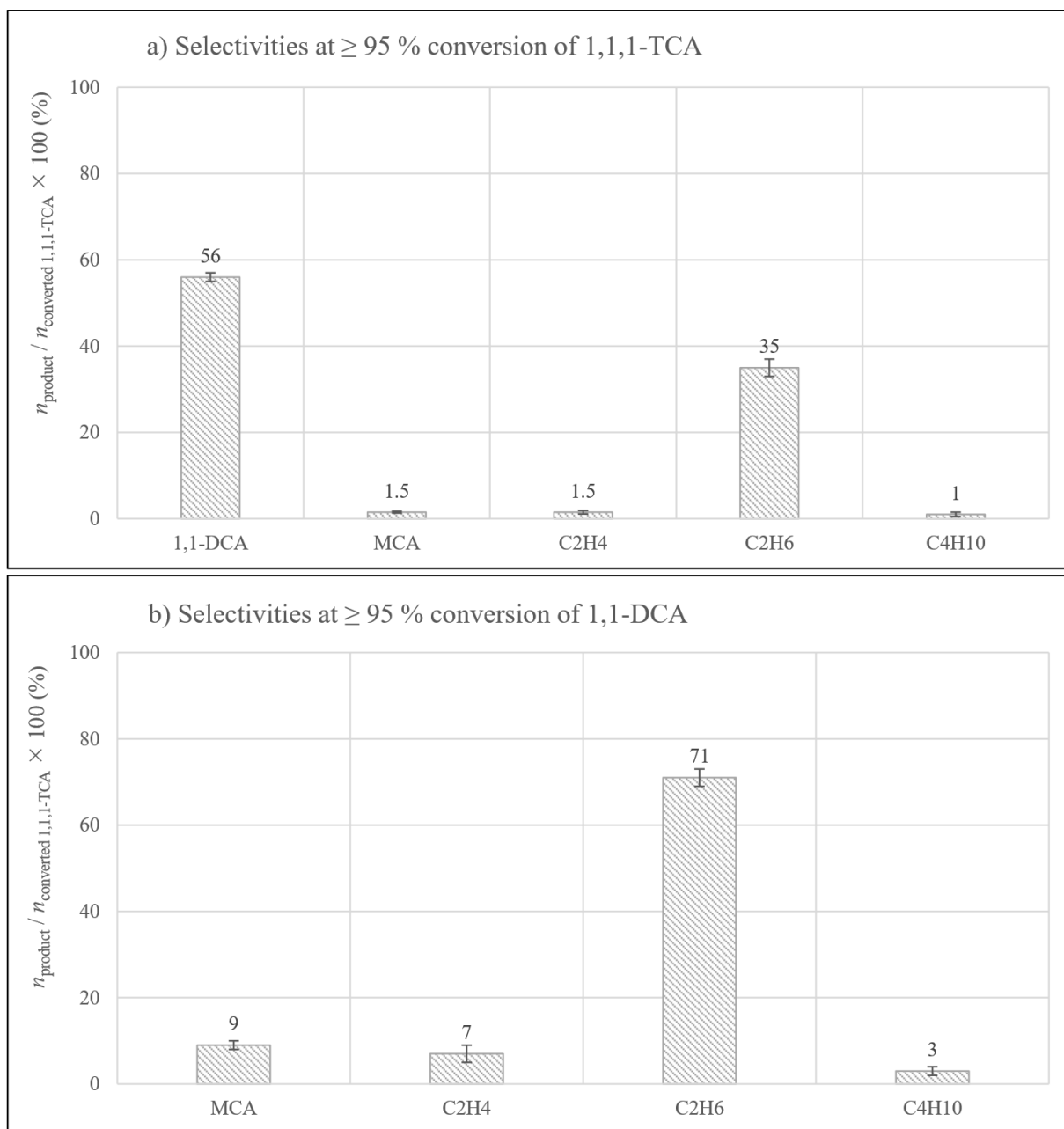


**Figure 19:** Product selectivity patterns during the dechlorination of 1,1,1-TCA using  $\text{Cu}^0 + \text{NaBH}_4$  a) Selectivities at  $\geq 95\%$  conversion of 1,1,1-TCA and b) Selectivities at  $\geq 95\%$  conversion of the 1,1-DCA intermediate ( $c_{\text{Cu}} = 1 \text{ mg/L}$ ;  $c_{0,1,1,1\text{-TCA}} = 20 \text{ mg/L}$ ;  $c_{0,\text{NaBH}_4} = 300 \text{ mg/L}$ ;  $\text{pH} = 10$ ).

As shown in Figure 19 (a), the selectivities to 1,1-DCA, MCA, C<sub>2</sub>H<sub>4</sub>, C<sub>4</sub>H<sub>10</sub> and C<sub>2</sub>H<sub>6</sub> were 56, 1.5, 1.5, 1 and 35 mol-%, respectively. The speculated first step during the dechlorination of 1,1,1-TCA involves the transfer of one electron to the adsorbed molecule according to the reaction

$\text{CCl}_3\text{CH}_3 + e^- \rightarrow \bullet\text{CCl}_2\text{CH}_3 + \text{Cl}^-$  (Fennelly and Roberts, 1998). 1,1-DCA as the major product could be formed by a second electron transfer step combined with protonation of the intermediate dichloroethyl radical anion according to the reaction ( $\bullet\text{CCl}_2\text{CH}_3 + e^- + \text{H}^+ \rightarrow \text{CHCl}_2\text{CH}_3$ ). Since the selectivity to 1,1-DCA was about 56 mol-%, hydrogenolysis can be considered the main reaction pathway for the initial dechlorination of 1,1,1-TCA.

As shown in Figure 19 (b), further dechlorination of 1,1-DCA leads to the increased amounts of MCA,  $\text{C}_2\text{H}_4$ ,  $\text{C}_4\text{H}_{10}$ , and  $\text{C}_2\text{H}_6$  to 9, 7, 3, and 71 mol-%, respectively. MCA was more-or-less a dead-end byproduct at the low catalyst concentration ( $c_{\text{Cu}} = 1 \text{ mg/L}$ ). Its dechlorination could be observed when the catalyst concentration was increased to  $c_{\text{Cu}} = 100 \text{ mg/L}$ . The specific Cu activity for the dechlorination of MCA was ( $A_{\text{Cu,MCA}} = (0.010 \pm 0.005) \text{ L}/(\text{g}\cdot\text{min})$ ). The formation of  $\text{C}_4\text{H}_{10}$  shows that radical coupling reactions are involved albeit to a minor extent. Fennelly and Roberts, (1998), suggested that the formation of  $\text{C}_2\text{H}_4$  from 1,1,1-TCA may occur through H-rearrangement reactions involving ethyl carbene ( $:\text{CHCH}_3$ ) intermediates.

For  $\text{CFCl}_3$  and  $\text{CCl}_4$ , the F and Cl substituents at the  $\text{CCl}_3$ -group have an electron-withdrawing effect on the carbon, making it more electrophilic, hence destabilizing C-centered radicals. For 1,1,1-TCA, the methyl substituent may stabilize radical intermediates via hyperconjugation. Since the selectivities for the generation of the first intermediates CF,  $\text{CHCl}_2\text{F}$ , and 1,1-DCA from  $\text{CCl}_4$ ,  $\text{CFCl}_3$ , and 1,1,1-TCA, respectively, were similar, electronic effects of the substituent play no significant role on the reaction selectivities. To further evaluate whether selectivity depends on the steric effects of the geminal R-substituent, the dechlorination of DCM and 1,1-DCA using  $\text{Cu}^0 + \text{NaBH}_4$  was investigated. The results are presented in Figure 20.

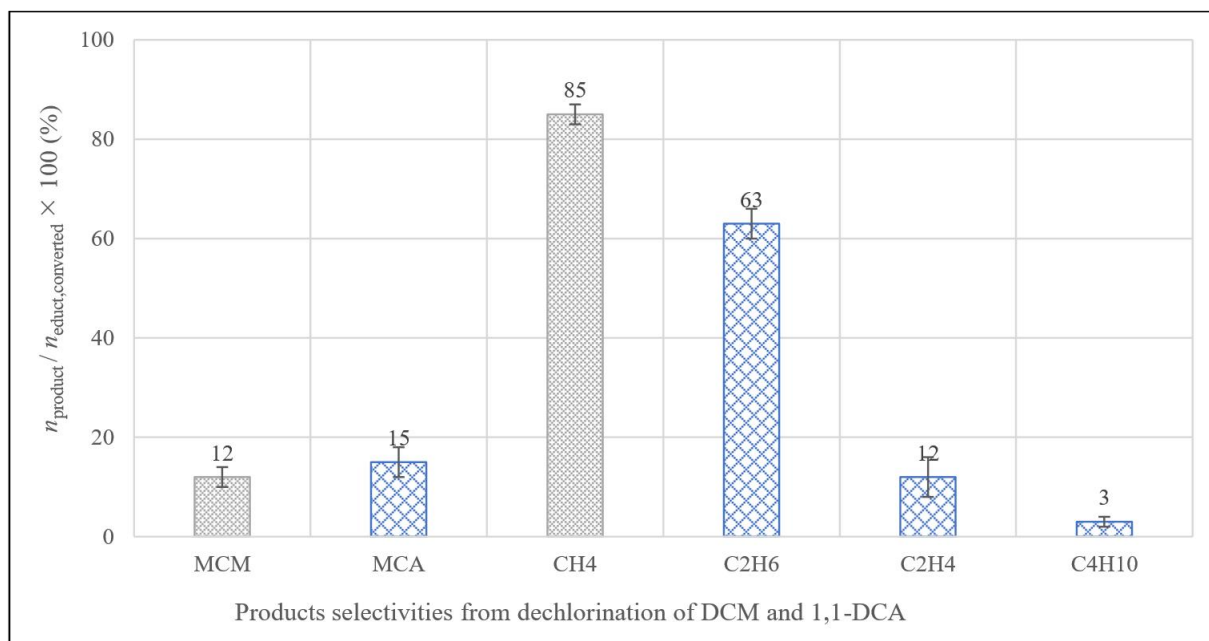


**Figure 20:** Product selectivity patterns for the dechlorination of DCM and 1,1-DCA using  $\text{Cu}^0 + \text{NaBH}_4$  ( $c_{\text{Cu}} = 50\text{-}100 \text{ mg/L}$ ;  $c_{0,\text{educt}} = 10\text{-}20 \text{ mg/L}$ ;  $c_{0,\text{NaBH}_4} = 300 \text{ mg/L}$ ;  $\text{pH} = 10$ ). Selectivity patterns determined at educt conversion  $\geq 95 \%$ . Grey and blue bars represent products from the dechlorination of DCM and 1,1-DCA, respectively.

As shown in Figure 20,  $\text{CH}_4$  and  $\text{C}_2\text{H}_6$  were the major products during the dechlorination of DCM and 1,1-DCA, respectively. Similar to 1,1,1-TCA, the formation of  $\text{C}_4\text{H}_{10}$  during dechlorination of 1,1-DCA shows that radical coupling reactions are involved albeit to a lower extent. Since  $\text{CH}_4$  and  $\text{C}_2\text{H}_6$  were the major products, it suggests that  $\alpha$ -elimination reaction is the main reaction pathway for the initial dechlorination of DCM and 1,1-DCA. As shown in Figure 18 (a), for  $\text{CCl}_4$ ,  $\text{CFCl}_3$ ,  $\text{CBrCl}_3$ , and 1,1,1-TCA (Figure 19 (a)), hydrogenolysis was the main reaction pathway. Therefore, the R-substituent that replaces the chloroform's H-substituent suggests that steric effects may be a limiting factor for the simultaneous removal of geminal chlorine atoms from the electrophilic carbon during the dehalogenation of  $\text{CCl}_3\text{-R}$  compounds via  $\alpha$ -elimination.

#### ***4.2 Application areas for Cu-, Pd- and nZVI-based systems***

As discussed in the earlier chapter 4.1 for the dechlorination of CF, the choice of the metallic reagent or catalyst determines the quantity and fate of the intermediate reaction byproducts, DCM and MCM. When reactivity, product selectivity, and the fate of intermediates are considered,  $\text{Cu}^0 + \text{NaBH}_4$  was best suited for the dechlorination of CF in comparison to  $\text{Pd} + \text{H}_2$  and nZVI. An evaluation of the three reduction systems also for a broader span of water contaminants is therefore advised. The evaluation of the dehalogenation capabilities of nZVI-, Pd- and Cu-based systems are not comparing like with like. Pd and Cu metals are true catalysts while nZVI is a reagent that is consumed by the target reaction. Besides, nZVI undergoes corrosion, where depending on the conditions, a considerable proportion of reduction equivalents is “lost”. Furthermore, various mechanisms are used by the three metals. nZVI is predominately an electron-transfer reagent and the activation of hydrogen plays a minor role. Metallic Pd as an effective catalyst for hydrogenation and HDC reactions can adsorb and dissociate hydrogen forming adsorbed surface hydrogen (Conrad et al., 1974) and absorb “subsurface hydrogen” (Teschner et al., 2010). Metallic Cu itself is not a potent reducing agent hence an external reducing agent such as  $\text{NaBH}_4$  should be supplied where H-species may act as reducing agents. Since CuH has been detected (Bennett et al., 2015; Schlesinger et al., 1953; Vaškelis et al., 1998), hydrides may as well be involved especially as dehalogenation agents at the surface. However, as in hydrosilylation (Díez-González and Nolan, 2008), where insertion of Cu-species leads to the cleavage of the C–X bond, such insertion may as well be implicated here. The variation in active reducing species concerning Cu-, Pd- and nZVI-based systems also suggests a wide range of underlying mechanisms and dehalogenation “abilities”. For all here-discussed systems, overall pollutant treatability, necessary metal input, expected treatment times, and knowledge about possible

byproducts are crucial decision tools needed for any application at field sites. Comparing metal-mass-based reaction rate constants or specific metal activities can therefore be used to transport these information sets to users.

#### *4.2.1 Specific metal activities for the reduction of HOCs using Cu-, Pd- and nZVI-based systems*

The appropriate kinetic parameter for a heterogeneous reaction such as dechlorination in aqueous suspension should be a surface-normalized parameter rather than a mass-related one. However, when comparing solid metal particles with no inner surface, the mass is a good alternative as a reference when the particles are roughly in the same size range and therefore having a similar surface area. The mass-related specific metal activities can then be used to provide an approximate comparison base. Mackenzie et al. (2006) have determined the specific Pd activities  $A_{Pd}$  for the reduction of various HOCs in water using a sieve fraction (63-125  $\mu\text{m}$ ) of the supported catalyst Pd/ $\gamma\text{-Al}_2\text{O}_3$ . However, it is inappropriate to directly use these data here for comparisons of specific Pd activities to those achieved with Pd nanoparticles for two reasons: (i) supported Pd clusters have a higher dispersity than the unsupported nanoparticles ( $n_{Pd \text{ surface}}: n_{Pd \text{ total}}$ ) and (ii) the reactants have to overcome two mass-transfer barriers in the porous catalyst: external film diffusion and intraparticle pore diffusion. The two phenomena act contrarily on the observable catalyst activities. The extent of the mass-transfer limitation depends on the specific reactivities; it is low for low reaction rate constants and vice versa. Nevertheless, the data can be used to gain insights into reactivity gradation of the reductive dehalogenation of HOCs belonging to a particular class and forecast reaction trends using other particle sizes or the same type of reductant.

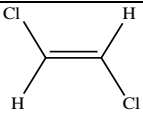
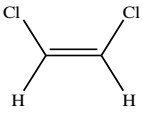
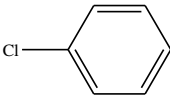
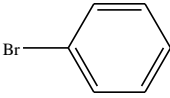
In the current study, specific Pd activities for the reductive dehalogenation of selected HOCs were determined experimentally at pH 10 (adjusted by 1 M NaOH) using colloidal Pd NPs

with mean particle sizes of 60 nm. pH 10 was applied to minimize self-poisoning of the catalyst by HX released during the dehalogenation reaction (Aramendía et al., 2002; Aramendía et al., 2001; Coq et al., 1986). For nZVI, HOCs reactivity data were obtained from batch experiments (at unbuffered pH 7-8) using particles with a mean size of 75 nm and also from the literature for nZVI with particle sizes 80-100 nm (Song and Carraway, 2005). Even though nZVI is usually consumed during dehalogenation reactions, it is generally accepted that the core-shell structure and overall particle size of nZVI with its metal-core and oxidic shell more-or-less remain during iron oxidation (Nurmi et al., 2005). Therefore, the  $k_{\text{obs}}$  values for the dechlorination of chlorinated ethanes obtained from the literature were further processed using equation 19 by taking into account the initial nZVI concentration. Table 8 shows an overview of the specific metal activities for the dehalogenation of various HOCs in water using Cu-, Pd- and nZVI-based systems. Also presented are the weakest C–X bond dissociation energy values for the various HOCs. The particle size distribution ( $d_{50}$  and  $d_{90}$ ) as determined by NTA analysis for Cu, Pd, and nZVI nanoparticles are presented in the appendix Table A2-3.

**Table 8:** Specific metal activities for the dehalogenation of single HOCs in water using Cu-, Pd- and nZVI-based systems together with the corresponding weakest C–X bond dissociation energies ( $c_{Cu} = 0.2\text{-}2500$  mg/L;  $c_{0,NaBH_4} = 300$  mg/L;  $c_{Pd} = 0.2\text{-}1500$  mg/L;  $p_{H_2} = 100$  kPa;  $c_{nZVI} = 0.4\text{-}5$  g/L;  $c_{0,HOCs} = 2\text{-}50$  mg/L)

Halogenated organic compound classes		BDE (kJ/mol)	Specific metal activities $A_m$ [L/(g·min)]		
			m = Cu	m = Pd	m = nZVI
Saturated aliphatic compounds with a higher chlorination degree	CTC, CCl <sub>4</sub>	293 <sup>a</sup>	1100 ± 100	200 ± 20	0.30 ± 0.05
	CF, CHCl <sub>3</sub>	322 <sup>a</sup>	130 ± 10	5 ± 1	0.003 ± 0.001
	1,1,1-TCA, CCl <sub>3</sub> –CH <sub>3</sub>	309 <sup>a</sup>	170 ± 20	n.a.	0.102 ± 0.006 <sup>g</sup>
	1,1,2-TCA, CHCl <sub>2</sub> –CH <sub>2</sub> Cl	318 <sup>b</sup>	6 ± 1	1.3 ± 0.2	0.0016 ± 0.0002 <sup>g</sup>
	1,1,1,2-TeCA, CCl <sub>3</sub> –CH <sub>2</sub> Cl	295 <sup>a</sup>	900 ± 200	380 ± 20	0.36 ± 0.03 <sup>g</sup>
	1,1,2,2-TeCA, CHCl <sub>2</sub> –CHCl <sub>2</sub>	314 <sup>a</sup>	60 ± 5	n.a.	0.021 ± 0.003 <sup>g</sup>
	HCA, CCl <sub>3</sub> –CCl <sub>3</sub>	304 <sup>a</sup>	2500 ± 500	n.a.	0.52 ± 0.04 <sup>g</sup>
Saturated aliphatic compounds with lower chlorination degree	DCM, CH <sub>2</sub> Cl <sub>2</sub>	339 <sup>a</sup>	0.22 ± 0.02	n.a.	n.a.
	MCM, CH <sub>3</sub> Cl	351 <sup>a</sup>	0.0020 ± 0.0002	n.a.	n.a.
	MCA, CH <sub>2</sub> Cl–CH <sub>3</sub>	352 <sup>a</sup>	0.010 ± 0.005	n.a.	n.a.
	1,1-DCA, CHCl <sub>2</sub> –CH <sub>3</sub>	328 <sup>a</sup>	5 ± 1	3 ± 1	0.000014 ± 0.000003 <sup>g</sup>

	1,2-DCA, CH <sub>2</sub> Cl-CH <sub>2</sub> Cl	345 <sup>a</sup>	0.10 ± 0.04	0.0010 ± 0.0005	< 0.000003 <sup>g</sup>
	1,2-DCP, CH <sub>2</sub> Cl-CHCl-CH <sub>3</sub>	319 <sup>c</sup>	0.40 ± 0.08	0.006 ± 0.001	n.a.
	1,2,3-TCP, CH <sub>2</sub> Cl-CHCl-CH <sub>2</sub> Cl	n.a.	0.30 ± 0.01	0.007 ± 0.002	n.a.
	1,2-DCB, CH <sub>2</sub> Cl-CHCl-CH <sub>2</sub> -CH <sub>3</sub>	n.a.	0.50 ± 0.03	0.004 ± 0.002	n.a.
Brominated compounds	bromotrichloromethane, CBrCl <sub>3</sub>	231 <sup>a</sup>	1300 ± 100	n.a.	n.a.
	BF, CHBr <sub>3</sub>	275 <sup>a</sup>	2000 ± 300	300 ± 50	0.060 ± 0.005
	DBM, CH <sub>2</sub> Br <sub>2</sub>	276 <sup>a</sup>	390 ± 20	40 ± 10	0.03 ± 0.01
	MBM, CH <sub>3</sub> Br	294 <sup>a</sup>	20 ± 3	n.a.	n.a.
	VB, CHBr=CH <sub>2</sub>	338 <sup>a</sup>	67 ± 10	2500 ± 500	0.0028 ± 0.0002
Chlorofluoroorganic compounds	CFC-11, CFCl <sub>3</sub>	321 <sup>a</sup>	280 ± 30	4 ± 1	n.a.
	CFC-113, CCl <sub>2</sub> F-CClF <sub>2</sub>	359 <sup>a</sup>	1050 ± 150	n.a.	n.a.
Chlorinated ethylenes	VC, CHCl=CH <sub>2</sub>	452 <sup>c</sup>	4 ± 2	1600 ± 200	n.a.
	1,1-DCE, CCl <sub>2</sub> =CH <sub>2</sub>	394 <sup>d</sup>	10 ± 1	590 ± 50	n.a.
	<i>trans</i> -DCE,	373 <sup>d</sup>	17 ± 5	1200 ± 100	n.a.

					
	<i>cis</i> -DCE, 	370 <sup>d</sup>	5 ± 2	840 ± 60	n.a.
	TCE, CCl <sub>2</sub> =CHCl	392 <sup>d</sup>	17 ± 1	220 ± 50	0.00024 ± 0.00004
	PCE, CCl <sub>2</sub> =CCl <sub>2</sub>	382 <sup>d</sup>	3 ± 1	110 ± 10	0.00040 ± 0.00022
Halogenated aromatic compounds	CB, 	399 <sup>f</sup>	0.00004 ± 0.00001	500 ± 150	n.a.
	BB, 	337 <sup>f</sup>	80 ± 10	900 ± 100	n.a.

<sup>a</sup> Ref. (Luo, 2007).

<sup>b</sup> Ref. (Cioslowski et al., 1997).

<sup>c</sup> Ref. (Liu et al., 2000).

<sup>d</sup> Ref. (Desai D'sa et al., 1988).

<sup>e</sup> Ref. (Chen, 2003).

<sup>f</sup> Ref. (Lide, 1995).

<sup>g</sup>  $k_{obs}$  data for the reduction of chloroethanes were obtained from (Song and Carraway, 2005) where the nZVI mean particle sizes used for the study were in the range 80-100 nm. The  $k_{obs}$  data and nZVI concentrations were used to calculate the specific nZVI activities according to equation 19.

The specific metal activities for the reduction of HOCs using Cu-, Pd- and nZVI-based systems were calculated from three replica experiments using nanoparticles of comparable particle sizes i.e. 50 -75 nm. The error ranges are mean deviations of the single values from the average.

pH = 10 for HOCs dehalogenation experiments using Cu<sup>0</sup> + NaBH<sub>4</sub> and Pd + H<sub>2</sub>. pH<sub>0</sub> = 7-8 for nZVI experiments which increased to 9-9.5 at the termination of the reaction where the HOCs conversions were ≥ 95 %. BDE refers to the gas-phase weakest C–X bond at standard state (1 atm and 25 °C). n.a. = not analyzed.

As shown in Table 8, the reactivity of the different HOCs presented as specific metal activities is structure-sensitive and varies depending on the type of remediation system used.  $\text{Cu}^0 + \text{NaBH}_4$  and  $\text{Pd} + \text{H}_2$  can be applied to nearly all HOCs classes containing F, Cl, and Br. However, it is noteworthy to point out that where  $\text{Cu}^0 + \text{NaBH}_4$  and  $\text{Pd} + \text{H}_2$  were applied for the dehalogenation of  $\text{CFCl}_3$  and  $\text{CCl}_2\text{F}-\text{CClF}_2$ , fluoride, methane, and ethane were not detected. Thus these systems failed in the cleavage of C–F bonds. Cleavage of the C–F bond was only observed by using  $\text{Cu}^0 + \text{NaBH}_4 + \text{vitamin B12}$  for the dehalogenation of  $\text{CFCl}_3$  where the yields to  $\text{CH}_4$ ,  $\text{F}^-$  and  $\text{Cl}^-$  were  $(75 \pm 5)$  mol-%,  $(10 \pm 2)$  mol-%, and  $(70 \pm 5)$  mol-%, respectively. The dehalogenation of  $\text{CCl}_2\text{F}-\text{CClF}_2$  using  $\text{Cu}^0 + \text{NaBH}_4 + \text{vitamin B12}$  was not evaluated.

The two catalysts, Cu and Pd, show much higher specific activities for all HOCs classes than with nZVI as a reagent. The difference in the specific metal activities between catalysts and reagents can be considered as a combination of the intrinsic properties of the metal and their dehalogenation mechanisms. Since Pd and nZVI have been extensively studied for the reduction of various HOCs and relevant information regarding the rate-determining steps and product patterns are available, the dehalogenation pathways for reduction of HOCs using  $\text{Cu}^0 + \text{NaBH}_4$  were evaluated in this study. Figure 21 shows the correlation between specific metal activities for dehalogenation of the various HOCs using  $\text{Cu}^0 + \text{NaBH}_4$  and  $\text{Pd} + \text{H}_2$  presented as  $\log A_m$  versus BDE. It is noteworthy to point out that for heterogeneous systems, reactions are determined by both adsorption and dehalogenation steps. Non-dissociative adsorption cannot be correlated with bond strengths. The correlation between specific metal activities ( $\log A_m$ ) versus BDE in Figure 21 is used only to provide insights into the possible reduction steps for the different compound classes.

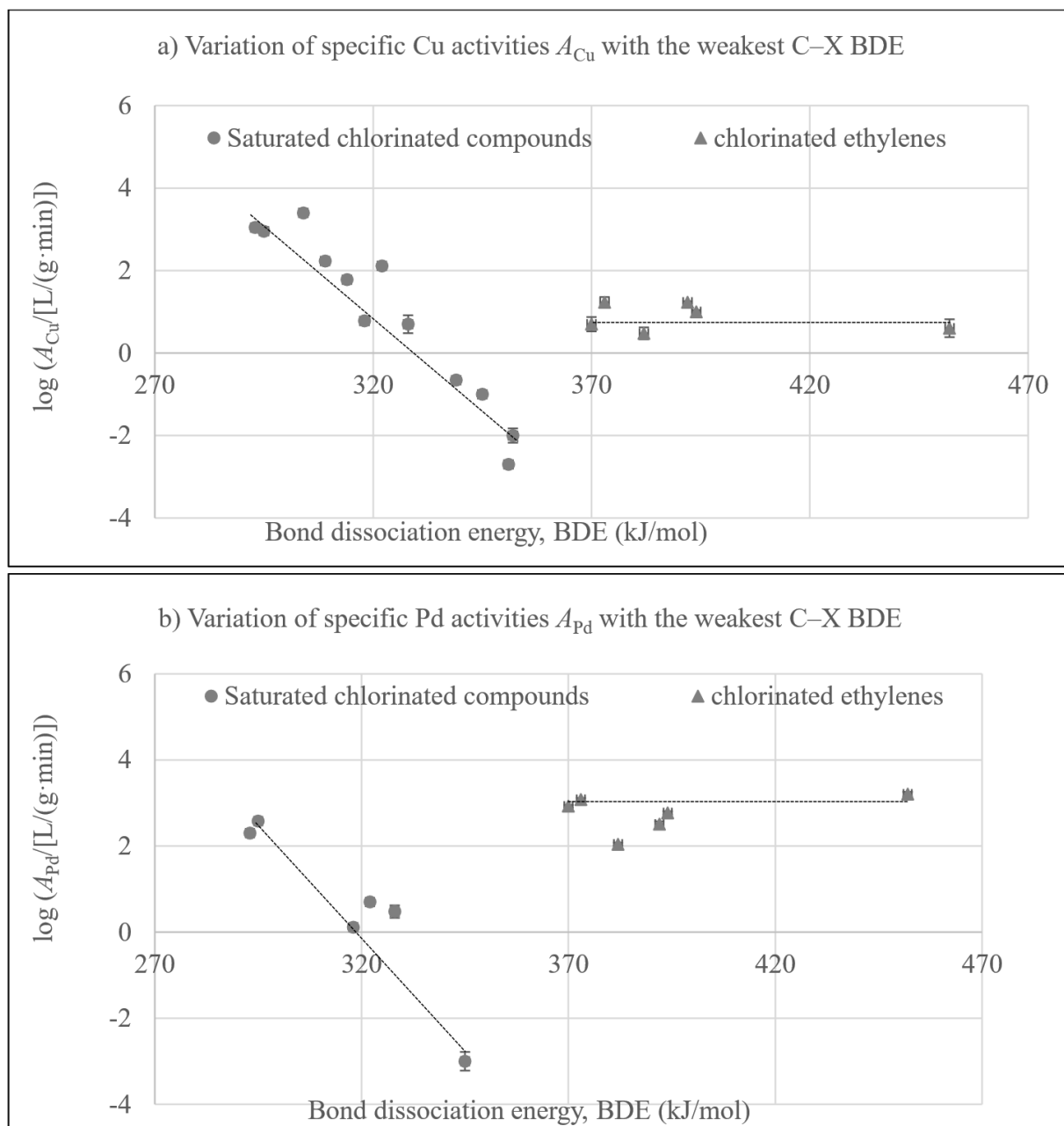


**Figure 21:** Correlation of specific metal activities as  $\log A_m$  with the weakest C–X bond dissociation energies for saturated chlorinated compounds and chlorinated ethylenes (a) using  $Cu^0 + NaBH_4$  and (b) using  $Pd + H_2$ . Dotted lines are used to indicate reactivity trends for the HOC classes.

As shown in Figure 21, the specific metal activities for the dehalogenation of saturated aliphatic compounds (chlorinated methanes and ethanes) using  $Cu^0 + NaBH_4$  and  $Pd + H_2$

decreases with an increase in BDE. For chlorinated ethylenes, no clear dependency between specific metal activities and BDE can be read from the graphs. This is an indication of two distinct rate-determining steps between saturated aliphatic chlorinated compounds and the chlorinated ethylenes. For the dehalogenation of HOCs carried out in the gas phase, dissociative adsorption and homolytic cleavage of the C–X bond were rate-determining using Pd (Chen, 2003; Rioux et al., 2000; Zhou et al., 1999) and Cu catalysts (Ahmed et al., 2018). Hence the HOC affinity to the catalyst's surface and the strength of the C–X bond are crucial in determining its reactivity. Therefore, for Cu and Pd catalysts, the homolytic cleavage of the weakest C–X bond for saturated aliphatic chlorinated compounds could be rate-determining ( $R-X \rightarrow R\cdot + X\cdot$ ).

Since the C–Br (285 kJ/mol) is weaker than the C–Cl bond (337 kJ/mol), specific Cu activities for the reduction of brominated compounds were higher than for their chlorinated counterparts. For example, as shown in Table 8, the specific Cu activities for the reduction of BF ( $A_{Cu,BF} = (2000 \pm 300) \text{ L}/(\text{g}\cdot\text{min})$ ) was higher by a factor of 15 than that of CF ( $A_{Cu,CF} = (130 \pm 10) \text{ L}/(\text{g}\cdot\text{min})$ ). Similarly, the specific Cu activities for the reduction of DBM ( $A_{Cu,DBM} = (390 \pm 20) \text{ L}/(\text{g}\cdot\text{min})$ ) was higher by a factor of 1800 than that of DCM ( $A_{Cu,DCM} = (0.22 \pm 0.02) \text{ L}/(\text{g}\cdot\text{min})$ ).

In addition to the strength of the C–X bond to be cleaved, the specific Cu activities were higher for compounds with an increased degree of substitution at the electrophilic carbon and also with longer alkyl chains. For example, as shown in Table 8, the specific Cu activity for the dechlorination of CF ( $A_{Cu,CF} = (130 \pm 10) \text{ L}/(\text{g}\cdot\text{min})$ ) was three orders of magnitude higher than that of DCM ( $A_{Cu,DCM} = (0.22 \pm 0.02) \text{ L}/(\text{g}\cdot\text{min})$ ). Similarly, the specific Cu activity for the dechlorination of 1,1,1-TCA ( $A_{Cu,1,1,1-TCA} = (170 \pm 20) \text{ L}/(\text{g}\cdot\text{min})$ ) was two orders of magnitude higher than that of 1,1-DCA ( $A_{Cu,1,1-DCA} = (5 \pm 1) \text{ L}/(\text{g}\cdot\text{min})$ ), respectively. This increase in catalyst

activity due to higher X-substitution degree at the electrophilic carbon could be due to i) the weakening of the C–X bonds, and ii) the stronger initial attachment of halogen atoms to the catalyst surface.

The saturated aliphatic chlorinated compounds with lower chlorination degrees such as 1,2-DCP, 1,2,3-TCP, and 1,2-DCB were easily dechlorinated using  $\text{Cu}^0 + \text{NaBH}_4$  compared to 1,2-DCA. The difference in specific Cu activities for these compounds could be due to the weakening of the C–Cl bond as a result of increased substitution. For example, 1,2-DCA with a stronger C–Cl bond (345 kJ/mol) was more difficult to dechlorinate than 1,2-DCP with a weaker C–Cl bond (319 kJ/mol). Therefore, the specific Cu activities for dechlorination of 1,2-DCA ( $A_{\text{Cu},1,2\text{-DCA}} = (0.10 \pm 0.04) \text{ L}/(\text{g}\cdot\text{min})$ ) was lower by a factor of 4 than that of 1,2-DCP ( $A_{\text{Cu},1,2\text{-DCP}} = (0.40 \pm 0.08) \text{ L}/(\text{g}\cdot\text{min})$ ). Since the specific Cu activities for the dechlorination of 1,2-DCP and 1,2,3-TCP were similar, it showed that the Cl-atoms substitution pattern within the alkyl chain has no marked effect on the reactivities. In other words, geminal substituents affect dechlorination rates much more than vicinal substituents.

Further comparison between Cu and Pd catalysts shows that the specific Cu activities for the dehalogenation of the saturated aliphatic HOCs with  $\geq 3$  halogen atoms are one to two orders of magnitude higher than those of Pd. Furthermore, the specific Cu activities for the dechlorination of compounds with lower chlorination degrees (i.e. 1,2-DCA, 1,2-DCP, 1,2,3-TCP, and 1,2-DCB) were two orders of magnitude higher than specific Pd activities. In contrast to Pd catalysts, Cu catalysts can be applied for the dehalogenation of nearly all saturated aliphatic compounds and eliminate the danger of accumulation of the lower chlorinated byproducts. Using the specific metal activities for the reduction of saturated aliphatic HOCs as a basis for comparing the dehalogenation abilities of the catalysts and reagent, the metal order is as follows:  $\text{Cu} \gg \text{Pd} \gg \text{nZVI}$ .

For chlorinated ethylenes, the specific Pd activities  $A_{Pd}$  were one to three orders of magnitude higher than the specific Cu activities  $A_{Cu}$ . The high specific Pd activities for these compounds have been attributed to the strong interaction between  $\pi$ -electrons at the Pd surfaces through di- $\delta$ -bond formation followed by the addition of active  $H^*$  to the double bond (Andersin and Honkala, 2011; Barbosa et al., 2002; Gómez-Sainero et al., 2002; Mackenzie et al., 2006). For the dechlorination of chlorinated ethylenes using  $Cu^0 + NaBH_4$ , such atomic  $H^*$  species are not available. In contrast to the saturated aliphatic chlorinated compounds, increased chlorination degree and the Cl-substitution pattern for chlorinated ethylenes have no marked effect on the specific Cu activities. For example, the specific Cu activities for dechlorination of VC, *cis*-DCE, and PCE were  $A_{Cu,VC} = (4 \pm 2) \text{ L}/(\text{g}\cdot\text{min})$ ,  $A_{Cu,cis-DCE} = (5 \pm 2) \text{ L}/(\text{g}\cdot\text{min})$  and  $A_{Cu,PCE} = (3 \pm 1) \text{ L}/(\text{g}\cdot\text{min})$ , respectively. Similar specific Cu activities  $A_{Cu}$  were also observed for the dechlorination of *trans*-DCE, 1,1-DCE, and TCE. Based on the specific metal activities for dechlorination of chlorinated ethylenes using the three remediation systems, the metal order is  $Pd \gg Cu \gg nZVI$ .

Despite existing literature claiming that bare nZVI is able to cleave aromatic C–Cl bonds especially those with lower chlorination degree e.g. chlorobenzene (Poursaberi et al., 2012; Ševců et al., 2017; Shih et al., 2011; Wang and Zhang, 1997), these results could not be confirmed by us and therefore should be considered artifacts. Successful cleavage of aromatic C–Cl bonds by nZVI were explained due to the presence of trace levels of hydrogenation-active metals such as Ni in ZVI precursors (Balda and Kopinke, 2020). In this study,  $Cu^0 + NaBH_4$  was able to cleave aromatic C–X bonds. As shown in Table 8, the specific Cu activities for the dehalogenation of CB and BB were  $A_{Cu,CB} = (0.00004 \pm 0.00001) \text{ L}/(\text{g}\cdot\text{min})$  and  $A_{Cu,BB} = (80 \pm 10) \text{ L}/(\text{g}\cdot\text{min})$ , respectively. The low specific Cu activity for dechlorination of CB is not significant for any

practical application. Hence  $\text{Cu}^0 + \text{NaBH}_4$  is more appropriate for the cleavage of aromatic C–Br bonds. In contrast to Cu catalysts, Pd catalysts can smoothly cleave aromatic C–X bonds. As shown in Table 8, the specific Pd activities for the reduction of CB and BB were  $A_{\text{Pd,CB}} = (500 \pm 150) \text{ L}/(\text{g}\cdot\text{min})$  and  $A_{\text{Pd,BB}} = (900 \pm 100) \text{ L}/(\text{g}\cdot\text{min})$ , respectively.

In conclusion, the specific metal activities for the reductive dehalogenation of HOCs with catalysts and reagents depend on: i) the strength of the C–X bond, ii) the presence of functional groups next to the C–X bond to be cleaved (i.e. geminal substitution pattern and presence of  $\pi$ -electrons), and iii) the intrinsic nature of the metal which determines the dehalogenation mechanisms. When comparing the reactivities of the three ‘metals’, one has to take into account that actually different ‘reduction systems’ are compared rather than metals because all three systems use their own reductants ( $\text{BH}_4^-$ ,  $\text{H}_2$ , and  $\text{Fe}^0$ ).

#### 4.2.2 Water matrix effects on the stability of Cu catalysts

The performance of a remediation system usually differs greatly when used under laboratory and field conditions. When treating HOCs present in real effluents, water matrix effects may alter the performance of the Cu catalysts. In this work, the performance of Cu catalysts for dechlorination of CF in the presence of common water solutes was evaluated and then compared with the baseline for Cu without co-solutes ( $A_{\text{Cu,CF,without co-solute}} = (130 \pm 10) \text{ L}/(\text{g}\cdot\text{min})$ ). The results are presented in Table 9. The aim was to identify which co-solutes have a negative or positive effect on the specific Cu activities. As a baseline for further comparison, the performance of Cu catalysts for dechlorination of CF was also evaluated in laboratory-supplied tap water and synthetic freshwater as shown in the appendix Table A3-5.

**Table 9:** Effect of various co-solutes on the specific Cu activities  $A_{Cu}$  for the dechlorination of CF compared to the baseline for Cu without co-solutes ( $A_{Cu,CF,without\ co-solute} = (130 \pm 10) \text{ L}/(\text{g}\cdot\text{min})$ ) ( $c_{0,CF} = 10 \text{ mg/L}$ ;  $c_{0,NaBH_4} = 300 \text{ mg/L}$ ; pH = 8 for  $\text{NaHCO}_3$ ; pH = 10 for the other experiments)

Aqueous co-solutes supplied		Solute concentration (mg/L)	Specific Cu activities $A_{Cu}$ in the presence of co-solute [ $\text{L}/(\text{g}\cdot\text{min})$ ]	$A_{Cu,CF,with\ co-solute}/A_{Cu,CF,without\ co-solute}$ [-]
Co-solutes with no marked effect on specific Cu activities	NaF	5	$140 \pm 20$	1.1
		20	$160 \pm 30$	1.2
	NaCl	5	$130 \pm 15$	1.0
		500	$140 \pm 40$	1.1
	KBr	5	$140 \pm 10$	1.1
		10	$130 \pm 20$	1.0
	Na <sub>2</sub> SO <sub>4</sub>	5	$130 \pm 15$	1.0
		500	$140 \pm 10$	1.1
	Na <sub>2</sub> SO <sub>3</sub>	5	$140 \pm 20$	1.1
		500	$130 \pm 10$	1.0
	SRHA as a surrogate for organic matter	5	$130 \pm 10$	1.0
		20	$140 \pm 10$	1.1
Co-solutes with a positive effect on	Na <sub>2</sub> CO <sub>3</sub>	100	$260 \pm 20$	2.0
	NaHCO <sub>3</sub>	100	$330 \pm 30$	2.5

specific Cu activities				
Co-solutes with a negative effect on specific Cu activities	MgSO <sub>4</sub> ·7H <sub>2</sub> O	50	90 ± 40	0.7
		500	60 ± 10	0.5
	CaCl <sub>2</sub> ·2H <sub>2</sub> O	50	120 ± 30	0.9
		500	80 ± 20	0.6
	FeSO <sub>4</sub> ·7H <sub>2</sub> O	10	100 ± 20	0.8
		100	30 ± 10	0.2
	MnSO <sub>4</sub> ·H <sub>2</sub> O	2	100 ± 20	0.8
		100	60 ± 10	0.5
Co-solutes containing redox-sensitive anions and their negative effect on specific Cu activities	NaNO <sub>3</sub>	10	100 ± 10	0.8
		20	90 ± 10	0.7
		50	60 ± 10	0.5
	NaNO <sub>2</sub>	10	100 ± 10	0.8
		20	90 ± 10	0.7
		50	70 ± 10	0.5
Co-solute that deactivates Cu catalysts	Na <sub>2</sub> S·H <sub>2</sub> O	1	13 ± 2	0.10
		10	3 ± 1	0.02

The co-solutes NaF, NaCl, and KBr have no significant effect on the specific Cu activities. Similar to Pd catalysts, the marginal effect on the stability of Cu catalysts by halide ions could be due to rapid desorption and solvation effects which may remove these ions from catalyst surfaces into the bulk solution. Also, Na<sub>2</sub>SO<sub>4</sub> and Na<sub>2</sub>SO<sub>3</sub> have no marked effect on the specific Cu activities. Therefore, the reduction of SO<sub>4</sub><sup>2-</sup> or SO<sub>3</sub><sup>2-</sup> to HS<sup>-</sup> (a known catalyst poison) under the experimental conditions may be considered not to occur. Compared to Pd catalysts which are readily deactivated by sulfite (Han et al., 2016; Lim and Zhu, 2008; Lowry and Reinhard, 2000), this study shows that Cu catalysts are moderately tolerant to deactivation by sulfite. This is a major advantage for Cu catalysts over Pd catalysts for reductive dehalogenation reactions in water.

Natural organic matter has been found to adsorb onto catalysts such as Pd leading to catalyst inhibition (Chaplin et al., 2006; Kopinke et al., 2010; Zhang et al., 2013). In this study, SRHA was used as a surrogate for NOM in the concentration range of  $c_{\text{SRHA}} = 5\text{-}20$  mg/L. Under the experimental conditions (pH = 10), SRHA had no marked effect on the specific Cu activities. SRHA like other humic substances contain phenolic and carboxylic functional groups that are deprotonated at pH > 7 (Baglieri et al., 2014; Brigante et al., 2007; Klučáková and Pekař, 2005). Deprotonated SRHA would have minimal interaction with the surface of Cu NPs hence no marked effect on catalysts performance. However, it should be noted that SRHA precipitation at neutral and acidic conditions may affect the performance of Cu catalysts (Qi et al., 2017; Wang et al., 2015).

As shown in Table 9, Na<sub>2</sub>CO<sub>3</sub> and NaHCO<sub>3</sub> increase the specific Cu activities by a factor of 2 and 2.5, respectively. So far, it's unclear how the addition of Na<sub>2</sub>CO<sub>3</sub> and NaHCO<sub>3</sub> enhances Cu performance. Despite having a positive effect on the specific Cu activities, Na<sub>2</sub>CO<sub>3</sub> and NaHCO<sub>3</sub> had no marked effect on the product selectivity patterns. The co-solutes CaCl<sub>2</sub>, MgSO<sub>4</sub>,

MnSO<sub>4</sub>, and FeSO<sub>4</sub> decreased the performance of the Cu catalysts. As shown in Table 9, increased concentrations of these co-solutes led to a decrease in catalysts performance. The precipitation of hydroxides of Ca, Mg, Mn, and Fe under the reaction conditions (pH = 10) may contribute to the loss of catalyst activities. The performance of Cu catalysts was also inhibited by NaNO<sub>3</sub> and NaNO<sub>2</sub>. The redox-sensitive species NO<sub>3</sub><sup>-</sup> and NO<sub>2</sub><sup>-</sup> may be subject to reduction to form N<sub>2</sub> and NH<sub>3</sub> under the experimental conditions (Chaplin et al., 2006; Guy et al., 2009; Lowry and Reinhard, 2001; Soares et al., 2008). Although NH<sub>3</sub> and N<sub>2</sub> were not measured in this study, the reduction of NO<sub>3</sub><sup>-</sup> and NO<sub>2</sub><sup>-</sup> by Cu<sup>0</sup> + NaBH<sub>4</sub> under the experimental conditions cannot be ruled out.

Replacing deionized water with tap water and synthetic freshwater for the dechlorination of CF led to a slight decrease in activities where  $A_{\text{Cu,CF,tap water or freshwater}}/A_{\text{Cu,CF,without co-solute}} = 0.8$  (data is shown in the appendix Table A3-5). The presence of cations such as Ca<sup>2+</sup>, Mg<sup>2+</sup>, and anions e.g. NO<sub>3</sub><sup>-</sup> in tap water and synthetic freshwater could contribute to the slight loss of catalyst activities. As shown in Table 9, the ratio of specific Cu activities in the absence and presence of Na<sub>2</sub>S were 0.1 and 0.02 for 1 and 10 mg/L Na<sub>2</sub>S, respectively. Under the experimental conditions pH = 10, HS<sup>-</sup> (pK<sub>a,HS<sup>-</sup></sub> = 12.9) is the main species (Linkous et al., 2004; Wu et al., 2018). Chemisorption of HS<sup>-</sup> onto copper to form sulfur-adlayers (Cu<sub>2</sub>S or CuS) blocks active sites for the CF dechlorination reaction (Jiang et al., 2020; Prokkola et al., 2020; Sugimasa et al., 2003; Twigg and Spencer, 2001). Deactivation of Cu catalysts by bisulfide is therefore detrimental to catalyst performance. Regeneration of sulfide-deactivated Cu NPs using oxidants such as KMnO<sub>4</sub> or hypochlorite was not attempted in this study.

In conclusion, this study shows that Cu catalysts are rather stable in the presence of common water solutes other than sulfide/bisulfide. Hence Cu<sup>0</sup> + NaBH<sub>4</sub> can be applied directly

for the treatment of HOCs in groundwater (only for pump & treat systems) or wastewater without the need for pre-treatment to remove water solutes. However, the protection of Cu catalysts against sulfide is still necessary.

#### *4.2.3 Regeneration and lifetime of Cu-doped cation-exchange resin*

The deactivation of catalysts such as Pd and Cu by solutes such as sulfide presents a major drawback in the treatment of contaminants. The frequent need for catalyst replacement or regeneration presents an economic burden and makes the utilization of such catalysts in environmental technologies less attractive. It has been shown that embedding catalysts such as Pd onto hydrophobic polymers e.g. poly(dimethylsiloxane) (PDMS) (Comandella et al., 2017; Comandella et al., 2016), silicone coatings (Kopinke et al., 2010; Navon et al., 2012), and Y-zeolites (Schüth et al., 2000) could minimize catalysts deactivation. In this study, the stability and regeneration of copper embedded onto amberlite cation-exchange resin were evaluated. The Cu/resin (1.4 wt-% Cu) was first soaked for 120 min in aqueous Na<sub>2</sub>S solutions whose concentrations were 1 mg/L and 20 mg/L to give molar Cu : S ratios of 8.6 and 0.43, respectively. The performances of the catalysts were evaluated before deactivation, upon deactivation, and regeneration by rinsing with deionized water. The variation in specific Cu activities  $A_{Cu}$  for the original, deactivated, and washed Cu/resin are presented in Figure 22.

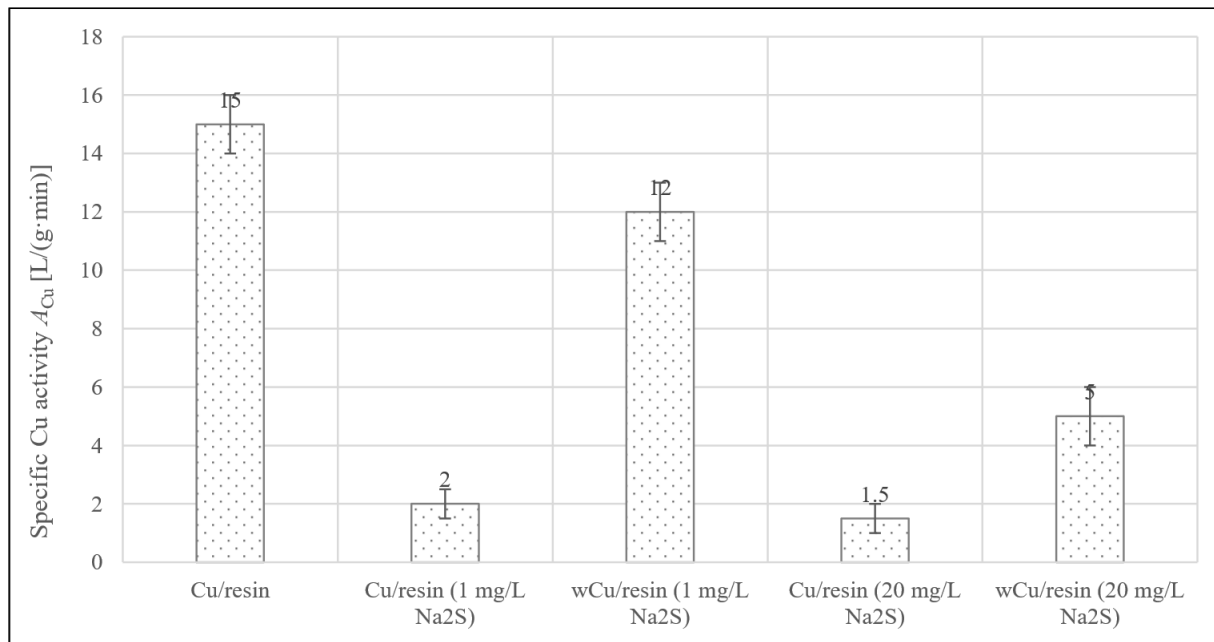


**Figure 22:** Variation of specific Cu activities when Cu/resin is deactivated with Na<sub>2</sub>S and regenerated upon rinsing with deionized water ( $c_{Cu/resin} = 300$  mg/L;  $c_{0,CF} = 10$  mg/L;  $c_{0,NaBH_4} = 300$  mg/L; pH = 10. “w” in the sample is the description for washed;  $A_{Cu}$  was calculated from 4.2 mg/L Cu within the resin).

As shown in Figure 22, the embedding of Cu in amberlite resin could not prevent its deactivation by sulfide. The ratio of specific Cu activities between the sulfide deactivated and non-deactivated catalysts ( $A_{Cu,CF,deactivated}/A_{Cu,CF,original}$ ) was in the range of 0.13 to 0.10 which was more-or-less similar despite the different concentrations of Na<sub>2</sub>S supplied. The implication was that already a small amount of sulfide led to the deactivation of the catalyst, whereas a significant fraction of Cu (about 10 %) was in a more protected state. Note that 10 mg/L Na<sub>2</sub>S·H<sub>2</sub>O led to 98% deactivation of freely suspended Cu NPs (compare Table 9). Rinsing the sulfide-deactivated Cu/resin with water restored partially the catalyst activity. For Cu/resin (1 mg/L Na<sub>2</sub>S), washing restored about 80 % of the original catalyst activity. Exposure to a high sulfide concentration (20 mg/L) and subsequent washing resulted in the restoration of a third of the original catalyst activity. Washing, therefore, may remove physisorbed sulfide. However, chemisorbed sulfide on

the copper may require stringent conditions such as oxidation processes especially under conditions with a high concentration of sulfide. Also, the contact to borohydride during the reduction process is not enough to fully re-reduce the copper function.

The lifetime and reusability of Cu/resin catalysts were further investigated through consecutive reaction cycles by multiple CF injections as shown in Figure 23.

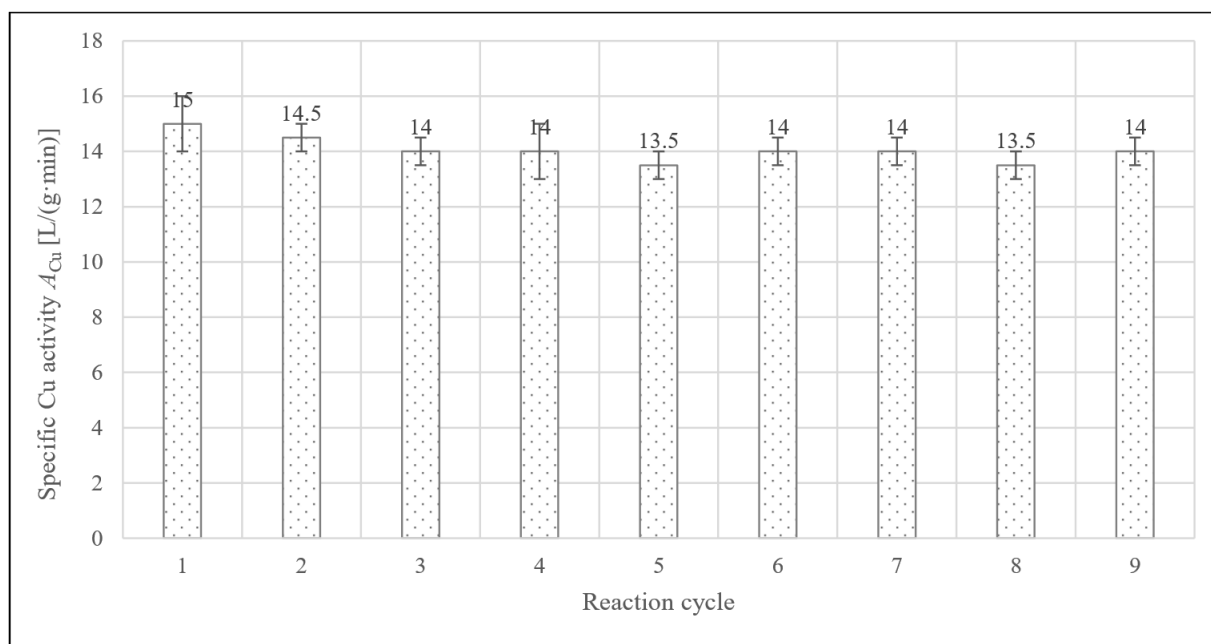


**Figure 23:** Variation in specific Cu activities during recycling of Cu/resin during dechlorination of CF ( $c_{Cu/resin} = 300$  mg/L;  $c_{0,CF} = 10$  mg/L;  $c_{0,NaBH_4} = 300$  mg/L; pH = 10). One cycle was 120 min where CF conversion was  $\geq 95$  % while  $A_{Cu}$  was calculated from 4.2 mg/L Cu within the resin.

As shown in Figure 23, there was no significant change in the specific Cu activities  $A_{Cu}$  for the dechlorination of CF even after 9 reaction cycles under laboratory operation. Since no Cu-species were detected from the effluent after each reaction cycle, this implied that the copper remained bound to the resin. This is a major advantage since it shows the system may be deployed for environmental clean-up in closed areas and the danger of copper leaching can be minimized.

Nevertheless, long-term tests may be necessary under application-near conditions with real wastewater and for longer periods to evaluate copper leaching from the resin especially at  $\text{pH} < 7$  and catalyst lifetime.

#### *4.2.4 Limitations of $\text{Cu}^0 + \text{NaBH}_4$ and the recommended application areas*

The estimated cost of  $\text{NaBH}_4$  is in the range of USD 15-40/kg (Chou et al., 2015) which is more expensive than the estimated cost of USD 6/kg for hydrogen (Hydrogen Council, 2020). The difference becomes even more evident when comparing costs on the basis of reduction equivalents: USD 15/kg  $\text{NaBH}_4$  corresponds to USD 71 per kmol reductant electrons (assuming that 8 electrons per  $\text{BH}_4^-$  can be used), whereas USD 6/kg  $\text{H}_2$  corresponds to USD 6 per kmol reductant electrons. This is a factor of 12 at least between the costs of the two reductants. The high cost of borohydride is a significant drawback for large-scale treatment of HOCs using  $\text{Cu}^0 + \text{NaBH}_4$ . However, the handling of  $\text{NaBH}_4$  is seen easier than that of hydrogen by many potential users. Hydrolysis of  $\text{NaBH}_4$  and formation of borates e.g. sodium metaborate ( $\text{NaBO}_2 \cdot n\text{H}_2\text{O}$ ) (Liu et al., 2006; Schlesinger et al., 1953) is also a problem. Boron and its derivatives are toxic to microorganisms, animals, and humans (Duydu et al., 2011; Fail et al., 1998; Schoderboeck et al., 2011). The recommended limits for boron in drinking water according to the World Health Organization (WHO) and the European Union are 0.5 and 1 mg/L, respectively (Weinthal et al., 2005; World Health Organization, 1998). Furthermore, the hydrolysis of  $\text{NaBH}_4$  in water produces effluents with pH between 9 and 10 (Liu et al., 2006; Schlesinger et al., 1953). Therefore, the pH of the treated effluent may need readjustment to between 6 and 9 before discharge into receiving water bodies and to municipal sewerage systems (Tilche and Orhon, 2002; U.S. EPA, 2012).

Copper is an essential metal present in several proteins essential for biological activities in humans (de Romaña et al., 2011; Wang et al., 2021). Despite the benefits of copper in trace amounts, higher dosages are toxic to humans. The drinking water limit for copper as recommended by WHO is 2 mg/L (World Health Organization, 2004). Therefore,  $\text{Cu}^0 + \text{NaBH}_4$  is best suited for small-scale *ex situ* applications where copper leaching into the environment can be controlled. In comparison to Cu NPs, supported Cu, e.g. Cu/resin should be considered to improve catalysts handling and regeneration. Sorption active materials e.g. zeolites may be useful as support for Cu catalysts to enhance the enrichment of the pollutants before reduction by the addition of borohydride. The recovery of leached copper from resin or any sorption-active supports can be done by placing metallic Fe (which can be prepared from scrap Fe as the cheaper source) at the exit of the effluent before discharge into the environment.

In conclusion,  $\text{Cu}^0 + \text{NaBH}_4$  is a robust system for the dehalogenation of HOCs in water under controlled conditions, but its application is limited to relatively small amounts of highly contaminated wastewaters and to chemical regeneration of adsorbents (such as ACs or zeolites) which are loaded with halogenated alkanes.

## 5 Summary

The present thesis contributes to the development of metallic copper in combination with  $\text{NaBH}_4$  as a reducing agent ( $\text{Cu}^0 + \text{NaBH}_4$ ), as an alternative system to Pd catalysts, and nZVI as a reagent for the reduction of HOCs in water.  $\text{Cu}^0 + \text{NaBH}_4$  can be applied to compounds such as  $\text{CH}_2\text{Cl}_2$  and  $\text{CH}_2\text{Cl}-\text{CH}_2\text{Cl}$  which are hardly transformed using  $\text{Pd} + \text{H}_2$  and nZVI. Since the dechlorination of compounds such as  $\text{CHCl}_3$  using  $\text{Cu}^0 + \text{NaBH}_4$  supports reaction pathways that lead to the fully dechlorinated hydrocarbons, e.g.  $\text{CH}_4$  from  $\text{CHCl}_3$ , as well as separate reaction pathways that lead to chlorinated byproducts such as  $\text{CH}_2\text{Cl}_2$ , selectivity patterns under various reaction conditions were studied and the effects of various additives were ascertained. Furthermore, optimal reaction conditions that minimize the accumulation of chlorinated byproducts are presented. In order to evaluate the suitability of  $\text{Cu}^0 + \text{NaBH}_4$  in water treatment applications, two priority research lines were followed: i) selectivity assessment and system optimization, and ii) comparison of reagents and catalysts in order to recommend the most appropriate application areas.

### Selectivity assessment and system optimization

In this part,  $\text{Cu}^0 + \text{NaBH}_4$  was applied in order to: i) determine product selectivity patterns during the dehalogenation of  $\text{CCl}_3\text{-R}$  compounds, where  $\text{R} = \text{Cl}, \text{F}, \text{Br}$  or  $\text{CH}_3$ , ii) evaluate the effects of reaction conditions upon the product selectivity patterns, and iii) optimize reaction conditions so as to minimize the accumulation of chlorinated byproducts.

**The product selectivity patterns during the reduction of  $\text{CCl}_3\text{-R}$  compounds were determined.** In environmental catalysis, the production of chlorinated byproducts is undesired but in many cases cannot be avoided.  $\text{CCl}_3\text{-R}$  compounds were selected and the product selectivity

patterns were determined and interpreted based upon i) electronic and steric effects of the R-substituent, ii) nature and type of reductants, and iii) influence of co-solutes.

**Product selectivity patterns are influenced by the degree of halogenation at the electrophilic carbon.** Using  $\text{CHCl}_3$  as a prominent member of the  $\text{CCl}_3\text{-R}$  compounds, the product selectivity patterns under various experimental conditions were successfully evaluated. The product selectivity patterns for dechlorination of  $\text{CHCl}_3$  using  $\text{Cu}^0 + \text{NaBH}_4$  divided to  $(84 \pm 2)$  mol-%,  $(13 \pm 2)$  mol-%, and  $(0.3 \pm 0.2)$  mol-% for  $\text{CH}_4$ ,  $\text{CH}_2\text{Cl}_2$ , and  $\text{CH}_3\text{Cl}$ , respectively. The term 'product selectivity pattern' is used in this study in the sense that the selectivities were calculated from converted educt under conditions where halogenated byproducts are more-or-less stable. Under identical conditions, it was observed that a combination of electronic and steric effects influences the selectivity patterns. For example, with the replacement of the chloroform's H-substituent, i.e. for the compounds  $\text{CCl}_4$ ,  $\text{CBrCl}_3$ ,  $\text{CFCl}_3$ , and  $\text{CCl}_3\text{-CH}_3$ , the product selectivities to the immediate halogenated intermediates were 50-72 mol-%. For these compounds, product selectivity patterns to the fully dechlorinated products,  $\text{CH}_4$  and  $\text{C}_2\text{H}_6$ , were only 16-35 mol-% and 33-37 mol-%, respectively.  $\text{CH}_4$  and fluoride as products were not detected during the reduction of  $\text{CFCl}_3$ , implying that cleavage of the C-F bond did not occur. The initial product selectivity patterns show that for  $\text{CCl}_4$ ,  $\text{CBrCl}_3$ ,  $\text{CFCl}_3$ , and  $\text{CCl}_3\text{-CH}_3$ , stepwise hydrogenolysis was the main dechlorination mechanism, in contrast to  $\alpha$ -elimination to the fully dechlorinated products.

With the replacement of the chloroform's Cl-substituent, e.g. for the target compounds  $\text{CH}_2\text{Cl}_2$  and  $\text{CHCl}_2\text{-CH}_3$ , selectivities to  $\text{CH}_4$  and  $\text{C}_2\text{H}_6$  were  $(85 \pm 2)$  mol-% and  $(63 \pm 2)$  mol-%, respectively. Hence, for  $\text{CHCl}_3$ ,  $\text{CH}_2\text{Cl}_2$ , and  $\text{CHCl}_2\text{-CH}_3$ ,  $\alpha$ -elimination reaction steps to the fully dechlorinated products,  $\text{CH}_4$  and  $\text{C}_2\text{H}_6$ , were the main dechlorination mechanisms, in contrast to

stepwise hydrogenolysis. Therefore, these results suggest that steric effects may be a limiting factor for the simultaneous removal of geminal chlorine atoms from the electrophilic carbon during the dehalogenation of  $\text{CCl}_3\text{-R}$  compounds in water via the  $\alpha$ -elimination mechanism.

**Product selectivity patterns are independent of the reactive species at the surfaces of Cu and Pd catalysts during the dechlorination of chloroform in water.** In this part of the thesis, combinations of different reductants for Cu and Pd catalysts were used for the dechlorination of  $\text{CHCl}_3$  under similar reaction conditions.  $\text{NaBH}_4$  and  $\text{H}_2$  were used as sources of active  $\text{H}^*$  for Pd. Since metallic copper is unable to activate molecular hydrogen under ambient conditions, it was combined with ZVI as a source of activated hydrogen in order to allow nascent hydrogen to interact with the Cu surface. ZVI-containing composite colloids (Carbo-Iron<sup>®</sup>) with and without sulfide doping for corrosion protection (CIC and S/CIC) were modified by 2 wt-% Cu in order to obtain Cu/CIC and Cu/S/CIC. Another set of experiments was performed where cathodic potentials in the range of -0.8 to -1.0 V at Cu-electrodes were applied in the presence or absence of  $\text{NaBH}_4$  to generate reactive species (electrons or active  $\text{H}^*$ ) for the surface-mediated dechlorination reaction. Also, electrochemical dechlorination of CF in water was done at Cu electrodes and cathodic potential of -1.1 V. Under all these reaction conditions where different reactive species (electrons or active  $\text{H}^*$ ) were generated at the surfaces of either Cu or Pd catalysts, similar product selectivity patterns (ratio of  $\text{CH}_2\text{Cl}_2$  :  $\text{CH}_4$ ) were observed. Therefore, this thesis work shows that product selectivity patterns during dechlorination of chloroform in water using either Cu or Pd catalysts are not system-specific but rather substance-specific (i.e. selectivity patterns are dependent upon the substitution degree at the electrophilic carbon).

**Inhibition and deactivation of Cu catalysts by sulfide increased the product selectivities in the undesired direction, towards  $\text{CH}_3\text{Cl}$  and  $\text{CH}_2\text{Cl}_2$ .** In this part of the thesis,

the product selectivities for dechlorination of  $\text{CHCl}_3$  were further evaluated using  $\text{Cu}^0 + \text{NaBH}_4$  in the presence of i) metal additives and ii) the co-solutes  $\text{NaNO}_3$ ,  $\text{NaNO}_2$ , and  $\text{Na}_2\text{S}$ . It was demonstrated that the metal additives Zn, Ce, Al, Sn, and Co led to inhibition of the dechlorination reaction accompanied with higher selectivities to  $\text{CH}_2\text{Cl}_2$  and  $\text{CH}_3\text{Cl}$ . For the metal mixtures comprised of Cu/Zn, Cu/Ce, Cu/Al, Cu/Sn, and Cu/Co, the product selectivities to  $\text{CH}_4$ ,  $\text{CH}_2\text{Cl}_2$ , and  $\text{CH}_3\text{Cl}$  were in the ranges of 65-72 mol-%, 22-25 mol-%, and 2-3 mol-%, respectively. These selectivities shifted towards the undesired direction where selectivities to  $\text{CH}_3\text{Cl}$  and  $\text{CH}_2\text{Cl}_2$  were nearly 7 and 2 times higher than the baseline of  $\text{Cu}^0 + \text{NaBH}_4$  in deionized water with  $S_{\text{CH}_3\text{Cl}} = (0.3 \pm 0.2)$  mol-% and  $S_{\text{CH}_2\text{Cl}_2} = (13 \pm 2)$  mol-%, respectively.

The redox-sensitive species  $\text{NO}_3^-$  and  $\text{NO}_2^-$  led to the loss of specific Cu activity (i.e. 20-50 % loss of catalyst activities) due to competition with  $\text{CHCl}_3$  molecules at the Cu surfaces for reduction. This resulted in higher  $\text{CH}_3\text{Cl}$  selectivities ( $S_{\text{CH}_3\text{Cl}} = 4-5$  mol-%), which were 13-17 times higher than the baseline of  $\text{Cu}^0 + \text{NaBH}_4$  with  $S_{\text{CH}_3\text{Cl}} = (0.3 \pm 0.2)$  mol-%.

Sulfide had the most negative effect on the performance of  $\text{Cu}^0 + \text{NaBH}_4$ , in terms of both product selectivity patterns and specific catalyst activities. Significant catalyst deactivation was observed in the presence of sulfide, where the ratio between the specific Cu activities in the presence of 1 mg/L  $\text{Na}_2\text{S}$  and deionized water  $A_{\text{Cu,CHCl}_3,\text{Na}_2\text{S}}/A_{\text{Cu,CHCl}_3,\text{deionized water}} = 0.1$ . The consequence of strong interaction between sulfide/bisulfide with Cu resulted in the modification of catalyst surface (formation of CuS). This modification altered the product selectivity patterns in the undesired direction, i.e. the selectivities to  $\text{CH}_2\text{Cl}_2$  and  $\text{CH}_3\text{Cl}$  were higher by a factor of 2 and 40, respectively in comparison to the baseline of  $\text{Cu}^0 + \text{NaBH}_4$  in deionized water. Therefore, the protection of Cu catalysts against inhibition or deactivation is necessary for stable performance under real water treatment conditions.

**Optimal reaction conditions that minimize the accumulation of chlorinated byproducts in the reactor were established.** Based on own and literature data, the dechlorination of  $\text{CCl}_4$  and  $\text{CHCl}_3$  using  $\text{Pd} + \text{H}_2$  and  $n\text{ZVI}$  usually produces  $\text{CH}_2\text{Cl}_2$  and  $\text{CH}_3\text{Cl}$  as undesired dead-end byproducts. Similarly, in the current work,  $\text{CH}_2\text{Cl}_2$  was an intermediate that was more-or-less a dead-end byproduct at low catalyst concentrations of  $c_{\text{Cu}} = 0.5\text{-}10 \text{ mg/L}$ . Since the formation and accumulation of the toxic chlorinated byproducts are undesired during water treatment, this thesis work presents the optimal conditions under which the further dechlorination of these intermediates could easily be achieved.

**The optimum catalyst and reductant concentrations needed were established.** In order to generate finally lower amounts of chlorinated byproducts, the optimal catalyst and reductant concentrations required were  $c_{\text{Cu}} \geq 100 \text{ mg/L}$  and  $c_{0,\text{NaBH}_4} \approx 300 \text{ mg/L}$ . Under these conditions, the chlorinated byproducts  $\text{CH}_2\text{Cl}_2$ ,  $\text{CH}_3\text{Cl}$ , and  $\text{CH}_2\text{Cl-CH}_3$  undergo sufficiently fast further dechlorination steps to the fully dechlorinated products,  $\text{CH}_4$  and  $\text{C}_2\text{H}_6$ . As stated earlier, compounds with lower chlorine substitution degrees, e.g.  $\text{CH}_2\text{Cl}_2$ ,  $\text{CH}_3\text{Cl}$ , and  $\text{CH}_2\text{Cl-CH}_3$  are rather resistant to dechlorination using  $\text{Pd} + \text{H}_2$  and  $n\text{ZVI}$ . In comparison to  $\text{Pd}$ - and  $n\text{ZVI}$ -based systems, this thesis work shows that maximized  $\text{Cu}$  and  $\text{NaBH}_4$  concentrations can prevent the accumulation of the less-chlorinated byproducts during the dechlorination of  $\text{CCl}_4$ ,  $\text{CHCl}_3$ ,  $\text{CCl}_3\text{CH}_3$ , and  $\text{CH}_2\text{Cl-CH}_3$  as educts. Hence, for the dehalogenation of  $\text{CCl}_3\text{-R}$  compounds,  $\text{Cu}^0 + \text{NaBH}_4$  is preferable to  $\text{Pd} + \text{H}_2$  and  $n\text{ZVI}$  when product selectivity patterns, specific metal activities, and the fate of chlorinated byproducts are considered.

**Desired selectivities towards less  $\text{CH}_2\text{Cl}_2$  and more  $\text{CH}_4$  were achieved using metallic Ag or bimetallic Ag/Cu particles.** For the first time, this thesis shows that in the presence of  $c_{0,\text{NaBH}_4} = 300 \text{ mg/L}$  as a reductant, lower concentrations of catalysts comprised of

Ag ( $c_{\text{Ag}} = 2 \text{ mg/L}$ ) or bimetallic Ag/Cu ( $c_{\text{Ag/Cu}} = 2 \text{ mg/L}$ ) can achieve the desired selectivities towards higher  $\text{CH}_4$  and lower  $\text{CH}_2\text{Cl}_2$  selectivities. For example, using Ag and bimetallic Ag/Cu particles for the dechlorination of  $\text{CHCl}_3$ , the selectivities to  $\text{CH}_4$ ,  $\text{CH}_2\text{Cl}_2$ , and  $\text{CH}_3\text{Cl}$  were found to be in the range of 90-92, 2-3, and 5-6 mol-%, respectively. The selectivity to  $\text{CH}_2\text{Cl}_2$ , in this case, is nearly 7 times lower than the baseline of  $\text{Cu}^0 + \text{NaBH}_4$  with  $S_{\text{CH}_2\text{Cl}_2} = (13 \pm 2) \text{ mol-\%}$ . Furthermore, the systems  $\text{Ag}^0 + \text{NaBH}_4$  and  $\text{Ag/Cu} + \text{NaBH}_4$  were more potent for the dechlorination of  $\text{CH}_2\text{Cl}_2$  than  $\text{Cu}^0 + \text{NaBH}_4$ . The specific metal activities for the dechlorination of  $\text{CH}_2\text{Cl}_2$  as the educt using either Ag or Ag/Cu were one order of magnitude higher than for the baseline of  $\text{Cu}^0 + \text{NaBH}_4$  i.e.,  $A_{\text{Ag,CH}_2\text{Cl}_2} = (2.1 \pm 0.5) \text{ L/(g}\cdot\text{min)}$ ,  $A_{\text{Ag/Cu,CH}_2\text{Cl}_2} = (1.0 \pm 0.5) \text{ L/(g}\cdot\text{min)}$  and  $A_{\text{Cu,CH}_2\text{Cl}_2} = (0.22 \pm 0.02) \text{ L/(g}\cdot\text{min)}$ , respectively. Although both Ag and bimetallic Ag/Cu particles could achieve the desired product selectivities (i.e. towards  $\text{CH}_4$  and the subsequent dechlorination of  $\text{CH}_2\text{Cl}_2$  as an intermediate), bimetallic Ag/Cu particles are recommended due to the higher specific metal activities for the dechlorination of  $\text{CHCl}_3$ , with  $A_{\text{m,CHCl}_3} = (80 \pm 5) \text{ L/(g}\cdot\text{min)}$  compared to the specific Ag activity with  $A_{\text{Ag,CHCl}_3} = (25 \pm 5) \text{ L/(g}\cdot\text{min)}$ . Also, Ag costs more than Cu by a factor of 90. Hence small amounts of Ag onto Cu should be considered as an alternative to pure Ag.

**$\text{Cu}^0 + \text{vitamin B12} + \text{NaBH}_4$  represents an optimal system combination for the dechlorination of  $\text{CHCl}_3$  in water.** For the system comprising  $\text{Cu}^0 + \text{NaBH}_4 + \text{vitamin B12}$ , the apparent selectivities to  $\text{CH}_4$ ,  $\text{CH}_2\text{Cl}_2$  and  $\text{CH}_3\text{Cl}$  were  $(90 \pm 2) \text{ mol-\%}$ ,  $(2 \pm 1) \text{ mol-\%}$  and  $(3 \pm 1) \text{ mol-\%}$ , respectively. The term ‘apparent selectivities’ is used in this case due to the accelerated dechlorination of  $\text{CH}_2\text{Cl}_2$  as an intermediate. For the system  $\text{Cu}^0 + \text{NaBH}_4 + \text{vitamin B12}$ , the specific metal activities for the dechlorination of  $\text{CHCl}_3$  and  $\text{CH}_2\text{Cl}_2$  were  $A_{\text{m,CHCl}_3} = (260 \pm 20) \text{ L/(g}\cdot\text{min)}$  and  $A_{\text{m,CH}_2\text{Cl}_2} = (15 \pm 3) \text{ L/(g}\cdot\text{min)}$ , respectively. These specific

metal activities were 2 and 68 times higher than the baseline of  $\text{Cu}^0 + \text{NaBH}_4$ , respectively. Therefore, the system  $\text{Cu}^0 + \text{NaBH}_4 + \text{vitamin B12}$  represents an optimal catalyst combination for the dechlorination of  $\text{CHCl}_3$  in water when the specific metal activities, product selectivity patterns, and the fate of chlorinated byproducts are considered.

### **Comparison of reagents and catalysts; recommended application areas**

In this part of the thesis, the dehalogenation potential of  $\text{Cu}^0 + \text{NaBH}_4$ ,  $\text{Pd} + \text{H}_2$ , and nZVI were investigated for various HOCs commonly encountered as water contaminants. Using own experimental data and literature data which were further processed, the specific metal activities for dehalogenation of similar HOCs using Cu-, Pd- and nZVI-based systems were determined by tuning the sizes of nanoparticles in the range of 50-75 nm. The scope and spectrum for application of each metal were evaluated based upon the following criteria: i) the reduction rates of the target compounds where specific metal activities were calculated, ii) the product yields iii) the fate of chlorinated intermediates, and iv) metal cost and catalyst stability in water. Based on these criteria, the recommended application areas for each remediation system are presented.

**$\text{Cu}^0 + \text{NaBH}_4$  should be considered for the dehalogenation of saturated aliphatic HOCs in water.** From experimental data, it was derived that  $\text{Cu}^0 + \text{NaBH}_4$  can be applied to nearly all HOC classes containing F, Cl, and Br at ambient conditions. However, as it was demonstrated for  $\text{CFCl}_3$  and  $\text{CCl}_2\text{F}-\text{CClF}_2$ , it is noteworthy to clarify that  $\text{Cu}^0 + \text{NaBH}_4$  fails for the cleavage of C–F bonds. Nevertheless, the cleavage of the C–F bonds during the dehalogenation of  $\text{CFCl}_3$  was easily achieved using the system comprised of  $\text{Cu}^0 + \text{NaBH}_4 + \text{vitamin B12}$ . Based on the specific metal activities for dehalogenation of saturated aliphatic HOCs, the following order of metal activities was observed:  $\text{Cu} \gg \text{Pd} \gg \text{nZVI}$ . For example, the specific metal activities for the dechlorination of chloroform using Cu, Pd and nZVI were  $A_{\text{Cu,CHCl}_3} = (130 \pm 10) \text{ L}/(\text{g}\cdot\text{min})$ ,

$A_{\text{Pd,CHCl}_3} = (5 \pm 1) \text{ L}/(\text{g}\cdot\text{min})$ , and  $A_{\text{nZVI,CHCl}_3} = (0.003 \pm 0.001) \text{ L}/(\text{g}\cdot\text{min})$ , respectively. Although these metal activities are mass-based ( $\text{L}/(\text{g}\cdot\text{min})$ ), the ranking can approximately be applied to surface activities because the investigated metal particles have similar sizes and are all non-porous. Furthermore, in this thesis, it was demonstrated that compounds with low chlorine substitution degrees which include  $\text{CH}_2\text{Cl}_2$ ,  $\text{CH}_3\text{Cl}$ ,  $\text{CH}_2\text{Cl}-\text{CH}_3$ ,  $\text{CH}_2\text{Cl}-\text{CH}_2\text{Cl}$ ,  $\text{CH}_2\text{Cl}-\text{CHCl}-\text{CH}_3$ , and  $\text{CH}_2\text{Cl}-\text{CHCl}-\text{CH}_2-\text{CH}_3$  which are difficult to dechlorinate using Pd and nZVI, were in this case easily dechlorinated by  $\text{Cu}^0 + \text{NaBH}_4$ . Based on the higher specific Cu activities for the reduction of saturated aliphatic compounds, copper catalysts which are cheaper by a factor of about 8500 than palladium catalysts on a mass basis are recommended for the dechlorination of these compounds in water treatment technologies. On the other hand,  $\text{NaBH}_4$  as a reductant costs more by a factor of 12 than  $\text{H}_2$  (comparison based on reduction equivalents), and the release of borate in the treated water may be an issue. Nevertheless,  $\text{Cu}^0 + \text{NaBH}_4$  is a promising system for small-scale *ex situ* applications; especially the regeneration of HOC-loaded adsorbents.

**Supported Cu catalysts as an alternative to Cu nanoparticles for treatment of saturated aliphatic HOCs in water.** As a precautionary measure, supported Cu catalysts should be considered as an alternative to Cu nanoparticles in order to allow copper recovery from the treated effluent. Supported Cu catalysts can also be handled more easily than Cu nanoparticles. Furthermore, Cu as a moderately toxic heavy metal is undesired in the environment and the allowable drinking-water limit as set by the World Health Organization is 2 mg/L. Despite the benefits of supported Cu catalysts, mass-transfer limitations and variation in particle sizes show that the specific catalyst activities for supported Cu catalysts were much lower than for Cu nanoparticles. Therefore, Cu/resin (refers to Cu-modified amberlite resin) was prepared and used for dechlorination of  $\text{CHCl}_3$  under reaction conditions similar to Cu nanoparticles. For example,

in this thesis the specific catalyst activities for the dechlorination of chloroform using Cu nanoparticles and Cu/resin catalysts in the presence of NaBH<sub>4</sub> were  $A_{\text{Cu,CHCl}_3} = (130 \pm 10) \text{ L}/(\text{g}\cdot\text{min})$  and  $A_{\text{Cu/resin,CHCl}_3} = (15 \pm 2) \text{ L}/(\text{g}\cdot\text{min})$ , respectively.

For the first time the reusability of Cu/resin catalysts is reported in this thesis where the catalysts were used in repeated reaction cycles under laboratory conditions. No copper leaching from the resin was observed, even after 9 reaction cycles, and the specific catalyst activities for dechlorination of chloroform using Cu/resin catalysts remained more-or-less the same during the entire operation. This is a significant improvement that could be of relevance for technical application when the Cu/resin catalysts are considered for long-term operation under field conditions.

**nZVI as a reagent should be considered for the dechlorination of chlorinated ethylenes.** Based on the specific metal activities for dechlorination of chlorinated ethylenes, the order of metal performance is as follows: Pd >> Cu >> nZVI. Although specific metal activities suggest that Pd should be preferred for the dechlorination of chlorinated ethylenes, nZVI is recommended due to the benefits it offers. The benefits of nZVI as a reagent include: i) it is much cheaper than Pd and Cu, ii) it is environmentally compatible, and iii) it does not require the addition of a further reductant e.g. H<sub>2</sub> or NaBH<sub>4</sub>. Cu<sup>0</sup> + NaBH<sub>4</sub> can to some extent be recommended for the reduction of the less-chlorinated ethylenes such as vinyl chloride and the dichloroethylene isomers, which are more difficult to dechlorinate using nZVI.

**Cu<sup>0</sup> + NaBH<sub>4</sub> should be considered for the reduction of brominated aromatics.** In this part, the comparison for dehalogenation of halogenated aromatics is made between Cu and Pd catalysts. Although in the literature several authors report that nZVI without amendment with hydrogenation-active metals can cleave aromatic C–Cl bonds especially for chlorinated aromatics

with lower chlorination degree e.g. chlorobenzene, own experimental data support the thesis that these results can be considered artifacts. Comparisons between Cu and Pd catalysts for the reduction of brominated and chlorinated aromatic compounds show that the specific Pd activities  $A_{Pd}$  are higher than the specific Cu activities  $A_{Cu}$ . For example, the specific Pd activities for the dehalogenation of chlorobenzene and bromobenzene in water were  $A_{Pd, chlorobenzene} = (500 \pm 150) \text{ L}/(\text{g}\cdot\text{min})$  and  $A_{Pd, bromobenzene} = (900 \pm 100) \text{ L}/(\text{g}\cdot\text{min})$ , respectively. Specific Cu activities for the reduction of chlorobenzene and bromobenzene were  $A_{Cu, chlorobenzene} = (4 \pm 1) \times 10^{-5} \text{ L}/(\text{g}\cdot\text{min})$  and  $A_{Cu, bromobenzene} = (80 \pm 10) \text{ L}/(\text{g}\cdot\text{min})$ , respectively. The low specific Cu activity for the dechlorination of chlorobenzene is therefore not significant for practical application. As stated earlier, Cu costs less by a factor of 8500 than Pd. The lower catalyst cost and adequate activity make  $\text{Cu}^0 + \text{NaBH}_4$  suitable for the reduction of aromatic C–Br bonds.

**Copper catalyst stability, reuse, and ease of regeneration of deactivated catalysts.** This part of the thesis shows that Cu nanoparticles and Cu/resin catalysts were readily deactivated by sulfide in water. For example, the specific Cu activity for the dechlorination of  $\text{CHCl}_3$  using Cu nanoparticles was decreased by the addition of  $\text{Na}_2\text{S}$  ( $n_{Cu} : n_S \approx 0.8$ ) at  $\text{pH} = 10$  from  $(130 \pm 10) \text{ L}/(\text{g}\cdot\text{min})$  to  $(13 \pm 2) \text{ L}/(\text{g}\cdot\text{min})$ , respectively. The dominant sulfur species is  $\text{HS}^-$  under the applied reaction conditions ( $\text{pH} = 10$ ). Incorporation of copper onto amberlite resin could not prevent bisulfide-induced catalyst deactivation. Nevertheless, 30-80 % original activity could be restored by rinsing the sulfide-deactivated Cu/resin with deionized water to remove physisorbed sulfide/bisulfide. For example, using Cu/resin catalysts for the dechlorination of  $\text{CHCl}_3$ , the specific activities for non-deactivated, deactivated (by 1 mg/L  $\text{Na}_2\text{S}$ ) and regenerated catalysts were  $(15 \pm 2) \text{ L}/(\text{g}\cdot\text{min})$ ,  $(1.0 \pm 0.5) \text{ L}/(\text{g}\cdot\text{min})$ , and  $(12 \pm 1) \text{ L}/(\text{g}\cdot\text{min})$ , respectively. This simple

regenerative treatment process (for conditions with lower sulfide concentrations) could contribute to the reuse of sulfide-deactivated catalysts, which is a critical application point in industrial and environmental catalysis.

**Niche application for Pd catalyst.** In this thesis, it was demonstrated that Cu nanoparticles were moderately resistant to deactivation by sulfite, which is an advantage over Pd catalysts. The deactivation of Pd by sulfite and sulfide is well known; extensive work in the literature has been devoted to protecting the catalysts against deactivation by macromolecular and ionic catalyst poisons, e.g. by incorporation onto hydrophobic polymers such as PDMS and silicone coatings. Since polymers such as PDMS are expensive and therefore may further increase treatment costs, the niche application for protected Pd catalysts should be the reduction of aromatic C–Cl bonds.

## Conclusions and Outlook

Dehalogenation reactions of various HOCs were successfully conducted using  $\text{Cu}^0 + \text{NaBH}_4$ ; the potential and limitations of the system are hereby presented.

*Regarding product selectivities.* In the current study with  $\text{CHCl}_3$  as a target pollutant, we observed similar product selectivity patterns (ratio of  $\text{CH}_2\text{Cl}_2 : \text{CH}_4$ ) for very different reduction systems. This supports the view that the nature of reactive species (electrons or active  $\text{H}^*$ ) at the surfaces of Cu and Pd catalysts have no marked effect on the product selectivity patterns. The product selectivity patterns were not system-specific but rather substance-specific. For compounds such as  $\text{CHCl}_3$ ,  $\text{CH}_2\text{Cl}_2$ , and  $\text{CHCl}_2\text{-CH}_3$ , selectivities were in preference of the fully dechlorinated products,  $\text{CH}_4$  and  $\text{C}_2\text{H}_6$ . In contrast by replacing the chloroform's H-substituent as in  $\text{CCl}_4$ ,  $\text{CFCl}_3$ ,  $\text{CBrCl}_3$ , and  $\text{CCl}_3\text{-CH}_3$ , product selectivities were in preference of the halogenated intermediates namely  $\text{CHCl}_3$ ,  $\text{CH}_2\text{Cl}_2$ ,  $\text{CHCl}_2\text{F}$ , and  $\text{CHCl}_2\text{-CH}_3$ . Hence for  $\text{CHCl}_3$ ,  $\text{CH}_2\text{Cl}_2$ , and  $\text{CHCl}_2\text{-CH}_3$ ,

$\alpha$ -elimination was the main dechlorination mechanism, whereas stepwise hydrogenolysis was the main mechanism for  $\text{CCl}_4$ ,  $\text{CFCl}_3$ ,  $\text{CBrCl}_3$ , and  $\text{CCl}_3\text{-CH}_3$ . In conclusion, this study suggests that steric effects could be the limiting factor for the simultaneous removal of geminal chlorine atoms at the electrophilic carbon during the dehalogenation of saturated aliphatic chloroalkanes in water via  $\alpha$ -elimination.

*Regarding the optimization of the system to generate fewer chlorinated byproducts.* In industrial and environmental catalysis, the accumulation of toxic halogenated byproducts such as  $\text{CH}_2\text{Cl}_2$  greatly affects the efficiency of the treatment system. In order to reduce chlorinated byproducts through a second dechlorination step, in this thesis the following optimal reaction conditions were established: i) use  $c_{\text{Cu}} \geq 100$  mg/L and  $c_{0,\text{NaBH}_4} \approx 300$  mg/L, ii) use either Ag or bimetallic Ag/Cu particles as catalysts, and iii) the optimal catalyst combination consists of  $\text{Cu}^0 + \text{NaBH}_4 + \text{vitamin B12}$ .

*Regarding copper catalysts stability, reuse, and regeneration.* This thesis work showed that Cu nanoparticles were stable against deactivation by sulfite, which is a major advantage over Pd. However, sulfide is still a major problem that led to the significant deactivation of Cu catalysts. For Cu/resin catalysts as an alternative to Cu nanoparticles, reusability and regeneration abilities were considered. After repeated reaction cycles, no copper leaching from the resin was observed, and the specific catalyst activities remained more-or-less constant. Furthermore, the sulfide-deactivated Cu/resin catalyst was easily regenerated by rinsing with deionized water and drying at 100 °C.

*Regarding application areas for reagents and catalysts.* From own experimental data as well as literature data, the recommended application areas for Cu, Pd, and nZVI are as follows: i)  $\text{Cu}^0 + \text{NaBH}_4$  is recommended for use in the treatment of saturated aliphatic HOCs and

chlorinated ethylenes as well as for the cleavage of aromatic C–Br bonds, ii) nZVI as a reagent is recommended for highly chlorinated HOCs, especially the chlorinated ethylenes, and iii) the niche application of sulfide-protected Pd catalysts is the cleavage of aromatic C–Cl bonds.

In conclusion, this research work has significantly broadened the scientific knowledge on the application of  $\text{Cu}^0 + \text{NaBH}_4$  as a robust reductive dehalogenation system for the treatment of water contaminated with HOCs. Although Cu/resin catalysts could minimize copper leaching into the water and therefore improve the reusability and regeneration of the catalysts, further catalyst development might be necessary in order to improve performance. Measures for the protection of Cu catalysts against deactivation by sulfide/bisulfide are also desirable in future works.

## 6 Bibliography

- Ahmed, O.H., Altarawneh, M., Al-Harabsheh, M., Jiang, Z.-T., Dlugogorski, B.Z. (2018): Catalytic de-halogenation of alkyl halides by copper surfaces. *Journal of Environmental Chemical Engineering* 6(6), 7214-7224.
- Ahn, J.-Y., Kim, C., Kim, H.-S., Hwang, K.-Y., Hwang, I. (2016): Effects of oxidants on *in situ* treatment of a DNAPL source by nanoscale zero-valent iron: A field study. *Water Research* 107, 57-65.
- Andersin, J., Honkala, K. (2011): First principles investigations of Pd-on-Au nanostructures for trichloroethene catalytic removal from groundwater. *Physical Chemistry Chemical Physics* 13(4), 1386-1394.
- Andrieux, C.P., Saveant, J.M., Su, K.B. (1986): Kinetics of dissociative electron transfer. Direct and mediated electrochemical reductive cleavage of the carbon-halogen bond. *The Journal of Physical Chemistry* 90(16), 3815-3823.
- Angeles-Wedler, D., Mackenzie, K., Kopinke, F.-D. (2008): Permanganate oxidation of sulfur compounds to prevent poisoning of Pd catalysts in water treatment processes. *Environmental Science & Technology* 42(15), 5734-5739.
- Angeles-Wedler, D., Mackenzie, K., Kopinke, F.-D. (2009): Sulphide-induced deactivation of Pd/Al<sub>2</sub>O<sub>3</sub> as hydrodechlorination catalyst and its oxidative regeneration with permanganate. *Applied Catalysis B: Environmental* 90(3), 613-617.
- Aramendía, M.A., Boráu, V., García, I.M., Jiménez, C., Lafont, F., Marinas, A., Marinas, J.M., Urbano, F.J. (2002): Liquid-phase hydrodechlorination of chlorobenzene over palladium-supported catalysts: Influence of HCl formation and NaOH addition. *Journal of Molecular Catalysis A: Chemical* 184(1), 237-245.
- Aramendía, M.A., Burch, R., García, I.M., Marinas, A., Marinas, J.M., Southward, B.W.L., Urbano, F.J. (2001): The effect of the addition of sodium compounds in the liquid-phase hydrodechlorination of chlorobenzene over palladium catalysts. *Applied Catalysis B: Environmental* 31(3), 163-171.
- Arnold, W.A., Ball, W.P., Roberts, A.L. (1999): Polychlorinated ethane reaction with zero-valent zinc: Pathways and rate control. *Journal of Contaminant Hydrology* 40(2), 183-200.
- Arnold, W.A., Roberts, A.L. (2000): Pathways and kinetics of chlorinated ethylene and chlorinated acetylene reaction with Fe(0) particles. *Environmental Science & Technology* 34(9), 1794-1805.
- Bae, S., Collins, R.N., Waite, T.D., Hanna, K. (2018): Advances in surface passivation of nanoscale zerovalent iron: A critical review. *Environmental Science & Technology* 52(21), 12010-12025.

- Bagley, D.M., Lalonde, M., Kaseros, V., Stasiuk, K.E., Sleep, B.E. (2000): Acclimation of anaerobic systems to biodegrade tetrachloroethene in the presence of carbon tetrachloride and chloroform. *Water Research* 34(1), 171-178.
- Baglieri, A., Vindrola, D., Gennari, M., Negre, M. (2014): Chemical and spectroscopic characterization of insoluble and soluble humic acid fractions at different pH values. *Chemical and Biological Technologies in Agriculture* 1(1), 9.
- Balda, M., Kopinke, F.-D. (2020): The role of nickel traces in fine chemicals for hydrodechlorination reactions with zero-valent iron. *Chemical Engineering Journal* 388, 124185.
- Balko, B.A., Tratnyek, P.G. (1998): Photoeffects on the reduction of carbon tetrachloride by zero-valent iron. *The Journal of Physical Chemistry B* 102(8), 1459-1465.
- Barbosa, L., Loffreda, D., Sautet, P. (2002): Chemisorption of trichloroethene on the PdCu alloy (110) surface: A periodical density functional study. *Langmuir* 18(7), 2625-2635.
- Barnes, R.J., Riba, O., Gardner, M.N., Scott, T.B., Jackman, S.A., Thompson, I.P. (2010): Optimization of nano-scale nickel/iron particles for the reduction of high concentration chlorinated aliphatic hydrocarbon solutions. *Chemosphere* 79(4), 448-454.
- Battke, J. (2006): Interaktion von Sorption und Reaktion bei der Dehalogenierung von halogenorganischen Verbindungen in Wasser. Doctoral Thesis, Otto-von-Guericke-Universität Magdeburg, UFZ-Umweltforschungszentrum Leipzig-Halle GmbH.
- Benitez, J.L., Del Angel, G. (2000): Effect of chlorine released during hydrodechlorination of chlorobenzene over Pd, Pt and Rh supported catalysts. *Reaction Kinetics and Catalysis Letters* 70(1), 67-72.
- Bennett, E., Wilson, T., Murphy, P., Refson, K., Hannon, A., Imberti, S., Callear, S., Chass, G., Parker, S. (2015): Structure and spectroscopy of CuH prepared via borohydride reduction. *Acta Crystallographica Section B Structural Science, Crystal Engineering and Materials* 71, 608-612.
- Beznis, N.V., Weckhuysen, B.M., Bitter, J.H. (2010): Cu-ZSM-5 zeolites for the formation of methanol from methane and oxygen: Probing the active sites and spectator species. *Catalysis Letters* 138(1), 14-22.
- Biçer, M., Şişman, İ. (2010): Controlled synthesis of copper nano/microstructures using ascorbic acid in aqueous CTAB solution. *Powder Technology* 198(2), 279-284.
- Bleyl, S., Kopinke, F.-D., Mackenzie, K. (2012): Carbo-Iron®—synthesis and stabilization of Fe(0)-doped colloidal activated carbon for *in situ* groundwater treatment. *Chemical Engineering Journal* 191, 588-595.
- Bransfield, S.J., Cwiertny, D.M., Roberts, A.L., Fairbrother, D.H. (2006): Influence of copper loading and surface coverage on the reactivity of granular iron toward 1,1,1-trichloroethane. *Environmental Science & Technology* 40(5), 1485-1490.

- Brigante, M., Zanini, G., Avena, M. (2007): On the dissolution kinetics of humic acid particles: Effects of pH, temperature and  $\text{Ca}^{2+}$  concentration. *Colloids and Surfaces A: Physicochemical and Engineering Aspects* 294(1), 64-70.
- Burris, D.R., Delcomyn, C.A., Smith, M.H., Roberts, A.L. (1996): Reductive dechlorination of tetrachloroethylene and trichloroethylene catalyzed by vitamin B12 in homogeneous and heterogeneous systems. *Environmental Science & Technology* 30(10), 3047-3052.
- Byrd, M.O., Ohrenberg, C.J. (2017): The use of ammonia as a qualitative test for determining when solid copper has completely precipitated from aqueous solutions containing copper(II) ions. *Georgia Journal of Science* 75(2), 1.
- Camacho-Flores, B.A., Martínez-Álvarez, O., Arenas-Arrocena, M.C., Garcia-Contreras, R., Argueta-Figueroa, L., de la Fuente-Hernández, J., Acosta-Torres, L.S. (2015): Copper: Synthesis techniques in nanoscale and powerful application as an antimicrobial agent. *Journal of Nanomaterials* 2015, 415238.
- Campbell, T., Burris, D., Roberts, A., Wells, J. (1997): Trichloroethylene and tetrachloroethylene reduction in a metallic iron–water-vapor batch system. *Environmental Toxicology and Chemistry* 16, 625-630.
- Chaplin, B.P., Reinhard, M., Schneider, W.F., Schüth, C., Shapley, J.R., Strathmann, T.J., Werth, C.J. (2012): Critical review of Pd-based catalytic treatment of priority contaminants in water. *Environmental Science & Technology* 46(7), 3655-3670.
- Chaplin, B.P., Roundy, E., Guy, K.A., Shapley, J.R., Werth, C.J. (2006): Effects of natural water ions and humic acid on catalytic nitrate reduction kinetics using an alumina supported Pd–Cu catalyst. *Environmental Science & Technology* 40(9), 3075-3081.
- Chaplin, B.P., Shapley, J.R., Werth, C.J. (2007): Regeneration of sulfur-fouled bimetallic Pd-based catalysts. *Environmental Science & Technology* 41(15), 5491-5497.
- Chen, N. (2003): Kinetics of the hydrodechlorination reaction of chlorinated compounds on palladium catalysts. Doctoral Thesis, Worcester Polytechnic Institute, Worcester, Massachusetts, USA.
- Chou, Y.-H., Yu, J.-H., Liang, Y.-M., Wang, P.-J., Li, C.-W., Chen, S.-S. (2015): Recovery of Cu(II) by chemical reduction using sodium dithionite: Effect of pH and ligands. *Water Science and Technology* 72(11), 2089-2094.
- Cioslowski, J., Liu, G., Moncrieff, D. (1997): Thermochemistry of homolytic C–C, C–H, and C–Cl bond dissociations in polychloroethanes: Benchmark electronic structure calculations. *Journal of the American Chemical Society* 119(47), 11452-11457.
- Comandella, D., Werheid, M., Kopinke, F.-D., Mackenzie, K. (2017): Optimization of PDMS-embedded palladium hydrodechlorination catalysts. *Chemical Engineering Journal* 319, 21-30.

- Comandella, D., Woszidlo, S., Georgi, A., Kopinke, F.-D., Mackenzie, K. (2016): Efforts for long-term protection of palladium hydrodechlorination catalysts. *Applied Catalysis B: Environmental* 186, 204-211.
- Conrad, H., Ertl, G., Latta, E.E. (1974): Adsorption of hydrogen on palladium single crystal surfaces. *Surface Science* 41(2), 435-446.
- Copper Prices. (2021): Copper prices - 45 year historical chart. Retrieved 21 April 2021 from <https://www.macrotrends.net/1476/copper-prices-historical-chart-data>
- Coq, B., Ferrat, G., Figueras, F. (1986): Conversion of chlorobenzene over palladium and rhodium catalysts of widely varying dispersion. *Journal of Catalysis* 101(2), 434-445.
- Cwiertny, D.M., Bransfield, S.J., Livi, K.J.T., Fairbrother, D.H., Roberts, A.L. (2006): Exploring the influence of granular iron additives on 1,1,1-trichloroethane reduction. *Environmental Science & Technology* 40(21), 6837-6843.
- Cwiertny, D.M., Bransfield, S.J., Roberts, A.L. (2007): Influence of the oxidizing species on the reactivity of iron-based bimetallic reductants. *Environmental Science & Technology* 41(10), 3734-3740.
- de Romaña, D.L., Olivares, M., Uauy, R., Araya, M. (2011): Risks and benefits of copper in light of new insights of copper homeostasis. *Journal of Trace Elements in Medicine and Biology* 25(1), 3-13.
- Dekant, W., Jean, P., Arts, J. (2021): Evaluation of the carcinogenicity of dichloromethane in rats, mice, hamsters and humans. *Regulatory Toxicology and Pharmacology* 120, 104858.
- Desai D'sa, E., Wentworth, W.E., Chen, E.C.M. (1988): Thermal electron attachment to chloro- and bromoethylenes. The demonstration of a new electron capture detector mechanism. *Journal of Physical Chemistry* 92(2), 285-290.
- Díez-González, S., Nolan, S.P. (2008): Copper, silver, and gold complexes in hydrosilylation reactions. *Accounts of Chemical Research* 41(2), 349-358.
- Dong, H., Li, L., Lu, Y., Cheng, Y., Wang, Y., Ning, Q., Wang, B., Zhang, L., Zeng, G. (2019): Integration of nanoscale zero-valent iron and functional anaerobic bacteria for groundwater remediation: A review. *Environment International* 124, 265-277.
- Duhamel, M., Wehr, S., Yu, L., Rizvi, H., Seepersad, D., Dworatzek, S., Cox, E., Edwards, E. (2002): Comparison of anaerobic dechlorinating enrichment cultures maintained on tetrachloroethene, trichloroethene, *cis*-dichloroethene and vinyl chloride. *Water Research* 36, 4193-4202.
- Duydu, Y., Başaran, N., Üstündağ, A., Aydın, S., Ündeğer, Ü., Ataman, O.Y., Aydos, K., Düker, Y., Ickstadt, K., Waltrup, B.S., Golka, K., Bolt, H.M. (2011): Reproductive toxicity parameters and biological monitoring in occupationally and environmentally boron-exposed persons in Bandırma, Turkey. *Archives of Toxicology* 85(6), 589-600.

- El-Sharnouby, O. (2016): Liquid phase nano metal catalyzed dechlorination of chlorinated organic compounds. Doctoral Thesis, The University of Western Ontario, Ontario, Canada.
- El-Sharnouby, O., Boparai, H.K., Herrera, J., O'Carroll, D.M. (2018): Aqueous-phase catalytic hydrodechlorination of 1,2-dichloroethane over palladium nanoparticles (nPd) with residual borohydride from nPd synthesis. *Chemical Engineering Journal* 342, 281-292.
- Erable, B., Goubet, I., Lamare, S., Legoy, M.-D., Maugard, T. (2006): Bioremediation of halogenated compounds: Comparison of dehalogenating bacteria and improvement of catalyst stability. *Chemosphere* 65(7), 1146-1152.
- Fail, P.A., Chapin, R.E., Price, C.J., Heindel, J.J. (1998): General, reproductive, developmental, and endocrine toxicity of boronated compounds. *Reproductive Toxicology* 12(1), 1-18.
- Feng, J., Lim, T.-T. (2005): Pathways and kinetics of carbon tetrachloride and chloroform reductions by nano-scale Fe and Fe/Ni particles: Comparison with commercial micro-scale Fe and Zn. *Chemosphere* 59(9), 1267-1277.
- Feng, J., Lim, T.T. (2007): Iron-mediated reduction rates and pathways of halogenated methanes with nanoscale Pd/Fe: Analysis of linear free energy relationship. *Chemosphere* 66(9), 1765-1774.
- Fennelly, J.P., Roberts, A.L. (1998): Reaction of 1,1,1-trichloroethane with zero-valent metals and bimetallic reductants. *Environmental Science & Technology* 32(13), 1980-1988.
- Fritsch, D., Kuhr, K., Mackenzie, K., Kopinke, F.-D. (2003): Hydrodechlorination of chloroorganic compounds in ground water by palladium catalysts: Part 1. Development of polymer-based catalysts and membrane reactor tests. *Catalysis Today* 82(1), 105-118.
- Garcia, N.A., Boparai, H.K., O'Carroll, D.M. (2016): Enhanced dechlorination of 1,2-dichloroethane by coupled nano iron-dithionite treatment. *Environmental Science & Technology* 50(10), 5243-5251.
- Gawande, M.B., Goswami, A., Felpin, F.-X., Asefa, T., Huang, X., Silva, R., Zou, X., Zboril, R., Varma, R.S. (2016): Cu and Cu-based nanoparticles: Synthesis and applications in catalysis. *Chemical Reviews* 116(6), 3722-3811.
- Gómez-Sainero, L.M., Seoane, X.L., Fierro, J.L.G., Arcoya, A. (2002): Liquid-phase hydrodechlorination of CCl<sub>4</sub> to CHCl<sub>3</sub> on Pd/carbon catalysts: Nature and role of Pd active species. *Journal of Catalysis* 209(2), 279-288.
- Guy, K.A., Xu, H., Yang, J.C., Werth, C.J., Shapley, J.R. (2009): Catalytic nitrate and nitrite reduction with Pd-Cu/PVP colloids in water: Composition, structure, and reactivity correlations. *The Journal of Physical Chemistry C* 113(19), 8177-8185.
- Han, Y., Liu, C., Horita, J., Yan, W. (2016): Trichloroethene hydrodechlorination by Pd-Fe bimetallic nanoparticles: Solute-induced catalyst deactivation analyzed by carbon isotope fractionation. *Applied Catalysis B: Environmental* 188, 77-86.

- Hara, J., Ito, H., Suto, K., Inoue, C., Chida, T. (2005): Kinetics of trichloroethene dechlorination with iron powder. *Water Research* 39(6), 1165-1173.
- Harper, D.B. (2000): The global chloromethane cycle: Biosynthesis, biodegradation and metabolic role. *Natural Product Reports* 17(4), 337-348.
- Hildebrand, H., Mackenzie, K., Kopinke, F.-D. (2009a): Highly active Pd-on-magnetite nanocatalysts for aqueous phase hydrodechlorination reactions. *Environmental Science & Technology* 43(9), 3254-3259.
- Hildebrand, H., Mackenzie, K., Kopinke, F.-D. (2009b): Pd/Fe<sub>3</sub>O<sub>4</sub> nano-catalysts for selective dehalogenation in wastewater treatment processes—influence of water constituents. *Applied Catalysis B: Environmental* 91(1), 389-396.
- Hirvonen, A., Tuhkanen, T., Kalliokoski, P. (1996): Formation of chlorinated acetic acids during UV/H<sub>2</sub>O<sub>2</sub>-oxidation of ground water contaminated with chlorinated ethylenes. *Chemosphere* 32(6), 1091-1102.
- Hu, M., Liu, Y., Yao, Z., Ma, L., Wang, X. (2017): Catalytic reduction for water treatment. *Frontiers of Environmental Science & Engineering* 12(1), 3.
- Huang, B., Lei, C., Wei, C., Zeng, G. (2014): Chlorinated volatile organic compounds (Cl-VOCs) in environment — sources, potential human health impacts, and current remediation technologies. *Environment International* 71, 118-138.
- Huang, C.-C., Lien, H.-L. (2010): Trimetallic Pd/Fe/Al particles for catalytic dechlorination of chlorinated organic contaminants. *Water Science and Technology* 62(1), 202-208.
- Huang, C.-C., Lo, S.-L., Lien, H.-L. (2012): Zero-valent copper nanoparticles for effective dechlorination of dichloromethane using sodium borohydride as a reductant. *Chemical Engineering Journal* 203, 95-100.
- Huang, C.-C., Lo, S.-L., Lien, H.-L. (2013): Synergistic effect of zero-valent copper nanoparticles on dichloromethane degradation by vitamin B12 under reducing condition. *Chemical Engineering Journal* 219, 311–318.
- Huang, C.-C., Lo, S.-L., Lien, H.-L. (2015): Vitamin B12-mediated hydrodechlorination of dichloromethane by bimetallic Cu/Al particles. *Chemical Engineering Journal* 273, 413-420.
- Huang, C.-C., Lo, S.-L., Tsai, S.-M., Lien, H.-L. (2011): Catalytic hydrodechlorination of 1,2-dichloroethane using copper nanoparticles under reduction conditions of sodium borohydride. *Journal of Environmental Monitoring* 13(9), 2406-2412.
- Hydrogen Council. (2020): Path to hydrogen competitiveness. A cost perspective. Oslo, Norway.
- Iglev, H., Trifonov, A., Thaller, A., Buchvarov, I., Fiebig, T., Laubereau, A. (2005): Photoionization dynamics of an aqueous iodide solution: The temperature dependence. *Chemical Physics Letters* 403(1), 198-204.

- Jafvert, C.T., Lee Wolfe, N. (1987): Degradation of selected halogenated ethanes in anoxic sediment-water systems. *Environmental Toxicology and Chemistry* 6(11), 827-837.
- Jiang, H., Guan, B., Peng, X., Wei, Y., Zhan, R., Lin, H., Huang, Z. (2020): Effect of sulfur poisoning on the performance and active sites of Cu/SSZ-13 catalyst. *Chemical Engineering Science* 226, 115855.
- Jin, X., Peldszus, S., Huck, P.M. (2012): Reaction kinetics of selected micropollutants in ozonation and advanced oxidation processes. *Water Research* 46(19), 6519-6530.
- Joo, S.H., Feitz, A.J., Waite, T.D. (2004): Oxidative degradation of the carbothioate herbicide, molinate, using nanoscale zero-valent iron. *Environmental Science & Technology* 38(7), 2242-2247.
- Khan, A., Rashid, A., Younas, R., Chong, R. (2016): A chemical reduction approach to the synthesis of copper nanoparticles. *International Nano Letters* 6(1), 21-26.
- Klučáková, M., Pekař, M. (2005): Solubility and dissociation of lignitic humic acids in water suspension. *Colloids and Surfaces A: Physicochemical and Engineering Aspects* 252(2), 157-163.
- Kojima, Y., Suzuki, K.-i., Fukumoto, K., Sasaki, M., Yamamoto, T., Kawai, Y., Hayashi, H. (2002): Hydrogen generation using sodium borohydride solution and metal catalyst coated on metal oxide. *International Journal of Hydrogen Energy* 27(10), 1029-1034.
- Kopinke, F.-D., Angeles-Wedler, D., Fritsch, D., Mackenzie, K. (2010): Pd-catalyzed hydrodechlorination of chlorinated aromatics in contaminated waters—effects of surfactants, organic matter and catalyst protection by silicone coating. *Applied Catalysis B: Environmental* 96(3), 323-328.
- Kopinke, F.-D., Mackenzie, K., Köhler, R. (2003): Catalytic hydrodechlorination of groundwater contaminants in water and in the gas phase using Pd/ $\gamma$ -Al<sub>2</sub>O<sub>3</sub>. *Applied Catalysis B: Environmental* 44(1), 15-24.
- Kopinke, F.-D., Speichert, G., Mackenzie, K., Hey-Hawkins, E. (2016): Reductive dechlorination in water: Interplay of sorption and reactivity. *Applied Catalysis B: Environmental* 181, 747-753.
- Kopinke, F.-D., Sühnholz, S., Georgi, A., Mackenzie, K. (2020): Interaction of zero-valent iron and carbonaceous materials for reduction of DDT. *Chemosphere* 253, 126712.
- Lehr, L., Zanni, M.T., Frischkorn, C., Weinkauff, R., Neumark, D.M. (1999): Electron solvation in finite systems: Femtosecond dynamics of iodide·(water)<sub>n</sub> anion clusters. *Science* 284(5414), 635-638.
- Li, B., Lin, K., Zhang, W., Lu, S., Liu, Y. (2012): Effectiveness of air stripping, advanced oxidation, and activated carbon adsorption-coupled process in treating chlorinated solvent-contaminated groundwater. *Journal of Environmental Engineering* 138, 903-914.

- Li, T., Farrell, J. (2000): Reductive dechlorination of trichloroethene and carbon tetrachloride using iron and palladized-iron cathodes. *Environmental Science & Technology* 34(1), 173-179.
- Li, T., Farrell, J. (2001): Electrochemical investigation of the rate-limiting mechanisms for trichloroethylene and carbon tetrachloride reduction at iron surfaces. *Environmental Science & Technology* 35(17), 3560-3565.
- Lide, D.R. (1995): *CRC handbook of chemistry and physics*. CRC Press, New York.
- Lien, H.-L., Zhang, W.-X. (2007): Nanoscale Pd/Fe bimetallic particles: Catalytic effects of palladium on hydrodechlorination. *Applied Catalysis B: Environmental* 77(1), 110-116.
- Lim, T.-T., Zhu, B.-W. (2008): Effects of anions on the kinetics and reactivity of nanoscale Pd/Fe in trichlorobenzene dechlorination. *Chemosphere* 73(9), 1471-1477.
- Lin, C.J., Lo, S.L., Liou, Y.H. (2004): Dechlorination of trichloroethylene in aqueous solution by noble metal-modified iron. *Journal of Hazardous Materials* 116(3), 219-228.
- Lin, Y.H., Tseng, H.H., Wey, M.Y., Lin, M.D. (2010): Characteristics of two types of stabilized nano zero-valent iron and transport in porous media. *Science of The Total Environment* 408(10), 2260-2267.
- Linkous, C.A., Huang, C., Fowler, J.R. (2004): UV photochemical oxidation of aqueous sodium sulfide to produce hydrogen and sulfur. *Journal of Photochemistry and Photobiology A: Chemistry* 168(3), 153-160.
- Liu, B.H., Li, Z.P., Suda, S. (2006): Nickel- and cobalt-based catalysts for hydrogen generation by hydrolysis of borohydride. *Journal of Alloys and Compounds* 415(1), 288-293.
- Liu, W.-J., Qian, T.-T., Jiang, H. (2014): Bimetallic Fe nanoparticles: Recent advances in synthesis and application in catalytic elimination of environmental pollutants. *Chemical Engineering Journal* 236, 448-463.
- Liu, Y., Choi, H., Dionysiou, D., Lowry, G.V. (2005a): Trichloroethene hydrodechlorination in water by highly disordered monometallic nanoiron. *Chemistry of Materials* 17(21), 5315-5322.
- Liu, Y., Lowry, G.V. (2006): Effect of particle age ( $\text{Fe}^0$  content) and solution pH on nZVI reactivity:  $\text{H}_2$  evolution and TCE dechlorination. *Environmental Science & Technology* 40(19), 6085-6090.
- Liu, Y., Majetich, S.A., Tilton, R.D., Sholl, D.S., Lowry, G.V. (2005b): TCE dechlorination rates, pathways, and efficiency of nanoscale iron particles with different properties. *Environmental Science & Technology* 39(5), 1338-1345.
- Liu, Z., Betterton, E.A., Arnold, R.G. (2000): Electrolytic reduction of low molecular weight chlorinated aliphatic compounds: Structural and thermodynamic effects on process kinetics. *Environmental Science & Technology* 34(5), 804-811.

- Lowry, G.V., Reinhard, M. (1999): Hydrodehalogenation of 1- to 3-carbon halogenated organic compounds in water using a palladium catalyst and hydrogen gas. *Environmental Science & Technology* 33(11), 1905-1910.
- Lowry, G.V., Reinhard, M. (2000): Pd-catalyzed TCE dechlorination in groundwater: Solute effects, biological control, and oxidative catalyst regeneration. *Environmental Science & Technology* 34(15), 3217-3223.
- Lowry, G.V., Reinhard, M. (2001): Pd-catalyzed TCE dechlorination in water: Effect of  $[H_2](aq)$  and  $H_2$ -utilizing competitive solutes on the TCE dechlorination rate and product distribution. *Environmental Science & Technology* 35(4), 696-702.
- Luo, Y.-R. (2007): *Comprehensive handbook of chemical bond energies*. CRC Press, Boca Raton, FL.
- Mabey, W., Mill, T. (1978): Critical review of hydrolysis of organic compounds in water under environmental conditions. *Journal of Physical and Chemical Reference Data* 7(2), 383-415.
- Mackenzie, K., Bleyl, S., Georgi, A., Kopinke, F.D. (2012): Carbo-Iron - an Fe/AC composite - as alternative to nano-iron for groundwater treatment. *Water Research* 46(12), 3817-3826.
- Mackenzie, K., Frenzel, H., Kopinke, F.-D. (2006): Hydrodehalogenation of halogenated hydrocarbons in water with Pd catalysts: Reaction rates and surface competition. *Applied Catalysis B: Environmental* 63(3), 161-167.
- Mackenzie, K., Kopinke, F.-D., Remmler, M. (1996): Reductive destruction of halogenated hydrocarbons in liquids and solids with solvated electrons. *Chemosphere* 33(8), 1495-1513.
- Mackenzie, P.D., Horney, D.P., Sivavec, T.M. (1999): Mineral precipitation and porosity losses in granular iron columns. *Journal of Hazardous Materials* 68(1), 1-17.
- Matheson, L.J., Tratnyek, P.G. (1994): Reductive dehalogenation of chlorinated methanes by iron metal. *Environmental Science & Technology* 28(12), 2045-2053.
- Matzek, L.W., Carter, K.E. (2016): Activated persulfate for organic chemical degradation: A review. *Chemosphere* 151, 178-188.
- McCormick, M.L., Adriaens, P. (2004): Carbon tetrachloride transformation on the surface of nanoscale biogenic magnetite particles. *Environmental Science & Technology* 38(4), 1045-1053.
- Mueller, N.C., Braun, J., Bruns, J., Černík, M., Rissing, P., Rickerby, D., Nowack, B. (2012): Application of nanoscale zero valent iron (nZVI) for groundwater remediation in Europe. *Environmental Science and Pollution Research* 19(2), 550-558.
- Munoz, M., Kolb, V., Lamolda, A., de Pedro, Z.M., Modrow, A., Etzold, B.J.M., Rodriguez, J.J., Casas, J.A. (2017): Polymer-based spherical activated carbon as catalytic support for hydrodechlorination reactions. *Applied Catalysis B: Environmental* 218, 498-505.

- Navon, R., Eldad, S., Mackenzie, K., Kopinke, F.-D. (2012): Protection of palladium catalysts for hydrodechlorination of chlorinated organic compounds in wastewaters. *Applied Catalysis B: Environmental* 119-120, 241-247.
- Noubactep, C. (2008): A critical review on the process of contaminant removal in Fe<sup>0</sup>-H<sub>2</sub>O systems. *Environmental Technology* 29(8), 909-920.
- Nurmi, J.T., Tratnyek, P.G., Sarathy, V., Baer, D.R., Amonette, J.E., Pecher, K., Wang, C., Linehan, J.C., Matson, D.W., Penn, R.L., Driessen, M.D. (2005): Characterization and properties of metallic iron nanoparticles: Spectroscopy, electrochemistry, and kinetics. *Environmental Science & Technology* 39(5), 1221-1230.
- Oh, W.-D., Dong, Z., Lim, T.-T. (2016): Generation of sulfate radical through heterogeneous catalysis for organic contaminants removal: Current development, challenges and prospects. *Applied Catalysis B: Environmental* 194, 169-201.
- Ordóñez, S., Sastre, H., Díez, F.V. (2000): Hydrodechlorination of aliphatic organochlorinated compounds over commercial hydrogenation catalysts. *Applied Catalysis B: Environmental* 25(1), 49-58.
- Orth, W.S., Gillham, R.W. (1996): Dechlorination of trichloroethene in aqueous solution using Fe<sup>0</sup>. *Environmental Science & Technology* 30(1), 66-71.
- Palladium Prices. (2021): Palladium prices - interactive historical chart. Retrieved 21 April 2021 from <https://www.macrotrends.net/2542/palladium-prices-historical-chart-data>
- Peters, C.J., Young, R.J., Perry, R. (1980): Factors influencing the formation of haloforms in the chlorination of humic materials. *Environmental Science & Technology* 14(11), 1391-1395.
- Phenrat, T., Schoenfelder, D., Losi, M., Yi, J., Peck, S.A., Lowry, G.V. (2009): Treatability study for a TCE contaminated area using nanoscale- and microscale-zerovalent iron particles: Reactivity and reactive life time. *Environmental Applications of Nanoscale and Microscale Reactive Metal Particles* 1027, 183-202.
- Poursaberi, T., Konoz, E., Sarrafi, A., Hassanisadi, M., Hajifathli, F. (2012): Application of nanoscale zero-valent iron in the remediation of DDT from contaminated water. *Chemical Science Transactions* 1, 658-668.
- Prokkola, H., Nurmesniemi, E.-T., Lassi, U. (2020): Removal of metals by sulphide precipitation using Na<sub>2</sub>S and HS<sup>-</sup>-solution. *ChemEngineering* 4(3), 51.
- Qi, X., Dong, Y.n., Wang, H., Wang, C., Li, F. (2017): Application of Turbiscan in the homoaggregation and heteroaggregation of copper nanoparticles. *Colloids and Surfaces A: Physicochemical and Engineering Aspects* 535, 96-104.
- Raut, S.S., Kamble, S.P., Kulkarni, P.S. (2016): Efficacy of zero-valent copper (Cu(0)) nanoparticles and reducing agents for dechlorination of mono chloroaromatics. *Chemosphere* 159, 359-366.

- Rioux, R.M., Thompson, C.D., Chen, N., Ribeiro, F.H. (2000): Hydrodechlorination of chlorofluorocarbons  $\text{CF}_3\text{-CFCl}_2$  and  $\text{CF}_3\text{-CCl}_3$  over Pd/carbon and Pd black catalysts. *Catalysis Today* 62(2), 269-278.
- Roberts, A.L., Totten, L.A., Arnold, W.A., Burris, D.R., Campbell, T.J. (1996): Reductive elimination of chlorinated ethylenes by zero-valent metals. *Environmental Science & Technology* 30(8), 2654-2659.
- Rosbero, T.M.S., Camacho, D.H. (2017): Green preparation and characterization of tentacle-like silver/copper nanoparticles for catalytic degradation of toxic chlorpyrifos in water. *Journal of Environmental Chemical Engineering* 5(3), 2524-2532.
- Rosenthal, S.L. (1987): A review of the mutagenicity of chloroform. *Environmental Molecular Mutagenesis* 10(2), 211-226.
- Ruangchainikom, C., Liao, C.H., Anotai, J., Lee, M.T. (2006): Effects of water characteristics on nitrate reduction by the  $\text{Fe}^0/\text{CO}_2$  process. *Chemosphere* 63(2), 335-343.
- Scherer, M.M., Balko, B.A., Gallagher, D.A., Tratnyek, P.G. (1998): Correlation analysis of rate constants for dechlorination by zero-valent iron. *Environmental Science & Technology* 32(19), 3026-3033.
- Schlesinger, H.I., Brown, H.C., Finholt, A.E., Gilbreath, J.R., Hoekstra, H.R., Hyde, E.K. (1953): Sodium borohydride, its hydrolysis and its use as a reducing agent and in the generation of hydrogen<sup>1</sup>. *Journal of the American Chemical Society* 75(1), 215-219.
- Schlosser, P.M., Bale, A.S., Gibbons, C.F., Wilkins, A., Cooper, G.S. (2015): Human health effects of dichloromethane: Key findings and scientific issues. *Environmental Health Perspectives* 123(2), 114-119.
- Schoderboeck, L., Mühlegger, S., Losert, A., Gausterer, C., Hornek, R. (2011): Effects assessment: Boron compounds in the aquatic environment. *Chemosphere* 82(3), 483-487.
- Schrauzer, G.N. (1976): New developments in the field of vitamin B12: Reactions of the cobalt atom in corrins and in vitamin B12 model compounds. *Angewandte Chemie International Edition English* 15(7), 417-426.
- Schüth, C., Disser, S., Schüth, F., Reinhard, M. (2000): Tailoring catalysts for hydrodechlorinating chlorinated hydrocarbon contaminants in groundwater. *Applied Catalysis B: Environmental* 28(3), 147-152.
- Ševců, A., El-Temsah, Y.S., Filip, J., Joneš, E.J., Bobčíková, K., Černík, M. (2017): Zero-valent iron particles for PCB degradation and an evaluation of their effects on bacteria, plants, and soil organisms. *Environmental Science and Pollution Research* 24, 21191-21202.
- Shey, J., van der Donk, W.A. (2000): Mechanistic studies on the vitamin B12-catalyzed dechlorination of chlorinated alkenes. *Journal of the American Chemical Society* 122(49), 12403-12404.

- Shih, Y.-h., Hsu, C.-y., Su, Y.-f. (2011): Reduction of hexachlorobenzene by nanoscale zero-valent iron: Kinetics, pH effect, and degradation mechanism. *Separation and Purification Technology* 76(3), 268-274.
- Shimakoshi, H., Maeyama, Y., Kaieda, T., Matsuo, T., Matsui, E., Naruta, Y., Hisaeda, Y. (2005): Hydrophobic vitamin B12. Part 20: Supernucleophilicity of Co(I) heptamethyl cobyrinate toward various organic halides. *Bulletin of the Chemical Society of Japan* 78(5), 859-863.
- Shirayama, H., Tohezo, Y., Taguchi, S. (2001): Photodegradation of chlorinated hydrocarbons in the presence and absence of dissolved oxygen in water. *Water Research* 35(8), 1941-1950.
- Shubair, T., Eljamal, O., Khalil, A.M.E., Tahara, A., Matsunaga, N. (2018): Novel application of nanoscale zero valent iron and bimetallic nano-Fe/Cu particles for the treatment of cesium contaminated water. *Journal of Environmental Chemical Engineering* 6(4), 4253-4264.
- Silva, T.A., Diniz, J., Paixão, L., Vieira, B., Barrocas, B., Nunes, C.D., Monteiro, O.C. (2017): Novel titanate nanotubes-cyanocobalamin materials: Synthesis and enhanced photocatalytic properties for pollutants removal. *Solid State Sciences* 63, 30-41.
- Silver Prices. (2021): Silver prices - 100 year historical chart. Retrieved 23 April 2021 from <https://www.macrotrends.net/1470/historical-silver-prices-100-year-chart?q=>
- Singh, A., Kuhad, R.C., Ward, O.P. (2009): Biological remediation of soil: An overview of global market and available technologies. *Advances in Applied Bioremediation. Soil Biology* 17, 1-19.
- Soares, O.S.G.P., Órfão, J.J.M., Pereira, M.F.R. (2008): Activated carbon supported metal catalysts for nitrate and nitrite reduction in water. *Catalysis Letters* 126(3), 253-260.
- Song, H., Carraway, E. (2006): Reduction of chlorinated methanes by nano-sized zero-valent iron. Kinetics, pathways, and effect of reaction conditions. *Environmental Engineering Science* 23(2), 272-284.
- Song, H., Carraway, E.R. (2005): Reduction of chlorinated ethanes by nanosized zero-valent iron: Kinetics, pathways, and effects of reaction conditions. *Environmental Science & Technology* 39(16), 6237-6245.
- Song, H., Carraway, E.R. (2008): Catalytic hydrodechlorination of chlorinated ethenes by nanoscale zero-valent iron. *Applied Catalysis B: Environmental* 78(1), 53-60.
- Sugimasa, M., Inukai, J., Itaya, K. (2003): Structure of sulfur adlayer on Cu(111) electrode in alkaline solution. *Journal of the Electrochemical Society* 150(2), E110-E116.
- Sun, G.-R., He, J.-B., Pittman, C.U. (2000): Destruction of halogenated hydrocarbons with solvated electrons in the presence of water. *Chemosphere* 41(6), 907-916.
- Teel, A.L., Warberg, C.R., Atkinson, D.A., Watts, R.J. (2001): Comparison of mineral and soluble iron fenton's catalysts for the treatment of trichloroethylene. *Water Research* 35(4), 977-984.

- Teschner, D., Borsodi, J., Kis, Z., Szentmiklósi, L., Révay, Z., Knop-Gericke, A., Schlögl, R., Torres, D., Sautet, P. (2010): Role of hydrogen species in palladium-catalyzed alkyne hydrogenation. *The Journal of Physical Chemistry C* 114(5), 2293-2299.
- Tibor, P., Krebsz, M. (2020): Synthesis and application of zero-valent iron nanoparticles in water treatment, environmental remediation, catalysis, and their biological effects. *Nanomaterials* 10, 917.
- Tilche, A., Orhon, D. (2002): Appropriate basis of effluent standards for industrial wastewaters. *Water Science & Technology* 45(12), 1-11.
- Tobiszewski, M., Namiesnik, J. (2012): Abiotic degradation of chlorinated ethanes and ethenes in water. *Environmental Science and Pollution Research International* 19(6), 1994-2006.
- Totten, L.A., Roberts, A.L. (2001): Calculated one- and two-electron reduction potentials and related molecular descriptors for reduction of alkyl and vinyl halides in water. *Critical Reviews in Environmental Science and Technology* 31(2), 175-221.
- Twigg, M.V., Spencer, M.S. (2001): Deactivation of supported copper metal catalysts for hydrogenation reactions. *Applied Catalysis A: General* 212(1), 161-174.
- U.S. EPA. (2001): Toxicological review of chloroform in support of summary information on IRIS. United States Environmental Protection Agency, Washington, DC, EPA 635-R-01-001.
- U.S. EPA. (2002): Methods for measuring the acute toxicity of effluents and receiving waters to freshwater and marine organisms. United States Environmental Protection Agency, Washington, DC, Fifth Edition, EPA-821-R-02-012, 31-32.
- U.S. EPA. (2012): Guidelines for water reuse. United States Environmental Protection Agency, Washington, D.C., EPA/600/R-12/618.
- Urbano, F.J., Marinas, J.M. (2001): Hydrogenolysis of organohalogen compounds over palladium supported catalysts. *Journal of Molecular Catalysis A: Chemical* 173(1), 329-345.
- Vaškėlis, A., Juškėnas, R., Jačiauskienė, J. (1998): Copper hydride formation in the electroless copper plating process: *In situ* x-ray diffraction evidence and electrochemical study. *Electrochimica Acta* 43(9), 1061-1066.
- Velázquez, J., Leekumjorn, S., Nguyen, Q., Fang, Y.L., Heck, K., Hopkins, G., Reinhard, M., Wong, M. (2013): Chloroform hydrodechlorination behavior of alumina-supported Pd and PdAu catalysts. *AIChE Journal* 59, 4474-4482.
- Velimirovic, M., Larsson, P.-O., Simons, Q., Bastiaens, L. (2013): Reactivity screening of microscale zerovalent irons and iron sulfides towards different CAHs under standardized experimental conditions. *Journal of Hazardous Materials* 252-253, 204-212.
- Vogel, M., Georgi, A., Kopinke, F.-D., Mackenzie, K. (2019): Sulfidation of ZVI/AC composite leads to highly corrosion-resistant nanoremediation particles with extended life-time. *Science of The Total Environment* 665, 235-245.

- Vogel, M., Nijenhuis, I., Lloyd, J., Boothman, C., Pöritz, M., Mackenzie, K. (2018): Combined chemical and microbiological degradation of tetrachloroethene during the application of Carbo-Iron at a contaminated field site. *Science of The Total Environment* 628-629, 1027-1036.
- Wade, R.C. (1983): Catalyzed reduction of organofunctional groups with sodium borohydride. *Journal of Molecular Catalysis* 18(3), 273-297.
- Wang, C.-B., Zhang, W.-x. (1997): Synthesizing nanoscale iron particles for rapid and complete dechlorination of TCE and PCBs. *Environmental Science & Technology* 31(7), 2154-2156.
- Wang, H., Wang, J.L. (2008): The cooperative electrochemical oxidation of chlorophenols in anode-cathode compartments. *Journal of Hazardous Materials* 154(1), 44-50.
- Wang, J., Blowers, P., Farrell, J. (2004): Understanding reduction of carbon tetrachloride at nickel surfaces. *Environmental Science & Technology* 38(5), 1576-1581.
- Wang, J., Farrell, J. (2003): Investigating the role of atomic hydrogen on chloroethene reactions with iron using Tafel analysis and electrochemical impedance spectroscopy. *Environmental Science & Technology* 37(17), 3891-3896.
- Wang, L.-F., Habibul, N., He, D.-Q., Li, W.-W., Zhang, X., Jiang, H., Yu, H.-Q. (2015): Copper release from copper nanoparticles in the presence of natural organic matter. *Water Research* 68, 12-23.
- Wang, P., Yuan, Y., Xu, K., Zhong, H., Yang, Y., Jin, S., Yang, K., Qi, X. (2021): Biological applications of copper-containing materials. *Bioactive Materials* 6(4), 916-927.
- Wang, X., Chen, C., Chang, Y., Liu, H. (2009): Dechlorination of chlorinated methanes by Pd/Fe bimetallic nanoparticles. *Journal of Hazardous Materials* 161(2), 815-823.
- Wang, X., Zhu, M., Liu, H., Ma, J., Li, F. (2013): Modification of Pd-Fe nanoparticles for catalytic dechlorination of 2,4-dichlorophenol. *Science of The Total Environment* 449, 157-167.
- Weinthal, E., Parag, Y., Vengosh, A., Muti, A., Kloppmann, W. (2005): The EU drinking water directive: The boron standard and scientific uncertainty. *European Environment* 15(1), 1-12.
- Wiltchka, K., Neumann, L., Werheid, M., Bunge, M., Düring, R.-A., Mackenzie, K., Böhm, L. (2020): Hydrodechlorination of hexachlorobenzene in a miniaturized nano-Pd(0) reaction system combined with the simultaneous extraction of all dechlorination products. *Applied Catalysis B: Environmental* 275, 119100.
- Wols, B.A., Hofman-Caris, C.H.M., Harmsen, D.J.H., Beerendonk, E.F. (2013): Degradation of 40 selected pharmaceuticals by UV/H<sub>2</sub>O<sub>2</sub>. *Water Research* 47(15), 5876-5888.
- World Health Organization. (1998): Boron in drinking-water: Background document for development of WHO guidelines for drinking-water quality. Geneva, Switzerland, WHO/SDE/WSH/03.04/54.

- World Health Organization. (2004): Copper in drinking water: Background document for development of WHO guidelines for drinking-water quality. Geneva, Switzerland, WHO/SDE/WSH/03.04/88.
- World Health Organization. (2005): Trihalomethanes in drinking-water: Background document for development of WHO guidelines for drinking-water quality. Geneva, Switzerland.
- Wu, D., Peng, H., Abdalla, M. (2018): Effect of sodium sulfide waste water recycling on the separation of chalcopyrite and molybdenite. *Physicochemical Problems of Mineral Processing* 54(3), 629-638.
- Yamazaki, S., Matsunaga, S., Hori, K. (2001): Photocatalytic degradation of trichloroethylene in water using TiO<sub>2</sub> pellets. *Water Research* 35(4), 1022-1028.
- Yan, Y.E., Schwartz, F.W. (1999): Oxidative degradation and kinetics of chlorinated ethylenes by potassium permanganate. *Journal of Contaminant Hydrology* 37(3), 343-365.
- Yuan, G., Keane, M.A. (2004): Liquid phase hydrodechlorination of chlorophenols over Pd/C and Pd/Al<sub>2</sub>O<sub>3</sub>: A consideration of HCl/catalyst interactions and solution pH effects. *Applied Catalysis B: Environmental* 52(4), 301-314.
- Zhang, M., Bacik, D.B., Roberts, C.B., Zhao, D. (2013): Catalytic hydrodechlorination of trichloroethylene in water with supported CMC-stabilized palladium nanoparticles. *Water Research* 47(11), 3706-3715.
- Zhang, M., He, F., Zhao, D. (2015): Catalytic activity of noble metal nanoparticles toward hydrodechlorination: Influence of catalyst electronic structure and nature of adsorption. *Frontiers of Environmental Science & Engineering* 9(5), 888-896.
- Zhang, W.-x. (2003): Nanoscale iron particles for environmental remediation: An overview. *Journal of Nanoparticle Research* 5(3), 323-332.
- Zhang, Y., Douglas, G.B., Pu, L., Zhao, Q., Tang, Y., Xu, W., Luo, B., Hong, W., Cui, L., Ye, Z. (2017): Zero-valent iron-facilitated reduction of nitrate: Chemical kinetics and reaction pathways. *Science of The Total Environment* 598, 1140-1150.
- Zhou, G., Chan, C., Gellman, A.J. (1999): Dechlorination of fluorinated 1,1-dichloroethanes on Pd(111). *The Journal of Physical Chemistry B* 103(7), 1134-1143.
- Zhou, T., Li, Y., Lim, T.-T. (2010): Catalytic hydrodechlorination of chlorophenols by Pd/Fe nanoparticles: Comparisons with other bimetallic systems, kinetics and mechanism. *Separation and Purification Technology* 76(2), 206-214.
- Zhu, B.-W., Lim, T.-T. (2007): Catalytic reduction of chlorobenzenes with Pd/Fe nanoparticles: Reactive sites, catalyst stability, particle aging, and regeneration. *Environmental Science & Technology* 41(21), 7523-7529.

## Appendix

### A1 Additional experimental details

**Table A1-1:** Laboratory tap water characteristics (supplied by the city of Leipzig, 2018)

Water constituent	Concentration (mg/L, except pH)
pH	7.7
Ca	74.3
Fe	0.028
K	6.0
Na	29.8
Mg	14.9
Mn	0.003
Ni	0.0045
Cr	< 0.0005
Pb	< 0.001
SO <sub>4</sub> <sup>2-</sup>	160
NO <sub>3</sub> <sup>-</sup>	12.5
NO <sub>2</sub> <sup>-</sup>	< 0.01
NH <sub>4</sub> <sup>+</sup>	< 0.03
F <sup>-</sup>	0.4
Cl <sup>-</sup>	49.4

**Table A1-2:** Details of electrodes and Pt wires used in electrochemical studies

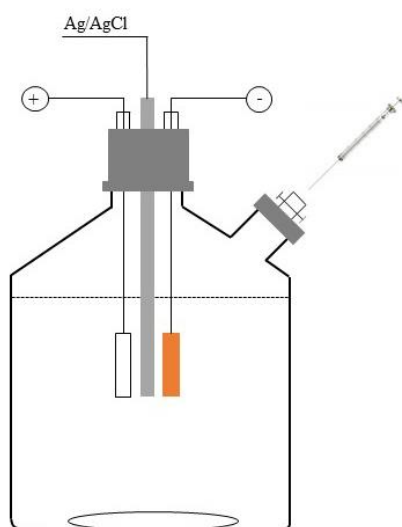
Details	Copper gauze	Platinum plate	Platinum wire
Manufacturer	Sigma-Aldrich, Germany	Sigma-Aldrich, Germany	Sigma-Aldrich, Germany
Form	100 × 100 mm mesh	25 × 25 mm foil	Wire
Assay	n.a.	99.99 %	99.99 %
Resistivity (μΩ·cm) at 20 °C	1.673	10.6	10.6
Thickness (mm)	0.25	1.0	0.2

n.a. = not available

*Electrochemical set-ups for the characterization of electrodes and chloroform dechlorination*

The electrochemical set-ups for characterization of the Cu and Cu/ACF electrodes and the dechlorination of chloroform are as presented in Figure A1-1. Charge-transfer measurements were conducted under diffusion-controlled conditions. The electrolytes were mixed using a magnetic stirrer during chloroform dechlorination experiments.

a) Electrochemical set-up for characterization of Cu electrode



b) Electrochemical set-up for characterization of Cu/ACF electrode

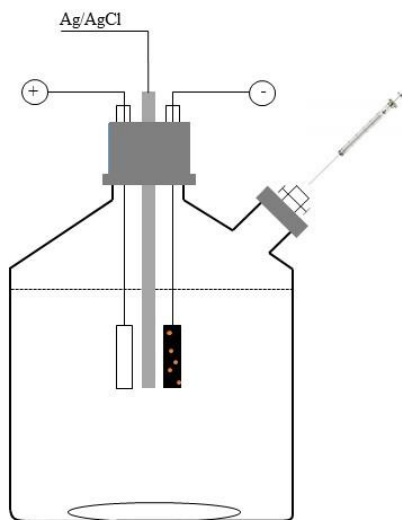


**Figure A1-1:** Experimental setup for electrochemical measurements using: a) Cu electrode and b) Cu/ACF electrode.

The cyclic voltammograms of Cu electrode by CV in the two electrolytes, 0.1 M NaOH and 0.1 M Na<sub>2</sub>SO<sub>4</sub> are as shown in Figure A1-2 and Figure A1-3, respectively. The CV profiles were obtained after immersing the Cu electrode for 30 min in the electrolytes.

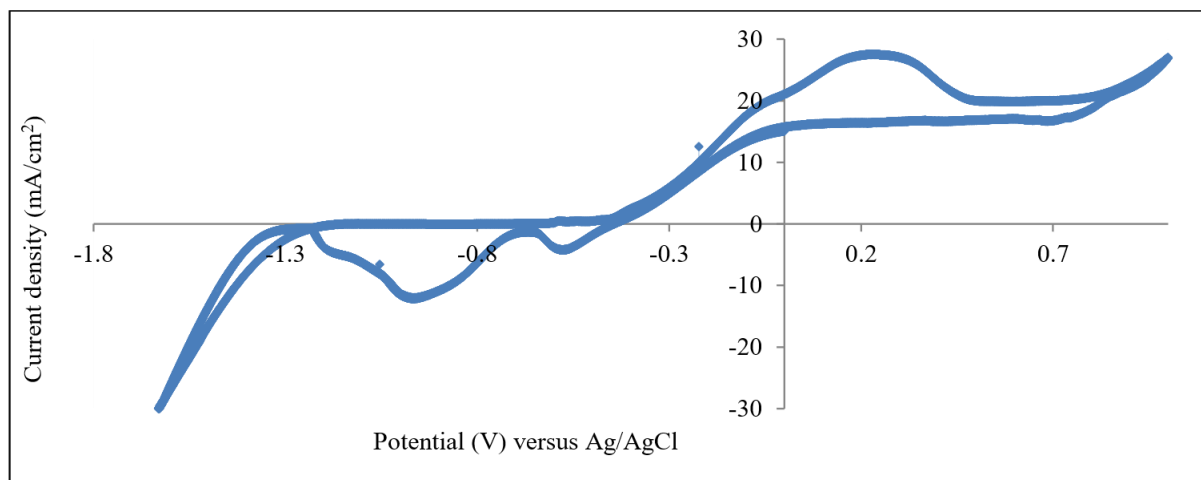


**Figure A1-2:** Cyclic voltammogram of Cu electrode in 0.1 M NaOH at 20 °C and a scan rate of 25 mV/s.

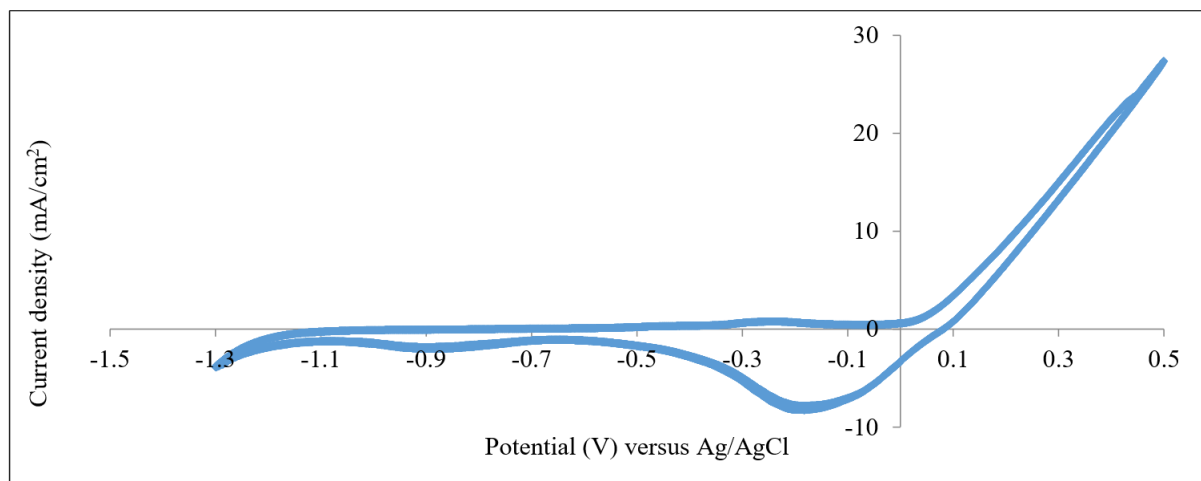


**Figure A1-3:** Cyclic voltammogram of Cu electrode in 0.1 M Na<sub>2</sub>SO<sub>4</sub> at 20 °C and a scan rate of 25 mV/s.

As shown in Figure A1-2, the anodic cycle in the presence of 0.1 M NaOH gives two distinct peaks. The small peak at -0.1 V was due to the formation of Cu<sub>2</sub>O while CuO is formed at 0.2 V. Further increase in potential beyond 0.7 V results in water hydrolysis. The cathodic cycle shows the reduction of CuO to Cu<sub>2</sub>O at -0.5 V. Further reduction of Cu<sub>2</sub>O results in the formation of metallic Cu at -0.9 V. The CV in the presence of Na<sub>2</sub>SO<sub>4</sub> (Figure A1-3) shows a very small broad peak at -0.2 V during the anodic cycle. This peak was ascribed to the formation of both Cu<sub>2</sub>O and CuO which precipitate as a result of reaction with electrolyte (the solution turned pale blue). During the reduction cycle, a single broad peak was observed at -0.2 V due to simultaneous reduction of Cu<sub>2</sub>O and CuO to metallic Cu. A further increase in negative potential beyond -1.0 V results in water electrolysis. Similarly, to minimize water electrolysis, the potential should not exceed -1.0 V for Cu/ACF as shown in Figure A1-4.

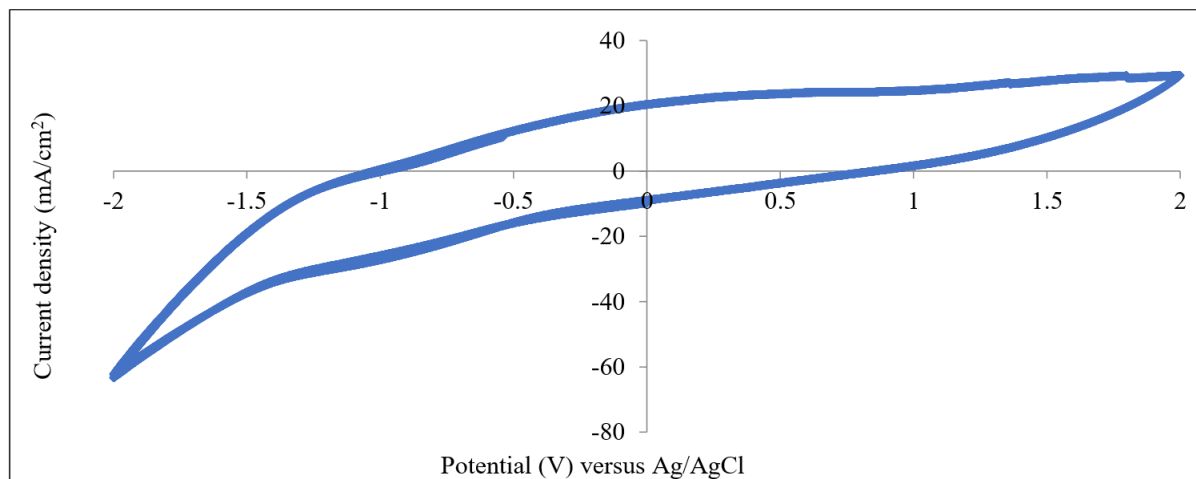


**Figure A1-4:** Cyclic voltammogram of Cu/ACF electrode in 0.1 M Na<sub>2</sub>SO<sub>4</sub> at 20 °C and a scan rate of 25 mV/s.

## A2 Characterization of particles and materials

**Table A2-1:** Results of iron analysis in CIC, S/CIC, and nZVI

Materials	Fe <sup>0</sup> content (wt-%)
CIC	26
S/CIC	24
nZVI	97

**Table A2-2:** Results of copper analysis in prepared materials determined by ICP-MS and UV-VIS spectrophotometry

Cu-modified material	Cu content (wt-%)
Cu/AC	0.5 and 1.0
Cu/ACF	0.5
Cu/resin	1.4
Cu/MFI 24 (i)	0.6
Cu/MFI 24 (w)	0.5
Cu/MFI 90 (i)	0.1
Cu/MFI 90 (w)	0.1

“i” in the sample is the description for Cu-modified zeolite prepared by ion-exchange method

“w” in the sample is the description for Cu-modified zeolite prepared by incipient wetness impregnation method

**Table A2-3:** Sizes of nanoparticles determined by NTA analysis

Nanoparticles type	Particle size (nm)	
	<i>d</i> <sub>50</sub>	<i>d</i> <sub>90</sub>
Cu	50	110
Pd	60	113
nZVI	75	127

**A3 Additional results from the dehalogenation of CCl<sub>3</sub>-R compounds**

**Table A3-1:** Chloride yields at  $\geq 95\%$  conversion of CF in various systems

Dechlorination system	Cl <sup>-</sup> yield (mol-%)
Pd/Cu	80 ± 2
Ni/Cu	81 ± 3
Cu/Zn	78 ± 3
Cu/Ce	77 ± 2
Cu/Al	81 ± 3
Cu/Sn	82 ± 2
Cu/Co	83 ± 2
Ag	95 ± 3
Ag/Cu (co-red)	94 ± 4
Ag/Cu (mix)	95 ± 3
Ag/Cu (sep)	94 ± 2
Cu + vitamin B12	96 ± 2

**Table A3-2:** Chloride yields and  $k_{\text{obs}}$  values for dechlorination of CF using bare and amended CIC and S/CIC

Dechlorination system	Cl <sup>-</sup> yield (mol-%)	$k_{\text{obs}}$ (1/min)
CIC	70 ± 4	0.0040 ± 0.0005
S/CIC	65 ± 2	0.005 ± 0.001
Cu/CIC	81 ± 2	0.013 ± 0.003
Cu/S/CIC	82 ± 2	0.008 ± 0.002
1.0 wt-% Pd/Cu/CIC	84 ± 2	0.0030 ± 0.0005
1.0 wt-% Ni/Cu/CIC	81 ± 1	0.0020 ± 0.0002
0.02 wt-% Ag/Cu/CIC	85 ± 3	0.045 ± 0.005
0.20 wt-% Ag/Cu/CIC	86 ± 2	0.075 ± 0.005
1.0 wt-% Ag/Cu/CIC	90 ± 2	0.30 ± 0.05
1.0 wt-% Ag/Cu/S/CIC	88 ± 2	0.0040 ± 0.0005

**Table A3-3:** Product selectivities determined at  $\geq 95$  % conversion of CF in water using Ag/Cu (H<sub>2</sub>-red) and Cu-modified materials ( $c_{\text{Cu-material}} = 500$  mg/L;  $c_{\text{O,NaBH}_4} = 300$  mg/L;  $c_{\text{O,CF}} = 10$  mg/L; pH = 10)

Catalyst system	Cu content (wt-%)	$n_{\text{product}} / n_{\text{converted CF}} \times 100$ (%)			Specific Cu activities $A_{\text{Cu}}$ [L/(g·min)]	Cl <sup>-</sup> yield (mol-%)
		MCM	DCM	CH <sub>4</sub>		
Ag/Cu (H <sub>2</sub> -red)	none	6 ± 2	3 ± 1	92 ± 2	3 ± 1	94 ± 2
Cu/AC	0.5	0.5 ± 0.2	14 ± 2	85 ± 2	4 ± 1	84 ± 2
Cu/AC	1.0	1 ± 0.5	14 ± 3	83 ± 2	8.5 ± 1	85 ± 2
Cu/ACF	0.5	1 ± 0.5	12 ± 2	82 ± 2	5 ± 2	86 ± 2
Cu/resin	1.4	1 ± 0.5	12 ± 1	86 ± 2	15 ± 2	85 ± 2
Cu/MFI 24 (i)	0.6	1 ± 0.5	16 ± 2	80 ± 2	15 ± 2	88 ± 5
Cu/MFI 24 (w)	0.5	1 ± 0.2	14 ± 2	76 ± 2	14 ± 1	90 ± 5
Cu/MFI 90 (i)	0.1	1 ± 0.5	12 ± 2	80 ± 2	6 ± 1	86 ± 2
Cu/MFI 90 (w)	0.1	1 ± 0.5	14 ± 2	77 ± 2	10 ± 2	88 ± 3

“i” in the sample is the description for Cu-modified zeolite prepared by ion-exchange method

“w” in the sample is the description for Cu-modified zeolite prepared by incipient wetness impregnation method

**Table A3-4:** Chloride yields upon dechlorination of the CCl<sub>3</sub>-R educt and the daughter HCCl<sub>2</sub>-R intermediates as well as the educts DCM and 1,1-DCA

Compound	Cl <sup>-</sup> yield (mol-%)
CCl <sub>4</sub>	30 ± 5
CFCl <sub>3</sub>	15 ± 3
CBrCl <sub>3</sub>	40 ± 4
1,1,1-TCA	92 ± 4
1,1-DCA	95 ± 4
DCM	93 ± 2

**Table A3-5:** Specific Cu activities,  $A_{Cu}$  for the dechlorination of CF in tap water and synthetic freshwater compared to the baseline for Cu ( $A_{Cu,CF,without\ co-solute} = (130 \pm 10) \text{ L}/(\text{g}\cdot\text{min})$ ) ( $C_{0,CF} = 10 \text{ mg/L}$ ;  $C_{0,NaBH_4} = 300 \text{ mg/L}$ ;  $\text{pH} = 10$ )

<b>Water type</b>	<b>Water hardness (mg/L)</b>	<b>Specific Cu activities <math>A_{Cu}</math> in the presence of co-solute [L/(g·min)]</b>	<b><math>A_{Cu,CF,tap\ water\ or\ freshwater}/A_{Cu,CF,without\ co-solute} [-]^c</math></b>
Tap water	Details are presented in the appendix Table A1-1	$100 \pm 10$	0.8
Synthetic freshwater	80-100 mg $\text{CaCO}_3/\text{L}$	$100 \pm 10$	0.8
(United States Environmental Protection Agency, 2002)	280-320 mg $\text{CaCO}_3/\text{L}$	$100 \pm 10$	0.8

#### **A4** *List of abbreviations*

1,1,1,2-TeCA	1,1,1,2-tetrachloroethane
1,1,1-TCA	1,1,1-trichloroethane
1,1,2,2-TeCA	1,1,2,2-tetrachloroethane
1,1,2-TCA	1,1,2-trichloroethane
1,1-DCA	1,1-dichloroethane
1,1-DCE	1,1-dichloroethylene
1,2,3-TCP	1,2,3-trichloropropane
1,2-DCA	1,2-dichloroethane
1,2-DCB	1,2-dichlorobutane
1,2-DCP	1,2-dichloropropane
AC	Activated carbon
ACF	Activated carbon felt
Ag/Cu/CIC	Silver-modified Cu/CIC
AOPs	Advanced oxidation processes
B <sub>12r</sub> or B <sub>12s</sub>	Reduced or super-reduced form of vitamin B12
BB	Bromobenzene
BDE	Bond dissociation energy
BET	Brunauer-Emmett-Teller
BF	Bromoform
C.E.	Counter electrode
C <sub>2</sub> H <sub>4</sub>	Ethylene
C <sub>2</sub> H <sub>6</sub>	Ethane

C <sub>3</sub> H <sub>8</sub>	Propane
CB	Chlorobenzene
CBrCl <sub>3</sub>	Bromotrichloromethane
CF	Chloroform
CFC-11	Trichlorofluoromethane
CFC-113	1,1,2-trichloro-1,2,2-trifluoroethane
CH <sub>4</sub>	Methane
CIC	Carbo-Iron <sup>®</sup> colloids
<i>cis</i> -DCE	<i>cis</i> -dichloroethylene
CMC	Carboxymethyl cellulose
CN	cyano group (–C≡N)
Co–R	Alkyl-cobalamin complexes
CTAB	Cetyltrimethyl ammonium bromide
CTC	Carbon tetrachloride
Cu NPs	Copper nanoparticles
Cu/AC	Copper-modified activated carbon
Cu/ACF	Copper-modified activated carbon felt
Cu/CIC	Copper-modified CIC
Cu/MFI 24 (i)	Copper-modified MFI 24 zeolite synthesized by ion-exchange
Cu/MFI 24 (w)	Copper-modified MFI 24 zeolite synthesized by incipient wetness impregnation
Cu/MFI 90 (i)	Copper-modified MFI 90 zeolite synthesized by ion-exchange

Cu/MFI 90 (w)	Copper-modified MFI 24 zeolite synthesized by incipient wetness impregnation
Cu/resin	Copper-doped cation-exchange resin
Cu/resin (1 mg/L Na <sub>2</sub> S)	Copper resin soaked in 1 mg/L Na <sub>2</sub> S
Cu/resin (20 mg/L Na <sub>2</sub> S)	Copper resin soaked in 20 mg/L Na <sub>2</sub> S
Cu/S/CIC	Copper-modified S/CIC
CV	Cyclic voltammetry
C–X	Carbon-halogen bond
DAAD	Germany Academic Exchange Service
DBM	Dibromomethane
DCEs	Dichloroethylene isomers
DCM	Dichloromethane
DNAPLs	Dense non-aqueous phase liquids
<i>E</i> <sub>1</sub> or <i>E</i> <sub>2</sub>	One-electron reduction potential or two-electron reduction potential
<i>E</i> <sub>LUMO</sub>	Energy of the lowest unoccupied molecular orbital
FID	Flame ionization detector
GC	Gas chromatography
GC-FID	Gas chromatography flame ionization detector
GC-MS	Gas chromatography mass spectrometry
HCA	Hexachloroethane
HDC	Hydrodechlorination
HOCs	Halogenated organic compounds
HS <sup>-</sup>	Bisulfide

HX	Hydrogen halide
IC	Ion chromatography
ICP	Inductively coupled plasma
ICP-MS	Inductively coupled plasma mass spectrometry
IHSS	International Humic Substances Society
LFERs	Linear free energy relationships
MBM	Monobromomethane
MCA	Monochloroethane
MCM	Monochloromethane
MeOH	Methanol
MS	Mass spectrometry
MTBE	Methyl tert-butyl ether
n.a.	not analyzed or not available
NOM	Natural organic matter
NTA	Nanoparticle tracking analysis
ORP	Oxidation-reduction potential
PAA	Poly(acrylic acid)
PCA	Pentachloroethane
PCE	Perchloroethylene
Pd NPs	Palladium nanoparticles
PDMS	Poly(dimethylsiloxane)
PRBs	Permeable reactive barriers
PSS	Poly(styrene sulfonate)

PTFE	Poly(tetrafluoroethylene)
PVP	Poly(vinylpyrrolidone)
R.E.	Reference electrode
R-H	Organic compound
RNIP	Reactive nanoscale iron particles
rpm	Revolutions per minute
R-X	Representative structure of any HOCs
S/CIC or S/nZVI	Sulfidated Carbo-Iron <sup>®</sup> colloids or Sulfidated nZVI
SET	Single electron transfer
SHE	Standard hydrogen electrode
SRHA	Suwannee river humic acid
TCD	Thermal conductivity detector
TCE	Trichloroethylene
<i>trans</i> -DCE	<i>trans</i> -dichloroethylene
USD	United States Dollar
UV	Ultraviolet radiation
VB	Vinyl bromide
VC	Vinyl chloride
W.E.	Working electrode
wCu/resin (1 mg/L Na <sub>2</sub> S)	Washed Cu/resin after deactivation by 1 mg/L Na <sub>2</sub> S
wCu/resin (20 mg/L Na <sub>2</sub> S)	Washed Cu/resin after deactivation by 20 mg/L Na <sub>2</sub> S
WHO	World Health Organization
ZVI or nZVI	Zero valent iron or nanoscale zero valent iron

## A5 List of symbols

Symbol	Units	Description
$A_{Ag}$	[L/(g·min)]	Specific Ag activity
$A_{Cu}$	[L/(g·min)]	Specific Cu activity
$A_m$	[L/(g·min)]	Specific metal activity
$A_{nZVI}$	[L/(g·min)]	Specific nZVI activity
$A_{Pd}$	[L/(g·min)]	Specific Pd activity
$a_s$	[m <sup>2</sup> /g]	Metal specific surface area
$c$	[mg/L or g/L]	Mass concentration
$c_i$	[mg/L]	Concentration of contaminant
$c_{i,product}$	[mg/L]	The concentration of a product $i$ at a given sampling time
$c_m$	[g/L]	Concentration of metal
$c_{product,max}$	[mg/L]	The maximum concentration of product
$c_{t1}$	[mg/L]	The concentration of a contaminant at sampling time $t_1$
$c_{t2}$	[mg/L]	The concentration of a contaminant at sampling time $t_2$
$d_{50}, d_{90}$	[μm]	Characteristics particle size distribution (50 % or 90 % of the particles are smaller than the specified value)
$E^\circ$ or $E$	[mV or V]	Electrical Potential at standard state or applied potential
$f$	[Hz]	Frequency
$HOC_{sw}$	[-]	The fraction of contaminant in water
$i$	[A]	Electrical current
$j$	[A/m <sup>2</sup> ]	Current density

$K_H$	[-]	Dimensionless Henry's constant
$k_{obs}$	[1/min]	Observed first-order rate constant
$k_{obs,corr}$	[1/min]	Corrected observed first-order rate constant
$k_{SA}$	[L/(m <sup>2</sup> ·min)]	Surface area-normalized rate constant
$m$	[g]	Metal mass
$M$	[mol/L]	The concentration of solute in moles per liter of water
$n$	[mol]	Moles of solute
$n_{converted,HOC}$	[mol]	Moles of educt converted at the given time
$n_{HOC,0}$	[mol]	Initial moles of educt fed into the reactor
$n_{HOC,t}$	[mol]	Moles of educt at a given time
$n_{i,product}$	[mol]	Moles of product i
$P$	[Watts]	Electrical power of a device
$R$	[Ω]	Electrical resistance
$S_{DCM}$ OR $S_{CH_2Cl_2}$	[mol-%]	Selectivity to dichloromethane
$S_{i,product}$	[mol-%]	Selectivity of a given product i
$S_{MCM}$ OR $S_{CH_3Cl}$	[mol-%]	Selectivity to monochloromethane
$T$	[°C]	Temperature
$t$	[s, min or h]	Time
$t_1, t_2$	[min]	Initial and final sampling times
$V_{electrolyte}$	[mL]	Volume of electrolyte
$V_h$	[mL]	The volume of the headspace in a reactor
$V_w$	[mL]	The volume of the aqueous phase in a reactor

$x_{Ag}$	[wt-%]	Mass fraction of Ag in a material
$x_{Cu}$	[wt-%]	Mass fraction of Cu in a material
$X_{HOC}$	[-]	Conversion of a contaminant
$Y_{i,product}$	[mol-%]	The yield of a product i
$\rho$	[N/m <sup>2</sup> , Pa or atm]	Pressure
$\tau_{1/2}$	[min]	The half-life of a contaminant in a reaction

## A6 List of figures

- Figure 1:** Speculated reaction step for the formation of trichloromethyl radical from carbon tetrachloride (Balko and Tratnyek, 1998; Matheson and Tratnyek, 1994; Song and Carraway, 2006). ..... 15
- Figure 2:** Speculated reaction step for the formation of chloroform from trichloromethyl radical (Balko and Tratnyek, 1998; Song and Carraway, 2006). ..... 16
- Figure 3:** Speculated reaction step for the formation of dichloromethyl radical from chloroform (Song and Carraway, 2006). ..... 16
- Figure 4:** Dechlorination pathways for chlorinated ethanes and ethylenes.  $\beta$ -elimination (1, 2, 7, 12, 18, 19, 20, 21, 23, 25); hydrogenolysis (3, 4, 6, 9, 10, 11, 13, 14, 15, 17, 22, 24, 26, 27, 28, 29);  $\alpha$ -elimination (16) and hydrogenation (5, 8) (Arnold et al., 1999; Tobiszewski and Namiesnik, 2012). ..... 18
- Figure 5:** Chemical structure of vitamin B12 where R = CN (Silva et al., 2017). ..... 33
- Figure 6:** Reaction progress during the dechlorination of CF in water using  $\text{Cu}^0 + \text{NaBH}_4$  a) Product yields and b) Product selectivities ( $c_{\text{Cu}} = 1 \text{ mg/L}$ ;  $c_{0,\text{NaBH}_4} = 300 \text{ mg/L}$ ;  $c_{0,\text{CF}} = 10 \text{ mg/L}$ ;  $\text{pH} = 10$ ). Note that for MCM, the values in both graphs are multiplied by a factor of 10. .... 69
- Figure 7:** Proposed reaction pathways for the dechlorination of CF in water using  $\text{Cu}^0 + \text{NaBH}_4$ . ( $c_{\text{Cu}} = 1\text{-}100 \text{ mg/L}$ ;  $c_{0,\text{NaBH}_4} = 300 \text{ mg/L}$ ;  $c_{0,\text{HOCs}} = 2\text{-}10 \text{ mg/L}$ ;  $\text{pH} = 10$ ). (Based on the product selectivity patterns in Figure 6, different arrow designs are used in this scheme to show which reaction is significant). ..... 71
- Figure 8:** Effect of Cu NPs concentration on the selectivity patterns during the dechlorination of CF ( $c_{0,\text{NaBH}_4} = 300 \text{ mg/L}$ ;  $c_{0,\text{CF}} = 10 \text{ mg/L}$ ;  $\text{pH} = 10$ ). Selectivity patterns were determined at the termination of reaction after 60 min where CF conversion  $\geq 95 \%$ . ..... 73
- Figure 9:** Effect of initial  $\text{NaBH}_4$  concentration on the selectivity patterns during the dechlorination of CF using Cu NPs ( $c_{\text{Cu}} = 1 \text{ mg/L}$ ;  $c_{0,\text{CF}} = 10 \text{ mg/L}$ ;  $\text{pH} = 10$ ). Selectivities determined at CF conversion  $\geq 95 \%$ . ..... 78
- Figure 10:** Effect of initial  $\text{NaBH}_4$  concentration on the specific Cu activities during the dechlorination of CF ( $c_{\text{Cu}} = 1 \text{ mg/L}$ ;  $c_{0,\text{CF}} = 10 \text{ mg/L}$ ;  $\text{pH} = 10$ ). ..... 78
- Figure 11:** Effect of initial CF concentration on the selectivity patterns during the dechlorination reactions using  $\text{Cu}^0 + \text{NaBH}_4$  ( $c_{\text{Cu}} = 1 \text{ mg/L}$ ;  $c_{0,\text{NaBH}_4} = 300 \text{ mg/L}$ ;  $\text{pH} = 10$ ). Selectivities determined at CF conversion  $\geq 95 \%$ . ..... 80

**Figure 12:** Effect of initial CF concentration on the specific Cu activities during the dechlorination reactions using  $\text{Cu}^0 + \text{NaBH}_4$  ( $c_{\text{Cu}} = 1 \text{ mg/L}$ ;  $c_{0,\text{NaBH}_4} = 300 \text{ mg/L}$ ;  $\text{pH} = 10$ ). ..... 80

**Figure 13:** Product selectivity patterns for the dechlorination of CF using  $\text{Cu}^0 + \text{NaBH}_4$  a) Co-solutes that have minor effects towards MCM and DCM selectivities and b) Co-solutes that increase selectivities towards MCM and DCM ( $c_{\text{Cu}} = 1 \text{ mg/L}$ ;  $c_{0,\text{NaBH}_4} = 300 \text{ mg/L}$ ;  $c_{0,\text{CF}} = 10 \text{ mg/L}$ ;  $\text{pH} = 10$ ;  $\text{pH}_{\text{NaHCO}_3} = 8$ ;  $c_{\text{solute}} = 10 \text{ mg/L}$ ;  $c_{\text{Na}_2\text{S}} = 1 \text{ mg/L}$ ). Selectivities determined at CF conversion  $\geq 95 \%$ . ..... 82

**Figure 14:** Selectivity patterns during the dechlorination of CF using  $\text{Ag}^0 + \text{NaBH}_4$  and  $\text{Cu}^0 + \text{NaBH}_4$  in the presence of metal additives and vitamin B12 ( $c_{\text{metal catalyst,total}} = 2 \text{ mg/L}$ ;  $c_{0,\text{NaBH}_4} = 300 \text{ mg/L}$ ;  $c_{\text{vitamin B12}} = 5 \text{ mg/L}$ ;  $c_{0,\text{CF}} = 10 \text{ mg/L}$ ;  $\text{pH} = 10$ ). Selectivities determined at CF conversion  $\geq 95 \%$ ; 25 wt-% Ag on Cu used for bimetallic Ag/Cu particles. For Cu + vitamin B12 ‘apparent selectivities’ results from subsequent dechlorination of DCM intermediate..... 84

**Figure 15:** Specific metal activities for dechlorination CF using  $\text{Ag}^0 + \text{NaBH}_4$  and  $\text{Cu}^0 + \text{NaBH}_4$  in the presence of metal additives and vitamin B12 ( $c_{\text{metal catalyst,total}} = 2 \text{ mg/L}$ ;  $c_{0,\text{NaBH}_4} = 300 \text{ mg/L}$ ;  $c_{\text{vitamin B12}} = 5 \text{ mg/L}$ ;  $c_{0,\text{CF}} = 10 \text{ mg/L}$ ;  $\text{pH} = 10$ ). Specific metal activities for Pd/Cu, Ni/Cu, Zn/Cu, Ce/Cu, Al/Cu, Sn/Cu, Co/Cu, and Cu + vitamin B12 were calculated based on the total metal concentration; 25 wt-% Ag on Cu used for the bimetallic Ag/Cu particles. .... 85

**Figure 16:** Product selectivity patterns during the dechlorination of CF using CIC, S/CIC, Cu/CIC, and Cu/S/CIC ( $c_{\text{CIC}} = c_{\text{Cu/CIC}} = c_{\text{Cu/S/CIC}} = 500 \text{ mg/L}$ ;  $c_{0,\text{CF}} = 10 \text{ mg/L}$ ;  $\text{pH} = 8$ ). Selectivities determined at CF conversion  $\geq 95 \%$ . ..... 90

**Figure 17:** Product selectivity patterns during the dechlorination of CF using metal-modified Cu/CIC and Cu/S/CIC ( $c_{\text{Pd/Cu/CIC}} = c_{\text{Ni/Cu/CIC}} = c_{\text{Ag/Cu/CIC}} = c_{\text{Ag/Cu/S/CIC}} = 500 \text{ mg/L}$ ;  $c_{0,\text{CF}} = 10 \text{ mg/L}$ ;  $\text{pH}_0 = 6.5$ ). Selectivities determined at CF conversion  $\geq 95 \%$ . ..... 92

**Figure 18:** Product selectivity patterns during the dehalogenation of  $\text{CCl}_4$ ,  $\text{CFCl}_3$  and  $\text{CBrCl}_3$  using  $\text{Cu}^0 + \text{NaBH}_4$  a) Selectivities at  $\geq 95 \%$  conversion of the parent  $\text{CCl}_3\text{-R}$  compound and b) Selectivities at  $\geq 95 \%$  conversion of the immediate  $\text{CHCl}_2\text{-R}$  intermediate ( $c_{\text{Cu}} = 0.2\text{-}2 \text{ mg/L}$ ;  $c_{0,\text{educt}} = 20 \text{ mg/L}$ ;  $c_{0,\text{NaBH}_4} = 300 \text{ mg/L}$ ;  $\text{pH} = 10$ ). ..... 97

**Figure 19:** Product selectivity patterns during the dechlorination of 1,1,1-TCA using  $\text{Cu}^0 + \text{NaBH}_4$  a) Selectivities at  $\geq 95 \%$  conversion of 1,1,1-TCA and b) Selectivities at  $\geq 95 \%$  conversion of the 1,1-DCA intermediate ( $c_{\text{Cu}} = 1 \text{ mg/L}$ ;  $c_{0,1,1,1\text{-TCA}} = 20 \text{ mg/L}$ ;  $c_{0,\text{NaBH}_4} = 300 \text{ mg/L}$ ;  $\text{pH} = 10$ ). ..... 99

**Figure 20:** Product selectivity patterns for the dechlorination of DCM and 1,1-DCA using  $\text{Cu}^0 + \text{NaBH}_4$  ( $c_{\text{Cu}} = 50\text{-}100 \text{ mg/L}$ ;  $c_{0,\text{educt}} = 10\text{-}20 \text{ mg/L}$ ;  $c_{0,\text{NaBH}_4} = 300 \text{ mg/L}$ ;  $\text{pH} = 10$ ). .....

Selectivity patterns determined at educt conversion  $\geq 95\%$ . Grey and blue bars represent products from the dechlorination of DCM and 1,1-DCA, respectively. .... 101

**Figure 21:** Correlation of specific metal activities as  $\log A_m$  with the weakest C–X bond dissociation energies for saturated chlorinated compounds and chlorinated ethylenes (a) using  $\text{Cu}^0 + \text{NaBH}_4$  and (b) using  $\text{Pd} + \text{H}_2$ . Dotted lines are used to indicate reactivity trends for the HOC classes. .... 109

**Figure 22:** Variation of specific Cu activities when Cu/resin is deactivated with  $\text{Na}_2\text{S}$  and regenerated upon rinsing with deionized water ( $c_{\text{Cu/resin}} = 300 \text{ mg/L}$ ;  $c_{0,\text{CF}} = 10 \text{ mg/L}$ ;  $c_{0,\text{NaBH}_4} = 300 \text{ mg/L}$ ;  $\text{pH} = 10$ . “w” in the sample is the description for washed;  $A_{\text{Cu}}$  was calculated from  $4.2 \text{ mg/L}$  Cu within the resin). .... 119

**Figure 23:** Variation in specific Cu activities during recycling of Cu/resin during dechlorination of CF ( $c_{\text{Cu/resin}} = 300 \text{ mg/L}$ ;  $c_{0,\text{CF}} = 10 \text{ mg/L}$ ;  $c_{0,\text{NaBH}_4} = 300 \text{ mg/L}$ ;  $\text{pH} = 10$ ). One cycle was 120 min where CF conversion was  $\geq 95\%$  while  $A_{\text{Cu}}$  was calculated from  $4.2 \text{ mg/L}$  Cu within the resin. .... 120

## A7 List of tables

<b>Table 1:</b> Specifications for chemicals and reagents and suppliers.....	43
<b>Table 2:</b> Specifications for gases and suppliers .....	46
<b>Table 3:</b> List of materials purchased and their key specifications .....	46
<b>Table 4:</b> ICP-MS parameters for the determination of Cu.....	62
<b>Table 5:</b> Calculated specific Cu activities $A_{Cu}$ for the dechlorination of CF, DCM, and MCM and to account for the formation of products during dechlorination of CF and DCM using $Cu^0 + NaBH_4$ ( $c_{Cu} = 1-100$ mg/L; $c_{0,NaBH_4} = 300$ mg/L; $p_{H_2} = 100$ kPa; $pH = 10$ ).....	72
<b>Table 6:</b> Selectivity patterns during the dechlorination of CF in water using $Cu^0 + NaBH_4$ , $Pd^0 + NaBH_4$ , $Pd + H_2$ , and $nZVI^{BH}$ remediation systems under ambient conditions ( $c_{Cu} = 1$ mg/L; $c_{Pd} = 3-5$ mg/L; $c_{NaBH_4} = 300$ mg/L; $c_{nZVI} = 5$ g/L).....	75
<b>Table 7:</b> Product selectivity patterns during the dechlorination of CF in water using Cu- and Cu/ACF-electrodes under an external electric potential and in the presence or absence of $NaBH_4$ ( $m_{Cu-electrode} = 370$ mg; $m_{0.5\text{ wt-\% Cu/AC}} = 6.3$ mg; $c_{0,CF} = 5$ mg/L; $c_{0,NaBH_4} = 300$ mg/L; $pH_0 = 7$ ; $V_{electrolyte} = 400$ mL of 0.1 M $Na_2SO_4$ ; $V_h = 100$ mL).....	95
<b>Table 8:</b> Specific metal activities for the dehalogenation of single HOCs in water using Cu-, Pd- and nZVI-based systems together with the corresponding weakest C–X bond dissociation energies ( $c_{Cu} = 0.2-2500$ mg/L; $c_{0,NaBH_4} = 300$ mg/L; $c_{Pd} = 0.2-1500$ mg/L; $p_{H_2} = 100$ kPa; $c_{nZVI} = 0.4-5$ g/L; $c_{0,HOCs} = 2-50$ mg/L) .....	105
<b>Table 9:</b> Effect of various co-solutes on the specific Cu activities $A_{Cu}$ for the dechlorination of CF compared to the baseline for Cu without co-solutes ( $A_{Cu,CF,without\ co-solute} = (130 \pm 10)$ L/(g·min)) ( $c_{0,CF} = 10$ mg/L; $c_{0,NaBH_4} = 300$ mg/L; $pH = 8$ for $NaHCO_3$ ; $pH = 10$ for the other experiments) .....	114

## **A8 Acknowledgments**

First and foremost, I sincerely thank Prof. Dr. Kopinke for accepting me to join the interesting research group. I also thank his valuable input during the PhD. work and critic in the development of the research topic and actualization of the thesis. I am also deeply indebted to Dr. Katrin Mackenzie for her guidance, motivation, and encouragement throughout my stay at the UFZ. I appreciate her input during the day-to-day work whether in the laboratory or the review of manuscripts and thesis. She also continuously rendered her support on how to spend my off-work activities in Leipzig and Germany. My sincere gratitude also goes to Dr. Anett Georgi who has been there to assist me whenever I needed her guidance and opinion. I would also like to sincerely thank my colleagues, Sarah Sühholz, Alina Gawel, Kai Zumpfe, and Jonas Jörns for their support in the laboratory which culminated in this thesis. Many thanks go to all the PhD students, Maria, Navid, Lisa, Lin and Jieying who have made my stay here interesting especially during the frequent get together for afternoon cake and evening barbecue every Summer I spent in Germany. I would also like the technical staff and personnel in the Department of Environmental Engineering at UFZ, who have always been ready to assist me whenever help was needed. Last but not least, my sincere appreciation goes to my employer, the Technical University of Mombasa for granting me study leave to pursue the research work. My sincere appreciation also goes to DAAD for awarding me the scholarship and their support throughout my stay in Germany. Finally, I would like to thank my spouse Rauhiya, my grandfathers Mzee Japan and Mzee Mwalimu, my grandmother Mariga, friends, and relatives who have always been there to encourage and cheer me up in every step of my life and career that enabled me to accomplish this task.

## **A9 Curriculum vitae**

### **Contact**

---

Ali Shee

E-mail: [sheekali@tum.ac.ke](mailto:sheekali@tum.ac.ke) or [ali.shee@ufz.de](mailto:ali.shee@ufz.de)

Theodor-Neubauer Str. 23

Cell phone: +49 177 340 7245 or +254717513076

04318 Leipzig, Germany.

### **Personal data**

---

Nationality: Kenyan

Date of birth: 23<sup>rd</sup> March 1986

Place of birth: Kwale - Kenya

Address: P.o box 16062 - 80110, Mombasa - Kenya.

### **Education**

---

October 2016 - present

PhD student in Chemistry, Faculty of Chemistry and Mineralogy, University of Leipzig.

The topic of the PhD thesis: Evaluation of Copper-Based-Catalysts for Treatment of Halogenated Organic Compounds in Water (conducted in the Department of Environmental Engineering, Helmholtz Centre for Environmental Research - UFZ).

April - May 2016	Deutsch als Fremdsprache, Grundkurs Goethe Institute, Nairobi-Kenya
June - September 2016	Deutsch als Fremdsprache Carl Duisberg Centre, Berlin
September 2011- December 2014	Master of Science in Chemistry Master's thesis: Comparative adsorption of methylene blue and congo red dyes onto coconut husks, mangroves and polylactide blended films
October 2006 - September 2010	Bachelor of Science in Industrial Chemistry Bachelor thesis: Phytochemical investigation of <i>Teclea nobilis</i> roots for anti-plasmodium activity

### **Short courses**

---

2016 - 2021	Various courses covering Scientific Skills and Transferable Skills for completion of the HIGRADE Curriculum of the Graduate School at the Helmholtz Centre for Environmental Research - UFZ, Leipzig-Germany.
2005 - 2008	International Computer Driving License, Institute of Advanced Technology, Mombasa.
July 25 - 27, 2012	KDSA Research proposal writing workshop
August 24 - 28, 2015	GC-MS Workshop offered by the Pan-African Chemistry Network, Nairobi-Kenya.
June 26 - 30, 2017	MDKL Catalysis course, Leipzig, Germany

## Internship/working experience

---

October 2016 - present	Research assistant, Department of Environmental Engineering, Helmholtz Centre for Environmental Research-UFZ, Leipzig, Germany
June 2015 - present	Tutorial Fellow Technical University of Mombasa, Mombasa, Kenya
January 2012 - May 2015	Teaching/Graduate Assistant Technical University of Mombasa

## Oral Presentations

---

1. The International Conference on Characterization and Remediation of Per and Polyfluoroalkyl Substances and Other Emerging Contaminants (PFAS). May 10 - 12, 2021, Virtual conference. **Reduction of Halogenated Organic Compounds in Water: Comparison of Catalysts and Reagents.**
2. Joint Integrated Project day at UFZ. November 5, 2019, Leipzig, Germany. **Reduction of Halogenated Organic Compounds in Water: Comparison of Reagents and Catalysts.**

3. The 16<sup>th</sup> International Conference on Environmental Science Technology (CEST 2019).  
September 4-7, 2019, Rhodes Island, Greece. **Reduction of Halogenated Organic Compounds in Water: Comparison of Application Areas for Cu, Pd and nZVI.**

## Awards

---

- |                          |   |
|--------------------------|---|
| March 2016 - August 2021 | Doctoral Scholarship offered by the Germany Academic Exchange Service (DAAD).   |
| September 7, 2019        | Best Oral Presentation Prize at the CEST 2019 Conference, Rhodes Island, Greece. Certificate from Chemical Engineering Journal and USD 200 prize. |

ISSN 1860-0387

PHD DISSERTATION 10 | 2021

Helmholtz Centre for  
Environmental Research – UFZ  
Permoserstraße 15  
04318 Leipzig | Germany  
[www.ufz.de](http://www.ufz.de)

NOT FOR SALE.

Ali Shee | Evaluation of Copper-Based-Catalysts for Treatment of Halogenated...